TISSUE ENGINEERING STRATEGIES FOR TOTAL DISC REPLACEMENT: STRUCTURE AND MECHANICAL FUNCTION OF THE INTERVERTEBRAL DISC

A Dissertation

Presented to the Faculty of the Graduate School

of Cornell University

In Partial Fulfillment of the Requirements for the Degree of

Doctor of Philosophy

by

Marianne Lintz

August 2021

TISSUE ENGINEERING STRATEGIES FOR TOTAL DISC REPLACEMENT: STRUCTURE AND MECHANICAL FUNCTION OF THE INTERVERTEBRAL DISC

Marianne Lintz, Ph.D.

Cornell University 2021

Degenerative disc disease (DDD) is implicated as one of the primary causes of lower back pain (LBP), the leading cause of disability worldwide. This degeneration is characterized by irreversible detrimental changes to the structure of the intervertebral disc (IVD) which then severely impairs its mechanical function in the spine. The gel-like nucleus pulposus (NP) at its core loses its ability to hydrate while damage propagates through the surrounding annulus fibrosus (AF) in the form of tears and lesions, rendering it unable to resist elastic deformation. Current surgical interventions treat the painful symptoms of the disease rather than the underlying causes, providing only a temporary solution. Tissue-engineered (TE) repair strategies have been proposed for the last two decades as a means of preventing disease advancement in the long term, aiming to restore the native disc's structure as well as repair damage to the cell population. While promising, recapitulating the disc's complex fibrous architecture and mechanical behavior represents an enduring challenge in the field, particularly in attempts to scale up to larger animal models for clinical translation.

This thesis sought to augment engineered constructs *in vitro* by investigating the interplay between matrix composition and mechanical behavior, as well as provide mechanical support to constructs for *in vivo* delivery. In particular, it describes how the manipulation of fiber formation through media glucose content *in vitro* plays a critical role in governing matrix structure and mechanical integrity (Chapter 1); how these same mechanisms function in a diseased state *in vivo* to influence the developing disc

(Chapter 2); and how providing a supplemental cage structure to immature TE-IVDs can prevent initial displacement and collapse following implantation to eventually ensure successful tissue integration. Collectively, the work presented here offers crucial insight into how to continue the advancement of biologically based TDR strategies towards use in the clinic.

BIOGRAPHICAL SKETCH

Marianne was born in Santiago, Chile and grew up in Weston, Florida with her parents and younger sister. She attended the Massachusetts Institute of Technology, where she graduated with a degree in Biological Engineering in 2015. As a sophomore she began conducting research under Dr. Alan Jasanoff, investigating behavioral responses to assist in mapping neural networks in rodents. She went on to work with Dr. Alan Grodzinsky, utilizing techniques in atomic force microscopy to facilitate imaging and characterization of mouse aggrecan.

Following her graduation in 2015, Marianne began her Ph.D. in Biomedical Engineering working in the Reinhart-King laboratory under Dr. Cynthia Reinhart-King to investigate the influence of cellular metabolism and tumor microenvironment on single-cell invasive migration and intravasation. In the summer of 2016 she participated in a two-month clinical immersion at New York Presbyterian Hospital / Weill Cornell Medical Center and shadowed Dr. Timothy D'Alfonso, an anatomic pathology specialist. In January of 2017 she began working under Dr. Lawrence Bonassar to continue her Ph.D. work. In collaboration with Dr. Roger Härtl and his team of neurosurgery fellows at Weill Cornell Medical Center, her research focused on tissue-engineered strategies for total disc replacement. In particular her thesis sought to establish mechanisms for supplementing the mechanical behavior of tissue-engineered constructs to enable clinical translation. During her time at Cornell Marianne was awarded the Cornell Engineering Colman Fellowship as well as the Provost Diversity Fellowship for Advanced Doctoral Students.

Upon completing her Ph.D. Marianne is interested in transitioning to industry, applying her skills to further research and development in cell therapies for regenerative medicine.

Dedicated to all of my loved ones, in thanks for your unwavering support

ACKNOWLEDGMENTS

I'd like to begin by sincerely thanking Dr. Lawrence Bonassar for his mentorship during my graduate experience. In addition to sharing his expertise and wisdom in guiding the development of this project, the patience and support—and ultimately kindness—he has extended during the more difficult times of this journey have been invaluable. Larry, it has been a privilege working under your guidance. I would also like to thank my committee members, Dr. David Putnam and Dr. Jonathan Cheetham, for their support and guidance. Thank you for devoting so much of your time and your excellent suggestions to the advancement of this project.

Great thanks go to Dr. Roger Härtl for his continued advice and grounding of this project in long-term clinical goals. I am a scientist by training and having you consistently contribute your unique perspective has been instrumental to shaping my understanding of regenerative medicine. Special thanks as well to Sertaç Kirnaz, Jacob Goldberg, Branden Medary, and Christoph Wipplinger from the Weill Medical team for your collaborative efforts but also for being excellent peers and friends. It has been a pleasure to work alongside of you.

Thank you to labmates and friends for sharing in this experience with me. Your presence, your patience, and your tremendous emotional support have helped push me forward through all of the ups and downs of the last six years. To the past and current members of the Bonassar lab, you have my deepest gratitude for sharing your brilliance and your time with me. Without you I would be hopelessly stuck in either the culture room or the basement. So thank you to all of you, including Mary Clare McCorry, Ben Cohen, Alex Boys, Chris DiDomenico, Jorge Mojica Santiago, Jill Middendorf, Nicole Diamantides, Sierra Cook, Liz Feeney, Jongkil Kim, Steven Ayala, Eric Yoon, Sera Lopez, Karan Vishwanath, Leigh Slyker, Sean Kim, Rachel Yerden, Emily Jiang, Ellaine Chou, Jared Matthews, and Maho Koga. To the new members of the lab

family—Caroline Thompson, Alikhan Fidai, Alicia Matavosian—I wish you all the best as you begin your graduate studies. Thank you also to Dr. Lisa Fortier for her kindness and support these last few years, to Belinda Floyd for always always fighting for us, to Jami Joyner for the care she devotes to DPE and the student body, and to Suzanne Koehl for never failing to make me smile. Thank you to Dr. Cynthia Reinhart-King and the members of her lab for welcoming me during the early stages of my Ph.D. It was a pleasure to work with you in the brief time you were at Cornell. And a very fond thank you is due to Dr. Alan Grodzinsky for being instrumental in kickstarting my research journey, for the incredible kindness he extends to each and every person who has the privilege of his mentorship, and for welcoming me back to the family so warmly. Al, here's to you.

And finally, thank you to my family for their unending love and belief in me. Thank you to my parents, Soraya and Diether, for giving so much so often. To Tania, my sister, for friendship and silliness but also for understanding. And to Annie, of course, who may as well have an honorary Ph.D. at this point.

Funding for this work was provided by the Colin MacDonald Fund, the Daedalus Innovation Fund, and the Center for Advanced Technology from the New York State Advanced Research Fund (NYSTAR).

TABLE OF CONTENTS

LIST OF FIGURES

Figure 3.2. A) Whole disc sGAG concentration, **B)** whole disc collagen content, and **C)** whole disc DNA content normalized to wet weight for each group. **D)** AGE content normalized to hydroxyproline for each group. Significant differences ($p<0.05$) are indicated using (*) and bars. Error bars represent standard deviation. (n=8-9)

Figure 3.3. Representative histological images for Safranin-O staining of wild type (top) and diabetic (bottom) discs of **A)** the entire disc at 40x and **B)** the inner AF at 100x magnification. Significant differences ($p<0.05$) are indicated using (*) and bars. Error bars represent standard deviation while scale bars indicate 0.15 mm. (n=5-6)

Supplemental Figure 3.1. A) Fraction of total disc area occupied by the NP for each group. **B)** Percent of total disc area occupied by Safranin-O staining. Significant differences ($p<0.05$) are indicated using (*) and bars. Error bars represent standard deviation while scale bars indicate 0.15 mm. (n=5-6)

Figure 3.4. Representative SHG images for wild type (top) and diabetic (bottom) discs of **A)** the entire disc and **B)** the inner AF. **C)** Normalized fiber orientation distributions for wild type (top) and diabetic (bottom) discs. Scale bars indicate 200 (**A**) or 100 μm (**B**). (n=6-7)

Figure 3.5. A) Dynamic stiffness for each group over 13 frequencies. **B)** Equilibrium modulus and **C)** hydraulic permeability determined from stiffness and phase angle values following cyclic tests for each group. **D)** Compressive modulus and **E)** hydraulic permeability determined from stress/relaxation tests for each group. Significant differences ($p<0.05$) are indicated using (*) and/or bars. Error bars represent standard deviation. (n=7-9)

Figure 4.1. Schematic outlining surgical procedure for implantation of one-and two-piece cages into the minipig cervical spine. Implantation photograph as well as outcome measures collected during the 4 week study timeline are presented.

Supplemental Figure 4.1. Trilineage differentiation potential for MSCs cultured in **A)** osteogenic, **B)** adipogenic, and **C)** growth media. Samples were stained with either Alizarin Red S (top) or Oil Red O (bottom). Scale bars indicate 0.15 mm.

Figure 4.2. A) X-ray monitoring of controls and implants at pre-op, immediately post-op, and 4 week followup timepoints. **B)** Disc height indices in surgically-treated levels at different timepoints. **C)** One-piece implants recovered post-sacrifice from the C3/4 (top) and C5/6 (bottom) experimental levels.

Figure 4.3. A) Representative SEM images taken at implant failure site. **B)** Experimental set up for unconfined compression mechanical tests. **C)** Stress vs. displacement plot of cage construct as compared to human intradiscal pressure (IDP).

Figure 4.4. A) Failure locations in the cage based on post-mortem assessment. **B)** Reconstructed 3D model of a minipig cervical vertebrae showing presence of posterior bony extrusion.

Figure 4.5. Photographs of composite TE-IVDs cultured in cages between media changes. Scale bars represent 17.5 mm while the red arrow indicates the location of the NP within the construct.

Figure 3.2. A) Whole disc sGAG concentration, **B)** whole disc collagen content, and **C)** whole disc DNA content normalized to wet weight for each group. **D)** AGE content normalized to hydroxyproline for each group. Significant differences ($p<0.05$) are indicated using (*) and bars. Error bars represent standard deviation. (n=8-9)

Figure 3.3. Representative histological images for Safranin-O staining of wild type (top) and diabetic (bottom) discs of **A)** the entire disc at 40x and **B)** the inner AF at 100x magnification. Significant differences ($p<0.05$) are indicated using (*) and bars. Error bars represent standard deviation while scale bars indicate 0.15 mm. (n=5-6)

Supplemental Figure 3.1. A) Fraction of total disc area occupied by the NP for each group. **B)** Percent of total disc area occupied by Safranin-O staining. Significant differences ($p<0.05$) are indicated using (*) and bars. Error bars represent standard deviation while scale bars indicate 0.15 mm. (n=5-6)

Figure 3.4. Representative SHG images for wild type (top) and diabetic (bottom) discs of **A)** the entire disc and **B)** the inner AF. **C)** Normalized fiber orientation distributions for wild type (top) and diabetic (bottom) discs. Scale bars indicate 200 (**A**) or 100 μm (**B**). (n=6-7)

Figure 3.5. A) Dynamic stiffness for each group over 13 frequencies. **B)** Equilibrium modulus and **C)** hydraulic permeability determined from stiffness and phase angle values following cyclic tests for each group. **D)** Compressive modulus and **E)** hydraulic permeability determined from stress/relaxation tests for each group. Significant differences ($p<0.05$) are indicated using (*) and/or bars. Error bars represent standard deviation. (n=7-9)

Figure 4.1. Schematic outlining surgical procedure for implantation of one-and two-piece cages into the minipig cervical spine. Implantation photograph as well as outcome measures collected during the 4 week study timeline are presented.

Supplemental Figure 4.1. Trilineage differentiation potential for MSCs cultured in **A)** osteogenic, **B)** adipogenic, and **C)** growth media. Samples were stained with either Alizarin Red S (top) or Oil Red O (bottom). Scale bars indicate 0.15 mm.

Figure 4.2. A) X-ray monitoring of controls and implants at pre-op, immediately post-op, and 4 week followup timepoints. **B)** Disc height indices in surgically-treated levels at different timepoints. **C)** One-piece implants recovered post-sacrifice from the C3/4 (top) and C5/6 (bottom) experimental levels.

Figure 4.3. A) Representative SEM images taken at implant failure site. **B)** Experimental set up for unconfined compression mechanical tests. **C)** Stress vs. displacement plot of cage construct as compared to human intradiscal pressure (IDP).

LIST OF TABLES

LIST OF ABBREVIATIONS

AF – annulus fibrosus

AGE – advanced glycation end product

ANOVA – analysis of variance

bFGF – basic fibroblast growth factor

BMP – bone morphogenic protein

CEP – cartilaginous endplate

DDD – degenerative disc disease

DHI – disc height index

DMEM – Dulbecco's modified Eagle serum

DMMB – dimethylmethylene blue

DNA – deoxyribonucleic acid

DPBS – Dulbecco's phosphate buffered saline

ECM – extracellular matrix

ELISA – enzyme-linked immunosorbent assay

FA – fiber alignment

FBS – fetal bovine serum

FFT – fast fourier transform

FTIR – fourier transform infrared

GAG – glycosaminoglycan

GDF – growth differentiation factor

HA – hyaluronic acid

IACUC – Institutional Animal Care and Use Committee

IDP – intradiscal pressure

IVD – intervertebral disc

LBP – lower back pain

MMP – matrix metalloproteinase

MRI – magnetic resonance imaging

MSC – mesenchymal stem cell

NP – nucleus pulposus

PBS – phosphate buffered saline

PCL – poly(caprolactone)

PDGF – platelet-derived growth factor

PGA – poly(glycolic acid)

PLA – poly(lactic acid)

PLGA – poly(lactic-co-glycolic acid)

PLLA – poly(L-lactic acid)

PMMA – polymethyl methacrylate

ROS – reactive oxygen species

s-GAG – sulfated glycosaminoglycan

SD – standard deviation

SEM - scanning electron microscopy

SHG – second harmonic generation

SLRP – small leucine rich proteoglycan

SPI – spinal cord injury

T2D – type 2 diabetes

TE – tissue-engineered

TE-IVD – tissue-engineered intervertebral disc

TGF - transforming growth factor

TDR – total disc replacement

μCT – micro-computed tomography

CHAPTER 1

Introduction

The Intervertebral Disc

The intervertebral disc (IVD) is a soft fibrocartilaginous tissue situated between the bony vertebrae in the spine, with a total of twenty-three discs occupying the length of the adult human spine. These discs are distributed among the four anatomic regions of the spine as follows: six in the cervical, twelve in the thoracic, and five in the lumbar[1-3]. A relatively similar structure is found throughout the majority of the discs with the exception of the first cervical level (C1/2) and the sacrum[3]. A composite joint structure, the IVD is comprised of three structurally distinct regions (Fig. 1.1): the nucleus pulposus (NP) at its core, the annulus fibrosus (AF) which surrounds and contains it, and the two cartilaginous endplates (CEPs) which serve as an interface between the disc and adjacent vertebral bodies. The resulting structure and composition of each of these regions contributes to the disc's mechanical role in the spinal column, allowing it to limit or enhance flexibility based on the magnitude of loads to which the body is subjected.

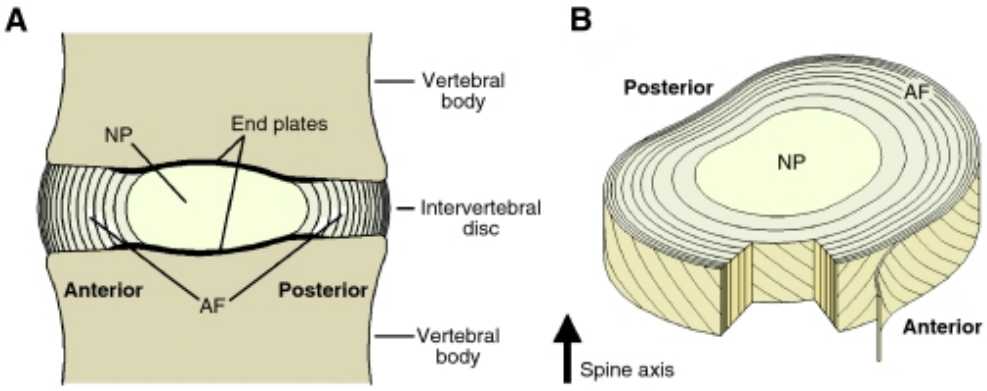

Figure 1.1. Schematic of **A)** the disc's position in the motion segment and **B)** the fiber organization of the AF region. Image adapted from Smith, et al.[4]

Structure and Composition

The NP at the center of the disc is a gelatinous structure consisting of mostly water at 70-90% of the tissue, though the total content varies with age[5-8]. Proteoglycans meanwhile account for the majority of the dry weight (35-65%) of the NP[5,9-14], including the negatively-charged aggregating proteoglycans aggrecan and versican as well as the small interstitial proteoglycans (or small leucine rich proteoglycans, SLRPs) biglycan, decorin, fibromodulin, and lumican[15]. As a result of the high concentration of negative charge associated with the large proteoglycans the NP is very hydrophilic, which in turn enables it to behave as a highly hydrated gel and retain water as well as resist deformation[4,16-18]. Particularly important for this role is the large keratan sulfate- / chondroitin sulfate-linked proteoglycan aggrecan, which aggregates with hyaluronan through stabilized interaction with link proteins[4,19-21]. The smaller proteoglycans are likely involved in extracellular matrix (ECM) maintenance and repair following injury[22-27]. Collagen type II fibers occupy a smaller fraction of the NP and account for 15-20% of its dry weight[5,9-14]. These fibers are arranged in a random, loose network throughout the NP and function to maintain its structural integrity.

The AF surrounding the NP is heterogeneous in nature and made up of highly oriented collagen fibers (Fig. 1.2). In contrast to the NP, the AF is approximately 65% water and has a reverse proteoglycan to collagen ratio, with collagen accounting for 65-70% of its dry weight while proteoglycans represent 10-20%[5,7,13,28]. The fibers which comprise the AF are arranged in 15-25 unique, concentric lamellae at alternating angles of approximately 25-45° to the horizontal axis, averaging around 28-30°, with the highest values present at the thinner outer layers[29-32]. An elastin fiber network can also be found between the lamellae[1,33,34]. The AF can be further divided into inner and outer regions based on structure, with the fibrous outer AF containing more aligned type I collagen arranged in an angle-ply fashion; meanwhile the structure of the inner AF is

more disorganized and contains a larger concentration of proteoglycans and type II collagen than its counterpart, similar to the NP[2,29,30,35-37]. Obliquely angled fiber bundles are present in both regions, joining the inner AF with the CEPs and attaching the outer AF directly to the vertebrae[2,4,38].

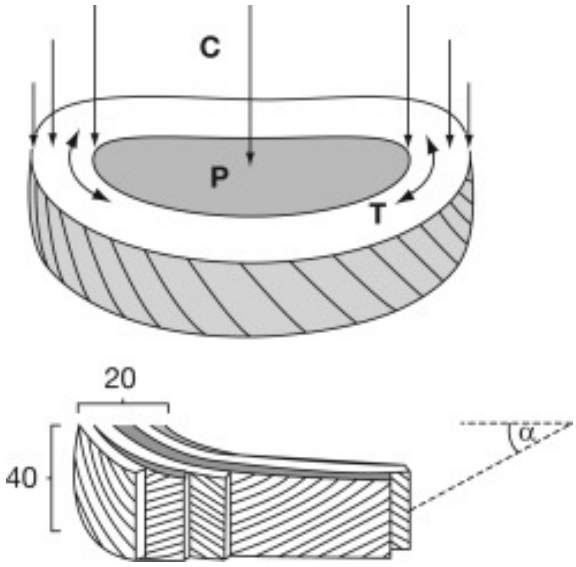

Figure 1.2. Representative schematic indicating orientation of the fiber lamellae throughout the AF. Figure adapted from Adams, et al.[39]

The CEP is a thin (~600 μm) hyaline cartilage boundary found at the superior and inferior regions of the IVD, positioned between the vertebral endplates and the NP, which plays a role in regulating nutrient distribution between the largely avascular mature IVD and adjacent vertebral bodies[19,40,41]. Along with transporting nutrients from the blood supply into the disc and waste out, the CEP also functions to contain the NP and provide structural support[40,42,43]. Like the remainder of the disc, the CEP is composed primarily of water (70-80%), proteoglycans, and collagen, with type II collagen fibers making up the bulk of the latter[40,44].

The cellular population throughout the IVD also varies with location, with unique cell types occupying the distinct regions and contributing to the health and

maintenance of the tissue. As a whole the disc displays fairly low cellularity at approximately 6,000 cells/mm^3, with the highest concentration of cells present in the very outer region of the AF and the lowest towards the NP: the mature AF contains about 2/3 while the NP is occupied by roughly 1/3 of the disc's cell population[1,45,46]. In the immature disc the NP is populated by large, vacuous notochordal cells which persist throughout the lifespan of most animals but disappear entirely in humans before the age of 20[20,47,48]. These notochordal cells are replaced by mature NP cells, thought to be derived from their precursors, which are smaller in comparison and display a rounded chondrocyte-like phenotype. Cell morphology in the AF meanwhile differs depending on region: cells in the inner AF resemble those in the NP and are spherical in nature, while those in the outer AF are elongated, oriented along the collagen fibers, and appear fibroblastic[46,49,50]. The CEP has a much higher cellularity than either the NP or AF at about 15,000 cells/mm^3, with morphology resembling the rounded chondrocyte-like cells of the NP[1,45,51].

Biomechanics and Function

The primary function of the IVD is to grant flexibility to the spine, allowing bending and twisting motions while absorbing compressive loads and distributing them to the vertebral bodies[2,9,39]. The previously described structure and biochemical composition are directly responsible for enabling the disc to do so. The presence of large amounts of proteoglycans in the NP results in a high water content and generates osmotic swelling in response to compression, increasing the tissue's hydrostatic pressure throughout[15,29,52,53]. Pressures generated in the primarily isotropic NP as a result of this swelling vary depending on the position of the individual's body, with values in a healthy lumbar disc ranging from 91-1330 kPa in prone and seated positions, respectively[54-57]. The surrounding AF in turn generates tensile circumferential stresses

to resist this buildup of pressure in the NP[9,58]. In fact, as a result of its highly organized collagen network and complex lamellar structure, the anisotropic AF functions differently in response to bending, twisting, or compressive movements. The resulting mechanical profile is not only dependent on location but time-dependent as well, resulting in nonlinear viscoelastic behavior. The inner AF, which has a higher type II collagen content enabling it to resist compressive forces, experiences the brunt of hydrostatic pressure from the NP while the outer AF, containing more type I collagen and therefore possessing greater tensile strength, experiences primarily tension[9,12,13,18,39]. Elastin fibers found throughout the AF also contribute to the tissue's ability to resist deformation and regain its structure following loading. The CEP meanwhile assists in the distribution and reduction of pressure generated by the NP it contains, bulging into the vertebral bodies in its stead[9,40,42,59,60].

Disc Development

Development of the disc during embryogenesis has been extensively studied. The spinal column, and therefore the discs contained within, arise during embryogenesis from the notochord, an embryonic structure stemming from the mesoderm which functions to a) transmit signals necessary for cell migration and adjacent tissue patterning, as well as b) directly develop into the NP[4,35,36,61,62]. Different transcriptional factors are secreted during this process, the highly specific combination of which guides the differentiation of different structures in the disc: the NP and AF, for example, arise simultaneously though distinctly.

Adjacent to the notochord are the somites, a pair of segmented spherical-shaped blocks of cells derived from the mesoderm. As the embryo matures, somite cells undergo an epithelial to mesenchymal transition and migrate towards the notochord. Here they begin to multiply, eventually surrounding the notochord to aggregate at

different locations and give rise to the sclerotome[4,63-65]. Depending on how the cells condense at these locations, the sclerotome gives rise to either the vertebral bodies or the AF: non-condensed regions become the former and condensed form the latter[66]. Following the establishment of the vertebrae the notochord begins to shrink, instead developing between the end-plates to form the immature NP[35,67]. As the NP develops the notochordal cells are replaced by the mature chondrocyte-like population; in humans there remain no traces of the notochord in adulthood, while in other species a distinct population of notochord cells can be found still within the NP.

Fiber formation in the AF is initiated during these stages[66], with matrix assembly largely guided by the involvement of proteoglycans[38,68,69]. SLRPs, a family of secreted proteoglycans that bind ECM molecules and are characterized by a leucine-rich core domain flanked by cysteine-rich end clusters, are known to play a critical role in tissue growth[22,23,70-72]. Hayes, et al. described how the AF was established in fetal rats, outlining the role that SLRPs play in regulating ECM assembly and collagen fibrillogenesis[38]. They showed that within the fetal disc, the initial phases of cellular differentiation are followed by organized fibrillar matrix deposition in the outer AF portions. Meanwhile in the inner AF a reinforcing structure of collagen fibers encircles the developing NP, both regions becoming more established as the disc develops to maturity. During development, fibromodulin plays the largest role in driving AF assembly and organization[66], while SLRPs such as biglycan and decorin are more associated with cartilage development in the regions surrounding the disc.

Degenerative Disc Disease

Lower back pain (LBP) is a common source of human injury and disability, with upwards of 70% of individuals experiencing some form of LBP during their lives, that increases in prevalence as the population ages[73]. Approximately 10% of individuals

suffering from LBP can remain permanently disabled, which in turn results in enormous medical costs associated with insurance, disability benefits, etc.[19]. Costs in the United States alone, for example, can average one to two billion dollars annually. Although the exact cause for the onset of the disease remains unknown, damage to the IVD has been implicated in many instances. Specifically, degeneration of the disc has been identified as one of the leading causes of this form of spinal injury and is associated with approximately 40% of LBP cases[73,74].

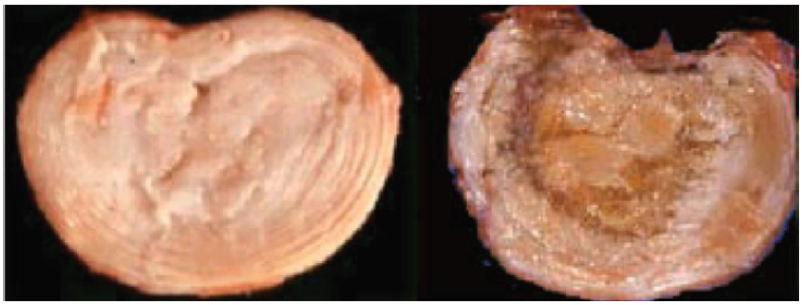

Figure 1.3. Photographs of a healthy (left) and degenerated (right) human IVD, highlighting the structural changes that affect the disc during DDD. Figure adapted from Urban, et al.[19]

Degenerative disc disease (DDD), though without an exact pathological definition, refers to pain and related sensory symptoms (i.e. numbness, muscle weakness) brought about by damage to the disc. This degeneration is characterized by an alteration to the disc's native structure and biomechanical properties (Fig. 1.3), and may lead to detrimental changes to the remainder of the spinal column, resulting in sciatica or spinal stenosis[19]. Though associated with natural degenerative processes brought about by age, DDD is considered a multi-factorial disease with a wide range of potential causes including mechanical stress, trauma/injury, genetic factors, inflammation, etc. DDD, like LBP, increases in incidence with age. 20% of adolescents reportedly experience mild symptoms from the first stages of degeneration, with this

number increasing to 40% and eventually 80% in 40- and 80-year-olds, respectively[75,76]. The Wakayama Spine Study which focused on individuals between the ages of 21 and 97, for example, found that more than 90% of those sampled over the age of 50 experienced DDD in some region of the spine[77], and that the incidence was additionally dependent on pre-existing conditions such as obesity though independent of sex. Corroborating these observations, peak incidence of the disease appears to occur in middle age, and while most individuals in this age group demonstrate some sort of degeneration the majority are asymptomatic[76]. In fact, studies have indicated that a large portion of the population as a whole has some degree of DDD, though a lack of symptoms results in the disease going undetected until progression to later stages and further degeneration.

Epidemiology and Pathogenesis

In very young individuals the regions of the IVD are easily distinguishable; however, as the disc matures and the process of degeneration unfolds, the boundaries become significantly less distinct. The NP, for example, becomes less gel-like and instead becomes stiffer and less compliant as its mechanical properties become irrevocably altered. The region experiences a decrease in proteoglycans and water content paired with an increase in glycation end products, the combination of which renders it unable to hydrate and therefore incapable of resisting elastic deformation[5,7,28,78]. Degenerated discs, when subjected to loads, deform more drastically than their healthy counterparts: disc height and water content decrease more rapidly while the disc returns to a normal state at a slower rate. An increasing loss of aggrecan content impacts the NP's ability to regulate its hydrostatic pressure and instead forces the AF to bear the brunt of compressive loading directly, resulting in damage propagating through the AF in the form of cracks or tears[19,78.79]. Such damage to the AF

is thought to trigger an inflammatory response and produce a degenerative cascade where factors contributing to matrix degradation (i.e. matrix metalloproteinases or MMPs) are upregulated. Ultimately, the anabolic nature of the ECM trends towards catabolism with an accumulation of degenerative changes.

Alongside these changes, the fibrillar architecture in both the NP and AF becomes increasingly more disorganized, with irregular continuity and spacing of the AF lamellae. Collagen type II content in the NP and outer AF decreases while the presence of collagen type I fibers increases in these regions[79]. The CEP meanwhile exhibits decreased permeability and calcifies with advanced degeneration, which may ultimately result in sclerosis. Further complications associated with disc degeneration involve the presence of necrotic and/or apoptotic cells, lack of nutrition, accumulation of cell waste, and enhanced growth of blood vessels and nerves in the disc resulting in severe pain to the individual or even bulging, herniation, or destabilization of the disc and/or motion segment[5].

Though the exact events which initiate degeneration have not been identified, it has been suggested that decreased permeability in the CEP is one of the main initiators of the degenerative cascade as these alterations would result in inhibited nutrient diffusion to the remainder of the disc, particularly the NP[3,43,80]. Due to the disc's largely avascular nature, the cell population is largely dependent on this nutrient exchange to preserve a proper pH balance; with impaired diffusion the disc environment can become increasingly more acidic, compromising the cells' ability to maintain the ECM as well as synthesize matrix components as they trend towards a senescent state[19,78]. Excessive or abnormal mechanical loading has also been implicated as a potential initiator of early degenerative changes, though repetitive controlled loading mechanisms such as standard exercise have been discounted as major contributors.

With regards to other diseases as potential risk factors diabetes has been established as a common comorbidity of DDD, with studies suggesting it may exacerbate degenerative pathways associated with its progression[81-93]. Long-term hyperglycemia associated with diabetes, for example, results in the accumulation of advanced glycation end products (AGEs) which trigger increased catabolism in the disc and stimulate the production of reactive oxygen species and MMPs, among other inflammatory factors. Hyperglycemia-induced apoptosis and senescence in the endogenous cell population also play a role in advancing degeneration, though the exact molecular mechanisms driving the process remain unclear.

Current Treatments

Conservative approaches for the treatment of DDD often include bedrest, pain-relieving injections (i.e. steroids), or physical therapy, and are mostly aimed at treating the patients' pain to enable them to return to their daily routines. Overall these approaches may provide temporary relief to patients suffering from painful DDD, but they are ultimately not viable for highly degenerated discs and do not provide long-term solutions.

A variety of more invasive surgical alternatives are also in place to treat disc degeneration. Typically, surgery is performed following T2-weighted preoperative magnetic resonance imaging (MRI) assessment to determine the extent of damage based on factors such as disc height, signal intensity, and integrity of the AF/NP boundary[94]. In certain cases where disc material has herniated and is causing pain by impinging on spinal nerves, portions of the herniated disc can be removed via discectomy. Although these are standard procedures and have been performed extensively there are still associated challenges, including difficulty maintaining stability and, most importantly, consequent degeneration of adjacent regions[95].

For more advanced degeneration and end-stage disease, standard surgical techniques involve the removal of the damaged disc in its entirety rather than simply portions of the AF and/or NP, followed by either spinal fusion or total disc replacement (TDR). Fusion is a surgical technique by which the vertebrae adjacent to the removed disc are permanently joined, preventing motion between them. The surgery involves the addition of bone graft—either auto-, allo-, or synthetic grafts—to provide cues that allow the bone to fuse into one continuous segment and heal almost as a broken bone does over a lengthy recovery period. While fusion was the gold standard for many years, particularly in the lumbar spine, there are a variety of complications that arise from the procedure. The most common reported post-operative side effects are pseudoarthrosis and graft site pain, observed in 16% and 9% of patients, respectively[96]. The resulting motion limitation and even total loss may also result in adjacent segment disease, as the rest of the spine must now overcompensate to account for the abnormal loading brought about by the fusion; uneven stress distributions and increased motion have been reported in these adjacent segments[94].

TDR meanwhile involves the introduction of an implant in place of the removed disc. Despite evidence suggesting that this procedure could provide successful long-term solutions to IVD degeneration and patients reporting satisfaction up to 24 months post-surgery[97], implantation rates continue to remain low[98]. Certain hurdles associated with this technique must be cleared before it is more widely adopted, some of these including difficult surgeries as well as high costs. Perhaps the most important issue to address, however, is the lack of available devices that properly mimic both the architecture and biomechanical properties of the native disc: TDR strategies are traditionally limited to mechanical implants. The primary issue with these approaches then is that the majority, whether through fixation of additional devices or not, focus on limiting mobility and improper weight loading rather than repairing the injured disc; that

is, they treat the symptoms of the disease rather than the underlying disease itself[99]. The long-term efficacy is uncertain, and as with discectomy and fusion there comes a substantial risk of reoperation brought about by adjacent segment disease. More substantial approaches are necessary for the treatment of end-stage disc disease, then, due to the depletion of the endogenous cell population and irreversible deterioration of tissue structure.

Experimental Approaches to Repair and Replacement

To resolve the issues present with the aforementioned approaches to treating DDD, investigators have proposed a variety of alternatives. These range from more conservative treatments aimed at restoring function in early stages of the disease, to more invasive approaches with the goal of replacing the damaged disc altogether.

NP and AF Repair

Following discectomies where portions of the AF and/or NP are removed, the structural integrity of the disc is weakened. In order to preserve some of the native function, strategies to repair or replace the damaged tissue have been developed. NP-like biomaterials such as hydrogels (collagen, alginate, chitosan, etc.) offer an attractive option as they are hydrophilic and can reproduce the NP's swelling capabilities, in theory restoring its ability to retain water[100-102]. They are, however, mechanically inferior; as a result, gels composed of synthetic polymers (i.e. polyethylene glycol) have been explored as an alternative. While the main benefit of these synthetic gels lies in the tunability of their mechanical and swelling properties, they demonstrate inferior bioactivity when compared to their counterparts, as well as significantly higher manufacturing costs[100]. For both classes of hydrogel, degradable and non-degradable options have been examined. The former is more biocompatible than the latter and can

also be remodeled by the cellular population, eventually replaced with newly deposited matrix. The majority of non-degradable gels, meanwhile, may not have the same degree of biocompatibility but they do present a more mechanically robust alternative[102]. In combination with the aforementioned gels, cell delivery by means of injection aims to supplement the remaining cellular population, replacing senescent cells to more actively produce proteoglycans and matrix components which provide cues for the repair of the disc. A variety of cell types including NP cells, mesenchymal stem cells (MSCs), and notochord cells have been tested as possible sources.

However, NP injections such as those detailed above do have their drawbacks, including stiffening of the material leading to gel fracture and endplate damage[101]. Research has also indicated that NP repair strategies cannot restore function to the damaged disc on their own; without sealing the AF defect, the injected gel is unable to provide the disc the mechanical support to withstand compressive loads and may lead to recurrence of the original herniation[103-105]. Nonbiologic options for repair involve the administration of sutures, metals, or synthetic polymers to physically seal AF lesions; however, these fail to restore native function due to inferior tissue integration and mechanical strength[106-109]. Bioactive and cell-laden materials such as hydrogels and sponges have also been proposed with the goal of enhancing healing and supplementing long-term remodeling of the AF. These biologic therapies have been shown to prevent degenerative changes, supplementing matrix remodeling following integration and highlighting the capacity for mechanical and structural restoration of native function[106]. More recently groups such as our own have investigated the feasibility of combination AF/NP repair strategies, which take into account the nature of the IVD as a composite structure. Results are promising and indicate that while individual approaches do have their benefits, combined repair is the most likely to salvage the disc by restoring NP hydration, AF morphology, and overall biomechanics in the long term[110].

While NP/AF repair has shown promise and is well on its way to being implemented in humans, it is important to remember that these techniques are only useful if the disc retains a viable cell population and some degree of intact structure. That is, implementation can only be successful in certain stages of degeneration; once the disease has progressed to a point that native tissue is no longer salvageable, other alternatives for treatment must be explored.

Tissue-Engineered Composite Discs

Over the better part of the last two decades, researchers have explored a variety of methods for treating end-stage DDD, attempting to generate synthetic discs (Fig. 1.4) that resemble native morphology as well as provide cues to ensure the continued health of the implant following surgical placement. Mizuno et al. first produced a synthetic composite disc in 2004 by placing an alginate gel core at the center of a poly(lactic acid) (PLA) / poly(glycolic acid) (PGA) scaffold, seeded with ovine NP and AF cells, respectively[111,112]. Following timepoints of up to 16 weeks of implantation in the dorsum of athymic mice, the discs were found to have biochemical and mechanical properties which were enhanced with time, eventually approximating their native counterparts.

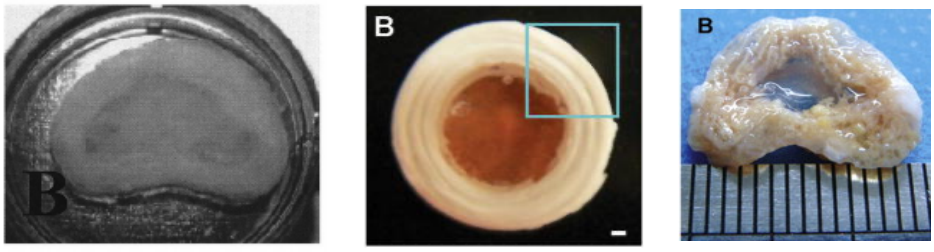

Figure 1.4. Representative photographs showcasing different approaches to generating composite TE-IVD constructs from a variety of material choices. Figure adapted from Mizuno, Nerurkar, and Park, et al.[111-114]

In the years that have followed, multiple groups have proposed their own solutions to the issues of a) recreating the aligned AF collagen network and b) re-introducing a viable cell population in composite cell-laden TE-IVDs utilizing a variety of unique approaches, summarized in Table 1.1[115]. AF material choices range from electrospun polymers such as poly(L-lactic acid) (PLLA) or poly(caprolactone) (PCL), demineralized bone gelatin, lamellar silk scaffolds, or collagen gels[111-126]. The choices for NP scaffolds include hyaluronic acid (HA), alginate, or agarose, all soft gel cores for the composite discs. Cell sources vary with regards to organism, ranging from human to bovine, porcine, leporine, etc., but all scaffolds are seeded with either primary IVD cells (AF or NP for their respective regions), chondrocytes, or MSCs. Certain groups also supplement the culture of their constructs by adding matrix components: in the case of Nesti et al., for example, cells were cultured in transforming growth factor-β (TGF-β) for almost a month in order to induce chondrogenesis[116].

The first *in vivo* study assessing the feasibility of a whole disc construct was executed in 2011 by our group in a rat caudal spine model[120,127-129]. The disc dimensions were determined based on parameters obtained from MRI and micro-computed tomography (μCT) images, then cultured and implanted in the rat spines for up to 6 months. Results indicated that the discs had integrated well with the host tissue, maintaining disc height and depositing ECM markers as indicated by biochemical analyses. Since then other groups have also utilized small animal *in vivo* models to show the efficacy of their designs, demonstrating comparable biochemical and biomechanical properties, as well as cell morphology, following implantation and subsequent tissue integration.

Despite the usefulness of small animal models as high-throughput systems for analyzing feasibility, they are extremely limited with regards to anatomy and disc geometry, as well as loading patterns. Rat IVDs, for example, are smaller and much

more permeable than those of humans and display progressive recovery over a short period of time[120,130]. As such, they are not a reliable model for clinical translation. More clinically relevant large animal models have subsequently been utilized in *in vivo* trials of TE-IVDs. In 2017 our group applied our findings from the rat model to the canine cervical spine due to a comparable loading profile to that seen in humans[123], as well as the fact that beagles are prone to spontaneous disc degeneration[131] and are actively treated for the disease. We observed a maintenance of disc height and hydration for the 16 week period, along with proteoglycan- and collagen-rich ECM deposition. We also noted that constructs at certain cervical levels were displaced immediately, most likely due to mechanical stresses varying between levels[132]. Work done by Gullbrand et al. utilized a goat cervical model to examine their own composite disc designs, as goats are an established model for spine research given comparable disc dimensions as well as a somewhat upright posture[125]. Following 8 weeks in culture their TE-IVDs also demonstrated structural, biochemical, and biomechanical behavior akin to their native counterparts.

Although these models are well-characterized and have yielded significant insight into IVD repair, there are still significant differences—both mechanically and anatomically—from the human spine. As a result, there exists the need to develop and investigate further large animal *in vivo* models that are more anatomically similar, and therefore more clinically relevant, than those currently used in scientific research in the hopes of addressing some of the challenges in translating to human models.

Authors (Year)	AF Material	NP Material	Cell Types	Type of Study	Animal Model	In Vivo Duration	Summary of Findings
Mizuno et al (2004, 2006)	PGA/PLA	Alginate	Ovine AF/NP cells	In vitro	N/A	N/A	First synthetic composite disc. Morphologically/histologically resembled native discs, with comparable biochemical markers.
Nesti et al (2008)	PLLA/HA	HA	Adult human MSC's	In vitro	N/A	N/A	First electrospun disc scaffold. Discs replicated AF micro-architecture while cells developed a chondrogenic phenotype in a time-dependent manner.
Nerurkar et al (2009-10)	PCL	Agarose	Bovine MSC's	In vitro	N/A	N/A	Discs had comparable mechanical properties to native values, though lesser in magnitude, and replicated AF architecture.
Bowles et al (2010-11)	Collagen I	Alginate	Ovine AF/NP cells	In vitro + in vivo	Rat caudal	6 months	First in vivo composite disc study. Host tissue integration, with maintained disc space height and secretion of matrix components. Comparable biochemical and mechanical properties to native values.
Zhuang et al (2011)	Demineralized bone matrix gelatin	Collagen (II) / hyaluronate / chondroitin-6-sulfate	Rabbit AF/NP cells	In vitro	N/A	N/A	Constructs morphologically/ histologically resembled native discs, with tissue formation and integration. Biochemical content also resembled native values.
Park et al (2012)	Silk protein	Fibrin/HA	Porcine AF cells / chondrocytes	In vitro	N/A	N/A	Lamellar scaffolds promoted AF/NP integration and native-like biochemical content compared to porous scaffolds.
Bowles et al (2012)	Collagen I	Alginate	Ovine AF/NP cells	In vivo	Rat lumbar	16 weeks	50% integrated with host tissue, maintained disc height, and deposited collagen- and proteoglycan-rich matrix. Failure likely a result of lumbar spine's complex loading profile compared to caudal.
Martin et al (2014, 2017)	PCL	Agarose	Bovine MSC's	In vivo	Rat caudal	5 weeks	External fixators and polymer:vertebrae interface minimized proteoglycan loss, driving integration and maintaining mechanical properties.
Moriguchi et al (2017)	Collagen I	Alginate	Canine AF/NP cells	In vivo	Canine cervical	16 weeks	Stably implanted discs maintained disc space height and hydration, deposited collagen- and proteoglycan-rich matrix.
Gullbrand et al (2018)	PCL	Agarose or HA	Bovine AF/NP cells	In vivo	Goat cervical	8 weeks	Similar results to previous rat model: maintained structure and achieved near-native mechanical properties.
Kim et al (2020)	PCL	HA	Bovine MSC's or bovine AF/NP cells	In vivo	Rat caudal	5 weeks	Both cell types behaved similarly and maintained structure throughout culture.

Table 1.1 Summary of *in vivo* and *in vitro* composite TE-IVD approaches. Table adapted from Kirnaz, et al.[115]

Research Objectives

The primary goals of this dissertation were to augment fiber orientation in TE-IVD constructs, determine the effect of diabetic hyperglycemia on the developing IVD, and characterize a support structure for ease of implantation in the porcine cervical spine. The primary hypotheses examined in this project were: (1) physiologic levels of glucose will guide optimal fiber formation and enhance mechanical properties in engineered constructs (Chapter 2), (2) super-physiologic levels of glucose disrupt the integrity of the young disc by interfering with mechanics, ECM composition, and fiber formation (Chapter 3), and (3) supplementing TE-IVDs with a resorbable delivery vehicle will stabilize the motion segment and provide sufficient mechanical support to enable proper tissue integration (Chapter 4).

Specific Aims

Specific Aim 1 (Chapter 2)

Evaluate the effect of glucose concentration on fiber morphology in the AF and overall biomechanics of composite TE-IVDs

Ovine MSCs were used to generate composite TE-IVDs, which were then cultured for four weeks in media glucose concentrations ranging from sub-physiologic (125, 250 mg/L), physiologic (500, 1000 mg/L), and super-physiologic (4500 mg/L) before being subjected to *in vitro* analysis of structural, compositional, and mechanical changes. Throughout culture the 4500 mg/L group was shown to be consistently glucose-saturated, consuming 50-60% of available glucose supply in comparison to the 85-100% consumed in the other groups. All groups demonstrated cellular remodeling throughout culture regardless of glucose status, with no significant differences in either DNA or collagen content, indicating consistent activity and health of the cellular population. Increasing glucose concentrations corresponded to an increase in sulfated

glycosaminoglycan (s-GAG) content, with the 4500 mg/L group (2.02 μg/mg) demonstrating a two-fold increase over the 125 mg/L group (0.99 μg/mg). Qualitative and quantitative analysis of fiber organization in the AF region indicated that by the end of the culture period, the 500 mg/L group showed the highest degree of alignment with a fiber alignment (FA) index of 1.30. Directionality decreased in the 125, 250, and 4500 mg/L groups, which all showed comparably disorganized fibers and FA indices of about 1.15-1.16, while the 1000 mg/L group showed slightly more alignment in comparison with an index of 1.19. These trends in fiber alignment were mirrored in mechanical characterization, with the 500 mg/L group demonstrating the highest equilibrium modulus at 27.3 kPa as compared to 10.9 and 15.8 kPa for the 125 and 4500 mg/L groups, respectively. Equilibrium modulus showed a stronger correlation with FA index as compared to GAG content, indicating that structure rather than composition ultimately drives optimal mechanics in engineered IVDs.

Specific Aim 2 (Chapter 3)

Investigate the effect of diabetic hyperglycemia on fiber organization and mechanical behavior in developing IVDs taken from the mouse caudal spine

Whole discs were collected from the caudal spines of db/db and db/+ mice for use in biochemical, histological, and mechanical analysis. Diabetic mice demonstrated a fasting blood glucose level of 263.6 mg/dL as compared to 52.1 mg/dL in their wild type counterparts. Both s-GAG and collagen content were higher in the diabetic discs, while DNA content was higher in the wild type. Qualitative and quantitative morphological differences were present in gross histological images taken from each group. The NP region in the diabetic discs was larger (by 29.0%) and more oval in shape than the wild type, with an irregular NP/AF boundary. Safranin-O staining for proteoglycan content extended further into the inner AF region in the diabetics than in

the wild type, occupying 65.8% and 55.0% of the whole disc area, respectively. Fiber organization at the AF/NP border was more disorganized and less aligned in the diabetic discs, with a flatter overall fiber orientation distribution as compared to the bimodal distribution attributed to the wild type. In response to both dynamic and compressive mechanical tests, diabetic discs demonstrated an approximately two-fold increase in resistance to deformation and took twice as long to recover from said deformation. These observations indicate that diabetes has a detrimental effect on the disc as early as development, altering ECM composition and ultimately impeding proper fiber formation and mechanical behavior.

Specific Aim 3 (Chapter 4)

Design and validate a biodegradable support structure to enhance mechanical stability of TE-IVDs prior to implantation in an in vivo porcine model

Göttingen minipigs were chosen as a new *in vivo* large animal model to address geometrical issues with a previous canine model. 3D-printed poly(lactic acid) (PLA) cage constructs were developed to facilitate delivery and implantation of composite TE-IVDs given the complex loading patterns inherent in the spines of larger animals. One- and two-piece designs were generated based on disc dimensions for the C3/4 and C5/6 levels in the porcine cervical spine, then subjected to mechanical testing for validation. One-piece designs were able to withstand uniformly applied stresses of up to 134 MPa, almost 70 times higher than what is seen *in vivo* in the human cervical spine. While both designs were successfully implanted and maintained disc height immediately post-operatively, two-piece designs demonstrated a 63.67% decrease in disc height index (DHI) and complete collapse of the disc space at the first follow-up. One-piece designs implanted at C3/4 and C5/6 remained stable for the four week study duration, with DHI decreasing 13.6% and 39.7% at these levels, respectively. Post-sacrificial analysis

revealed all implants were consistently damaged in the posterior region, regardless of design or experimental level. Reconstruction of the porcine cervical spine indicates endplate geometry, not material integrity, is responsible for structural failure: repetitive loading from a bony process in the posterior region of the vertebrae led to the cages fragmenting. Though additional investigation of prototypes is necessary prior to *in vivo* implementation of the cage in conjunction with the TE-IVDs, construct fabrication was successfully adapted for the culture of discs within the cages. These data suggest that with design modifications to account for the Göttingen minipig cervical spine anatomy, a resorbable cage for TE-IVDs could stabilize the motion segment and provide sufficient mechanical support for the soft construct to enable proper tissue integration and restoration of native biomechanical and biochemical properties.

REFERENCES

[1] Pattappa G, Li Z, Peroglio M, Wismer N, Alini M, Grad S. Diversity of intervertebral disc cells: phenotype and function. *J Anat*. 2012;221(6):480-496.

[2] Humzah MD, Soames RW. Human intervertebral disc: structure and function. *Anat Rec*. 1988;220(4):337-356.

[3] Moore RJ. The vertebral end-plate: what do we know? *Eur Spine J*. 2000;9(2):92-96.

[4] Smith LJ, Nerurkar NL, Choi KS, Harfe BD, Elliott DM. Degeneration and regeneration of the intervertebral disc: lessons from development. *Dis Model Mech*. 2011;4(1):31-41.

[5] Buckwalter JA. Aging and degeneration of the human intervertebral disc. *Spine (Phila Pa 1976)*. 1995;20(11):1307-1314.

[6] Coventry MB. Anatomy of the intervertebral disk. *Clin Orthop Relat Res*. 1969;67:9-15.

[7] Antoniou J, Steffen T, Nelson F, Winterbottom N, Hollander AP, Poole RA, Aebi M, Alini M. The human lumbar intervertebral disc: evidence for changes in the biosynthesis and denaturation of the extracellular matrix with growth, maturation, ageing, and degeneration. *J Clin Invest*. 1996;98(4):996-1003.

[8] Kraemer J, Kolditz D, Gowin R. Water and electrolyte content of human intervertebral discs under variable load. *Spine (Phila Pa 1976)*. 1985;10(1):69-71.

[9] Newell N, Little JP, Christou A, Adams MA, Adam CJ, Masouros SD. Biomechanics of the human intervertebral disc: A review of testing techniques and results. *J Mech Behav Biomed Mater*. 2017;69:420-434.

[10] Dickson IR, Happey F, Pearson CH, Naylor A, Turner RL. Variations in the protein components of human intervertebral disk with age. *Nature*. 1967;215(5096):52-53.

[11] Iatridis JC, Weidenbaum M, Setton LA, Mow VC. Is the nucleus pulposus a solid or a fluid? Mechanical behaviors of the nucleus pulposus of the human intervertebral disc. *Spine (Phila Pa 1976)*. 1996;21(10):1174-84.

[12] McDevitt, Cahir A. "Proteoglycans of the intervertebral disc." *The Biology of the Intervertebral Disc. Boca Raton, Fla* (1988).

[13] Eyre DR, Muir H. Types I and II collagens in intervertebral disc. Interchanging radial distributions in annulus fibrosus. *Biochem J*. 1976;157(1):267-270.

[14] Eyre, David R. "Collagens of the disc." *Biology of* (1988).

[15] Singh K, Masuda K, Thonar EJ, An HS, Cs-Szabo G. Age-related changes in the extracellular matrix of nucleus pulposus and anulus fibrosus of human intervertebral disc. *Spine (Phila Pa 1976)*. 2009;34(1):10-16.

[16] Lipson SJ, Muir H. Experimental intervertebral disc degeneration: morphologic and proteoglycan changes over time. *Arthritis Rheum*. 1981;24:12–21.

[17] Melching LI, Cs-Szabo G, Roughley PJ. Analysis of proteoglycan messages in human articular cartilage by a competitive PCR technique. *Matrix Biol*. 1997;16:1–11.

[18] Melrose J, Ghosh P, Taylor TK. A comparative analysis of the differential spatial and temporal distributions of the large (aggrecan, versican) and small (decorin, biglycan, fibromodulin) proteoglycans of the intervertebral disc. *J Anat*. 2001;198(Pt 1):3-15.

[19] Urban JP, Roberts S. Degeneration of the intervertebral disc. *Arthritis Res Ther*. 2003;5(3):120-130.

[20] Richardson SM, Mobasheri A, Freemont AJ, Hoyland JA. Intervertebral disc biology, degeneration and novel tissue engineering and regenerative medicine therapies. *Histol Histopathol*. 2007;22(9):1033-1041.

[21] Kiani C, Chen L, Wu YJ, Yee AJ, Yang BB. Structure and function of aggrecan. *Cell Res*. 2002;12(1):19-32.

[22] Iozzo RV, Schaefer L. Proteoglycan form and function: A comprehensive nomenclature of proteoglycans. *Matrix Biol*. 2015;42:11-55.

[23] Iozzo RV, Murdoch AD. Proteoglycans of the extracellular environment: clues from the gene and protein side offer novel perspectives in molecular diversity and function. *FASEB J*. 1996;10(5):598-614.

[24] Götz W, Barnert S, Bertagnoli R, Miosge N, Kresse H, Herken R. Immunohistochemical localization of the small proteoglycans decorin and biglycan in human intervertebral discs. *Cell Tissue Res*. 1997;289:185-190.

[25] Hildebrand A, Romarís M, Rasmussen LM, Heinegård D, Twardzik DR, Border WA, Ruoslahti E. Interaction of the small interstitial proteoglycans biglycan, decorin and fibromodulin with transforming growth factor beta. *Biochem J*. 1994;302(Pt 2):527-534.

[26] Heinegård D, Aspberg A, Franzén A, Lorenzo P. (2002). Chapter 4 - Glycosylated Matrix Proteins. In: Royce PM, Steinmann, B, eds. *Connective Tissue and Its Heritable*

Disorders: Molecular, Genetic, and Medical Aspects. 2nd Ed. Wiley-Liss; 2002:271-291.

[27] Gruber HE, Fisher EC Jr, Desai B, Stasky AA, Hoelscher G, Hanley EN Jr. Human intervertebral disc cells from the annulus: threedimensional culture in agarose or alginate and responsiveness to TGF-beta1. *Exp Cell Res*. 1997;235:13-21.
[28] Lyons G, Eisenstein SM, Sweet MB. Biochemical changes in intervertebral disc degeneration. *Biochim Biophys Acta*. 1981;673(4):443-453.

[29] Marcolongo M, Sarkar S, Ganesh, N. In: Ducheyne P, eds. 7.11 Trends in Materials for Spine Surgery. *Comprehensive Biomaterials II*. Elsevier; 2017:175-198.

[30] Marchand F, Ahmed AM. Investigation of the laminate structure of lumbar disc anulus fibrosus. *Spine (Phila Pa 1976)*. 1990;15(5):402-10.

[31] Baldit A. 11 - Micromechanics of the Intervertebral Disk. In: Ganghoff J-F, eds. *Multiscale Biomechanics*. Elsevier; 2018:455-467.

[32] Alonso F, Hart DJ. Intervertebral Disk. In: Aminoff MJ, Daroff RB, eds. *Encyclopedia of the Neurological Sciences*. 2nd ed. Academic Press; 2014:724-729.

[33] Yu J, Winlove PC, Roberts S, Urban JP. Elastic fibre organization in the intervertebral discs of the bovine tail. *J Anat*. 2002;201(6):465-475.

[34] Yu J, Fairbank JC, Roberts S, Urban JP. *Spine (Phila Pa 1976)*. 2005; 30(16):1815-1820.

[35] Peacock A. Observations on the prenatal development of the intervertebral disc in man. *J Anat*. 1951;85:260–274.

[36] Peacock A. Observations on the postnatal structure of the intervertebral disc in man. *J Anat*. 1952;86:162–179.

[37] Cassidy JJ, Hiltner A, Baer E. Hierarchical structure of the intervertebral disc. *Connect Tissue Res*. 1989;23(1):75-88.

[38] Hayes AJ, Isaacs MD, Hughes C, Caterson B, Ralphs JR. Collagen fibrillogenesis in the development of the annulus fibrosus of the intervertebral disc. *Eur Cell Mater*. 2011;22:226-241.

[39] Adams MA, Roughley PJ. What is intervertebral disc degeneration, and what causes it? *Spine (Phila Pa 1976)*. 2006;31(18):2151-61.

[40] DeLucca JF, Cortes DH, Jacobs NT, Vresilovic EJ, Duncan RL, Elliott DM. Human cartilage endplate permeability varies with degeneration and intervertebral disc site. *J Biomech*. 2016;49(4):550-557.

[41] Rajasekaran S, Babu JN, Arun R, Armstrong BR, Shetty AP, Murugan S. ISSLS prize winner: A study of diffusion in human lumbar discs: a serial magnetic resonance imaging study documenting the influence of the endplate on diffusion in normal and degenerate discs. *Spine (Phila Pa 1976)*. 2004;29(23):2654-2667.

[42] Grant MP, Epure LM, Bokhari R, Roughley P, Antoniou J, Mwale F. Human cartilaginous endplate degeneration is induced by calcium and the extracellular calcium-sensing receptor in the intervertebral disc. *Eur Cell Mater*. 2016;32:137-51.

[43] Moon SM, Yoder JH, Wright AC, Smith LJ, Vresilovic EJ, Elliott DM. Evaluation of intervertebral disc cartilaginous endplate structure using magnetic resonance imaging. *Eur Spine J*. 2013;22(8):1820-1828.

[44] Liu MH, Sun C, Yao Y, Fan X, Liu H, Cui YH, Bian XW, Huang B, Zhou Y. Matrix stiffness promotes cartilage endplate chondrocyte calcification in disc degeneration via miR-20a targeting ANKH expression. *Sci Rep*. 2016;6:25401.

[45] Maroudas A, Stockwell RA, Nachemson A, Urban J. Factors involved in the nutrition of the human lumbar intervertebral disc: cellularity and diffusion of glucose in vitro. *J Anat*. 1975;120(Pt 1):113-130.

[46] Bruehlmann SB, Rattner JB, Matyas JR, Duncan NA. Regional variations in the cellular matrix of the annulus fibrosus of the intervertebral disc. *J Anat*. 2002;201(2):159-171.

[47] Trout JJ, Buckwalter JA, Moore KC, Landas SK. Ultrastructure of the human intervertebral disc. I. Changes in notochordal cells with age. *Tissue Cell*. 1982;14(2):359-369.

[48] Hunter CJ, Matyas JR, Duncan NA. The notochordal cell in the nucleus pulposus: a review in the context of tissue engineering. *Tissue Eng*. 2003;9(4):667-677.

[49] Errington RJ, Puustjarvi K, White IR, Roberts S, Urban JP. Characterisation of cytoplasm-filled processes in cells of the intervertebral disc. *J Anat*. 1998;192 (Pt 3):369-378.

[50] Hastreiter D, Ozuna RM, Spector M. Regional variations in certain cellular characteristics in human lumbar intervertebral discs, including the presence of alpha-smooth muscle actin. *J Orthop Res*. 2001;19(4):597-604.

[51] Roughley PJ. Biology of intervertebral disc aging and degeneration: involvement of the extracellular matrix. *Spine (Phila Pa 1976)*. 2004;29:2691-2699.

[52] Keyes DC, Compere EL. The Normal and Pathological Physiology of the Nucleus Pulposus of the Intervertebral Disc. *J Bone Jt Surg*. 1932;14:897-935.

[53] McNally DS, Adams MA, Goodship AE. Development and validation of a new transducer for intradiscal pressure measurement. *J Biomed Eng*. 1992;14(6):495-498.

[54] Wilke HJ, Neef P, Caimi M, Hoogland T, Claes LE. New in vivo measurements of pressures in the intervertebral disc in daily life. *Spine (Phila Pa 1976)*. 1999;24(8):755-762.

[55] Nachemson A, Morris JM. Lumbar discometry. Lumbar intradiscal pressure measurements in vivo. *Lancet*. 1963;1(7291):1140-1142.

[56] Nachemson A, Morris JM. In Vivo Measurements of Intradiscal Pressure. Discometry, A Method for the Determination of Pressure in the Lower Lumbar Discs. *J Bone Joint Surg Am*. 1964;46:1077-1092.

[57] Sato K, Kikuchi S, Yonezawa T. In vivo intradiscal pressure measurement in healthy individuals and in patients with ongoing back problems. *Spine (Phila Pa 1976)*. 1999;24(23):2468-2474.

[58] Smolders LA, Forterre F. In: Fingeroth JM, Thomas WB, eds. Biomechanics of the Intervertebral Disc and Why Do Discs Displace? *Advances in Intervertebral Disc Disease in Dogs and Cats*. Wiley;2015.

[59] Brinckmann P, Frobin W, Hierholzer E, Horst M. Deformation of the vertebral end-plate under axial loading of the spine. *Spine (Phila Pa 1976)*. 1983;8(8):851-856.

[60] Holmes AD, Hukins DW, Freemont AJ. End-plate displacement during compression of lumbar vertebra-disc-vertebra segments and the mechanism of failure. *Spine (Phila Pa 1976)*. 1993;18(1):128-135.

[61] Fleming A, Keynes RJ, Tannahill D. The role of the notochord in vertebral column formation. *J Anat*. 2001;199(Pt 1-2):177-180.

[62] Walmsley R. The development and growth of the intervertebral disc. *Edinb Med J*. 1953;60(8):341-364.

[63] Bilezikian JP, Raisz LG, Rodan GA, Karaplis AC. In: Karaplis AC, eds. Embryonic development of bone and the molecular regulation of intramembranous and endochondral bone formation. *Principles of Bone Biology*. Academic Press; 2002:53-84

[64] Hunter CJ, Matyas JR, Duncan NA. The notochordal cell in the nucleus pulposus: a review in the context of tissue engineering. *Tissue Eng*. 2003;9(4):667-677.

[65] Stemple DL. Structure and function of the notochord: an essential organ for chordate development. *Development*. 2005;132(11):2503-2512.

[66] Aszódi A, Chan D, Hunziker E, Bateman JF, Fässler R. Collagen II is essential for the removal of the notochord and the formation of intervertebral discs. *J Cell Biol*. 1998;143(5):1399-1412.

[67] Pazzaglia UE, Salisbury JR, Byers PD. Development and involution of the notochord in the human spine. *J R Soc Med*. 1989;82(7):413-415.

[68] Lawson LY, Harfe BD. Developmental mechanisms of intervertebral disc and vertebral column formation. *Wiley Interdiscip Rev Dev Biol*. 2017;6(6).

[69] Colombier P, Clouet J, Hamel O, Lescaudron L, Guicheux J. The lumbar intervertebral disc: from embryonic development to degeneration. *Joint Bone Spine*. 2014;81(2):125-129.

[70] Kelleher CM, McLean SE, Mecham RP. Vascular extracellular matrix and aortic development. *Curr Top Dev Biol*. 2004;62:153-188.

[71] Banos CC, Thomas AH, Kuo CK. Collagen fibrillogenesis in tendon development: current models and regulation of fibril assembly. *Birth Defects Res C Embryo Today*. 2008;84(3):228-244.

[72] Kalamajski S, Oldberg A. The role of small leucine-rich proteoglycans in collagen fibrillogenesis. *Matrix Biol*. 2010;29(4):248-253.

[73] Molinos M, Almeida CR, Caldeira J, Cunha C, Gonçalves RM, Barbosa MA. Inflammation in intervertebral disc degeneration and regeneration [published correction appears in J R Soc Interface. 2015 Jul 6;12(108):20150429]. *J R Soc Interface*. 2015;12(104):20141191.

[74] Luoma K, Riihimäki H, Luukkonen R, Raininko R, Viikari-Juntura E, Lamminen A. Low back pain in relation to lumbar disc degeneration. *Spine (Phila Pa 1976)*. 2000;25(4):487-492.

[75] Kos N, Gradisnik L, Velnar T. A Brief Review of the Degenerative Intervertebral Disc Disease. *Med Arch*. 2019;73(6):421-424.

[76] Medical Advisory Secretariat. Artificial discs for lumbar and cervical degenerative disc disease–update: an evidence-based analysis. Ontario Health Technology Assessment Series 2006; 6(10).

[77] Teraguchi M, Yoshimura N, Hashizume H, Muraki S, Yamada H, Minamide A, Oka H, Ishimoto Y, Nagata K, Kagotani R, Takiguchi N, Akune T, Kawaguchi H, Nakamura K, Yoshida M. Prevalence and distribution of intervertebral disc degeneration over the entire spine in a population-based cohort: the Wakayama Spine Study. *Osteoarthritis Cartilage*. 2014;22(1):104-110.

[78] Colombini A, Lombardi G, Corsi MM, Banfi G. Pathophysiology of the human intervertebral disc. *Int J Biochem Cell Biol*. 2008;40(5):837-842.

[79] Dowdell J, Erwin M, Choma T, Vaccaro A, Iatridis J, Cho SK. Intervertebral Disk Degeneration and Repair. *Neurosurgery*. 2017;80(3S):S46-S54.

[80] Grignon B, Grignon Y, Mainard D, Braun M, Netter P, Roland J. The structure of the cartilaginous end-plates in elder people. *Surg Radiol Anat*. 2000;22(1):13-9.

[81] Cannata F, Vadalà G, Ambrosio L, Fallucca S, Napoli N, Papalia R, Pozzilli P, Denaro V. Intervertebral disc degeneration: A focus on obesity and type 2 diabetes. *Diabetes Metab Res Rev*. 2020;36(1):e3224.

[82] Alpantaki K, Kampouroglou A, Koutserimpas C, Effraimidis G, Hadjipavlou A. Diabetes mellitus as a risk factor for intervertebral disc degeneration: a critical review. *Eur Spine J*. 2019;28(9):2129-2144.

[83] Li X, Liu X, Wang Y, Cao F, Chen Z, Hu Z, Yu B, Feng H, Ba Z, Liu T, Li H, Jiang B, Huang Y, Li L, Wu D. Intervertebral disc degeneration in mice with type II diabetes induced by leptin receptor deficiency. *BMC Musculoskelet Disord*. 2020;21(1):77.

[84] Zhang Y, Proenca R, Maffei M, Barone M, Leopold L, Friedman JM. Positional cloning of the mouse obese gene and its human homologue [published correction appears in Nature 1995 Mar 30;374(6521):479]. *Nature*. 1994;372(6505):425-432.

[85] Kivimäki M, Virtanen M, Kawachi I, Nyberg ST, Alfredsson L, Batty GD, Bjorner JB, Borritz M, Brunner EJ, Burr H, Dragano N, Ferrie JE, Fransson EI, Hamer M, Heikkilä K, Knutsson A, Koskenvuo M, Madsen IEH, Nielsen ML, Nordin M, Oksanen T, Pejtersen JH, Pentti J, Rugulies R, Salo P, Siegrist J, Steptoe A, Suominen S, Theorell T, Vahtera J, Westerholm PJM, Westerlund H, Singh-Manoux A, Jokela M. Long working hours, socioeconomic status, and the risk of incident type 2 diabetes: a meta-analysis of published and unpublished data from 222 120 individuals. *Lancet Diabetes Endocrinol*. 2015;3(1):27-34.

[86] Jakoi AM, Pannu G, D'Oro A, Buser Z, Pham MH, Patel NN, Hsieh PC, Liu JC, Acosta FL, Hah R, Wang JC. The Clinical Correlations between Diabetes, Cigarette Smoking and Obesity on Intervertebral Degenerative Disc Disease of the Lumbar Spine. *Asian Spine J*. 2017;11(3):337-347.

[87] Sakellaridis N. The influence of diabetes mellitus on lumbar intervertebral disk herniation. *Surg Neurol*. 2006;66(2):152-154.

[88] Anekstein Y, Smorgick Y, Lotan R, Agar G, Shalmon E, Floman Y, Mirovsky Y. Diabetes mellitus as a risk factor for the development of lumbar spinal stenosis. *Isr Med Assoc J*. 2010;12(1):16-20.

[89] Teraguchi M, Yoshimura N, Hashizume H, Muraki S, Yamada H, Minamide A, Oka H, Ishimoto Y, Nagata K, Kagotani R, Takiguchi N, Akune T, Kawaguchi H, Nakamura K, Yoshida M. Prevalence and distribution of intervertebral disc degeneration over the entire spine in a population-based cohort: the Wakayama Spine Study. *Osteoarthritis Cartilage*. 2014;22(1):104-110.

[90] Mobbs RJ, Newcombe RL, Chandran KN. Lumbar discectomy and the diabetic patient: incidence and outcome. J Clin Neurosci. 2001;8(1):10-13

[91] Mahmoud M, Kokozidou M, Auffarth A, Schulze-Tanzil G. The Relationship between Diabetes Mellitus Type II and Intervertebral Disc Degeneration in Diabetic Rodent Models: A Systematic and Comprehensive Review. *Cells*. 2020;9(10):2208.

[92] Wang J, Hu J, Chen X, Huang C, Lin J, Shao Z, Gu M, Wu Y, Tian N, Gao W, Zhou Y, Wang X, Zhang X. BRD4 inhibition regulates MAPK, NF-κB signals, and autophagy to suppress MMP-13 expression in diabetic intervertebral disc degeneration. *FASEB J*. 2019;33(10):11555-11566.

[93] Jiang L, Zhang X, Zheng X, Ru A, Ni X, Wu Y, Tian N, Huang Y, Xue E, Wang X, Xu H.. Apoptosis, senescence, and autophagy in rat nucleus pulposus cells: Implications for diabetic intervertebral disc degeneration. *J Orthop Res*. 2013;31(5):692-702.

[94] Lee YC, Zotti MG, Osti OL. Operative Management of Lumbar Degenerative Disc Disease. *Asian Spine J*. 2016;10(4):801-819.

[95] Wu TK, Wang BY, Meng Y, Ding C, Yang Y, Lou JG, Liu H. Multilevel cervical disc replacement versus multilevel anterior discectomy and fusion: A meta-analysis. *Medicine (Baltimore)*. 2017;96(16):e6503.

[96] Frelinghuysen P, Huang RC, Girardi FP, Cammisa FP Jr. Lumbar total disc replacement part I: rationale, biomechanics, and implant types. *Orthop Clin North Am*. 2005;36(3):293-299.

[97] Blumenthal S, McAfee PC, Guyer RD, Hochschuler SH, Geisler FH, Holt RT, Garcia R Jr, Regan JJ, Ohnmeiss DD. A prospective, randomized, multicenter Food and Drug Administration investigational device exemptions study of lumbar total disc replacement with the CHARITE artificial disc versus lumbar fusion: part I: evaluation of clinical outcomes. *Spine (Phila Pa 1976)*. 2005;30(14):1565-75; discussion E387-91.

[98] Salzmann SN, Plais N, Shue J, Girardi FP. Lumbar disc replacement surgery-successes and obstacles to widespread adoption. *Curr Rev Musculoskelet Med*. 2017;10(2):153-159.

[99] Setton LA, Bonassar LJ, Masuda K. Regeneration and replacement of the intervertebral disc. In: Robert L, Robert L, Joseph V, eds. *Principles of Tissue Engineering*. 3rd ed. Boston: Elsevier Academic Press. 2007;877-96.

[100] van Uden S, Silva-Correia J, Oliveira JM, Reis RL. Current strategies for treatment of intervertebral disc degeneration: substitution and regeneration possibilities. *Biomater Res*. 2017;21:22.

[101] Tendulkar G, Chen T, Ehnert S, Kaps HP, Nüssler AK. Intervertebral Disc Nucleus Repair: Hype or Hope? *Int J Mol Sci*. 2019;20(15):3622.

[102] Schmitz TC, Salzer E, Crispim JF, Fabra GT, LeVisage C, Pandit A, Tryfonidou M, Maitre CL, Ito K. Characterization of biomaterials intended for use in the nucleus pulposus of degenerated intervertebral discs. *Acta Biomater*. 2020;114:1-15.

[103] Guterl CC, See EY, Blanquer SB, Pandit A, Ferguson SJ, Benneker LM, Grijpma DW, Sakai D, Eglin D, Alini M, Iatridis JC, Grad S. Challenges and strategies in the repair of ruptured annulus fibrosus. *Eur Cell Mater*. 2013;25:1-21.

[104] Veres SP, Robertson PA, Broom ND. ISSLS prize winner: microstructure and mechanical disruption of the lumbar disc annulus: part II: how the annulus fails under hydrostatic pressure. *Spine (Phila Pa 1976)*. 2008; 33:2711–2720.

[105] Thompson RE, Pearcy MJ, Downing KJ, Manthey BA, Parkinson IH, Fazzalari NL. Disc lesions and the mechanics of the intervertebral joint complex. *Spine (Phila Pa 1976)*. 2000; 25:3026–3035.

[106] Sloan SR Jr, Lintz M, Hussain I, Hartl R, Bonassar LJ. Biologic Annulus Fibrosus Repair: A Review of Preclinical In Vivo Investigations. *Tissue Eng Part B Rev*. 2018;24(3):179-190.

[107] Bron JL, van der Veen AJ, Helder MN, van Royen BJ, Smit TH. Biomechanical and in vivo evaluation of experimental closure devices of the annulus fibrosus designed for a goat nucleus replacement model. *Eur Spine J*. 2010;19(8):1347-1355.

[108] Bateman AH, Balkovec C, Akens MK, Chan AH, Harrison RD, Oakden W, Yee AJ, McGill SM. Closure of the annulus fibrosus of the intervertebral disc using a novel suture application device-in vivo porcine and ex vivo biomechanical evaluation. *Spine J*. 2016;16(7):889-895.

[109] Wang YH, Kuo TF, Wang JL. The implantation of non-cell-based materials to prevent the recurrent disc herniation: an in vivo porcine model using quantitative discomanometry examination. *Eur Spine J*. 2007;16(7):1021-1027.

[110] Sloan SR Jr, Wipplinger C, Kirnaz S, Navarro-Ramirez R, Schmidt F, McCloskey D, Pannellini T, Schiavinato A, Härtl R, Bonassar LJ. Combined nucleus pulposus augmentation and annulus fibrosus repair prevents acute intervertebral disc degeneration after discectomy. *Sci Transl Med*. 2020;12(534):eaay2380.

[111] Mizuno H, Roy AK, Vacanti CA, Kojima K, Ueda M, Bonassar LJ. Tissue-engineered composites of anulus fibrosus and nucleus pulposus for intervertebral disc replacement. *Spine (Phila Pa 1976)*. 2004;29(12):1290-1298.

[112] Mizuno H, Roy AK, Zaporojan V, Vacanti CA, Ueda M, Bonassar LJ. Biomechanical and biochemical characterization of composite tissue-engineered intervertebral discs. *Biomaterials*. 2006;27(3):362-370.

[113] Nerurkar NL, Sen S, Huang AH, Elliott DM, Mauck RL. Engineered disc-like angle-ply structures for intervertebral disc replacement. *Spine (Phila Pa 1976)*. 2010;35(8):867-873.

[114] Park SH, Gil ES, Cho H, Mandal BB, Tien LW, Min BH, Kaplan DL. Intervertebral disk tissue engineering using biphasic silk composite scaffolds. *Tissue Eng Part A*. 2012;18(5-6):447-458.

[115] Kirnaz S, Singh S, Lintz M, Goldberg JL, McGrath L, Medary B, Sommer F, Bonassar LJ, Härtl R. Innovative Biological Approaches for Treatment of Degenerative Disc Disease: A Literature Review of In Vivo Animal and Clinical Data. In press, 2021.

[116] Nesti LJ, Li WJ, Shanti RM, Jiang YJ, Jackson W, Freedman BA, Kuklo TR, Giuliani JR, Tuan RS. Intervertebral disc tissue engineering using a novel hyaluronic acid-nanofibrous scaffold (HANFS) amalgam. *Tissue Eng Part A*. 2008;14(9):1527-1537.

[117] Chang G, Kim HJ, Kaplan D, Vunjak-Novakovic G, Kandel RA. Porous silk scaffolds can be used for tissue engineering annulus fibrosus. *Eur Spine J*. 2007;16(11):1848-1857.

[118] Zhuang Y, Huang B, Li CQ, Liu LT, Pan Y, Zheng WJ, Luo G, Zhou Y. Construction of tissue-engineered composite intervertebral disc and preliminary morphological and biochemical evaluation. *Biochem Biophys Res Commun*. 2011;407(2):327-332.

[119] Bowles RD, Williams RM, Zipfel WR, Bonassar LJ. Self-assembly of aligned tissue-engineered annulus fibrosus and intervertebral disc composite via collagen gel contraction. *Tissue Eng Part A*. 2010;16(4):1339-1348.

[120] Bowles RD, Gebhard HH, Härtl R, Bonassar LJ. Tissue-engineered intervertebral discs produce new matrix, maintain disc height, and restore biomechanical function to the rodent spine. *Proc Natl Acad Sci U S A*. 2011;108(32):13106-13111.

[121] Bowles RD, Gebhard HH, Dyke JP, Ballon DJ, Tomasino A, Cunningham ME, Härtl R, Bonassar, LJ. Image-based tissue engineering of a total intervertebral disc implant for restoration of function to the rat lumbar spine. *NMR Biomed*. 2012;25(3):443-451.

[122] Martin JT, Milby AH, Chiaro JA, Kim DH, Hebela NM, Smith LJ, Elliott DM, Mauck RL. Translation of an engineered nanofibrous disc-like angle-ply structure for intervertebral disc replacement in a small animal model. *Acta Biomater*. 2014;10(6):2473-2481.

[123] Moriguchi Y, Mojica-Santiago J, Grunert P, Pennicooke B, Berlin C, Khair T, Navarro-Ramirez R, Ricart Arbona RJ, Nguyen J, Härtl R, Bonassar LJ. otal disc replacement using tissue-engineered intervertebral discs in the canine cervical spine. *PLoS One*. 2017;12(10):e0185716.

[124] Mojica-Santiago JA, Lang GM, Navarro-Ramirez R, Hussain I, Härtl R, Bonassar LJ. Resorbable plating system stabilizes tissue-engineered intervertebral discs implanted ex vivo in canine cervical spines. *JOR Spine*. 2018;1(3):e1031.

[125] Gullbrand SE, Kim DH, Bonnevie E, Ashinsky BG, Smith LJ, Elliott DM, Mauck RL, Smith HE. Towards the scale up of tissue engineered intervertebral discs for clinical application. *Acta Biomater*. 2018;70:154-164.

[126] Kim DH, Martin JT, Gullbrand SE, Elliott DM, Smith LJ, Smith HE, Mauck RL. Fabrication, Maturation, and Implantation of Composite Tissue-Engineered Total Discs Formed from Native and Mesenchymal Stem Cell Combinations [published online ahead of print, 2020 Jun 4]. *Acta Biomater*. 2020;S1742-7061(20)30318-4.

[127] Gebhard H, Bowles R, Dyke J, et al. Total disc replacement using a tissue-engineered intervertebral disc in vivo: new animal model and initial results. *Evid Based Spine Care J*. 2010;1(2):62-66.

[128] Grunert P, Borde BH, Hudson KD, Macielak MR, Bonassar LJ, Härtl R. Annular repair using high-density collagen gel: a rat-tail in vivo model. *Spine (Phila Pa 1976)*. 2014;39(3):198-206.

[129] James AR, Bowles RD, Gebhard HH, Bonassar LJ, Härtl R. Tissue-engineered total disc replacement: final outcomes of a murine caudal disc in vivo study. *Evid Based Spine Care J*. 2011;2(4):55-56.

[130] Navarro R, Juhas S, Keshavarzi S, Juhasova J, Motlik J, Johe K, Marsala S, Scadeng M, Lazar P, Tomori Z, Schulteis G, Beattie M, Ciacci JD, Marsala M. Chronic spinal compression model in minipigs: a systematic behavioral, qualitative, and quantitative neuropathological study. *J Neurotrauma*. 2012;29(3):499-513.

[131] Bach FC, Willems N, Penning LC, Ito K, Meij BP, Tryfonidou MA. Potential regenerative treatment strategies for intervertebral disc degeneration in dogs. *BMC Vet Res*. 2014;10:3.

[132] Panjabi MM, Crisco JJ, Vasavada A, Oda T, Cholewicki J, Nibu K, et al. Mechanical properties of the human cervical spine as shown by three-dimensional load-displacement curves. *Spine (Phila Pa 1976)*. 2001;26(24):2692–700.

CHAPTER 2

Physiologic Levels of Glucose Drive Fiber Alignment in Tissue-Engineered Intervertebral Discs[1]

Abstract

Tissue engineering of the intervertebral disc (IVD) represents a potential treatment for end stage disease, aiming to replace damaged discs with constructs that aim to a) recreate the disc's unique structure and b) restore the endogenous cell population. In native discs the highly aligned nature of the annulus fibrosus (AF) has led to persistent challenges in recapitulating its complex fibrous architecture. Proteoglycans have been shown to play a role in regulating fiber formation in fibrocartilaginous tissues such as the meniscus. In this study, we controlled fiber formation in self-aligning constructs by tuning media glucose concentrations (125-4500 mg/L). Increasing glucose concentration resulted in increased glycosaminoglycan (GAG) content in our discs; however, fiber alignment peaked at 500 mg/L glucose, which decreased at both higher and lower levels of glucose. The mechanical stability of the disc showed a similar response to changing glucose content, and variations in the mechanics were explained more by fiber alignment than GAG content. These results indicate that saturating engineered constructs with glucose may lead to the prioritization of proteoglycan deposition over fiber formation, and that for these constructs it is structure rather than composition that ultimately determines mechanical behavior.

[1] This chapter will be submitted to ACS Biomaterials Science & Engineering: Lintz M, Bonassar LJ. Physiologic Levels of Glucose Drive Fiber Alignment in Tissue-Engineered Intervertebral Discs. 2021

Graphical Abstract

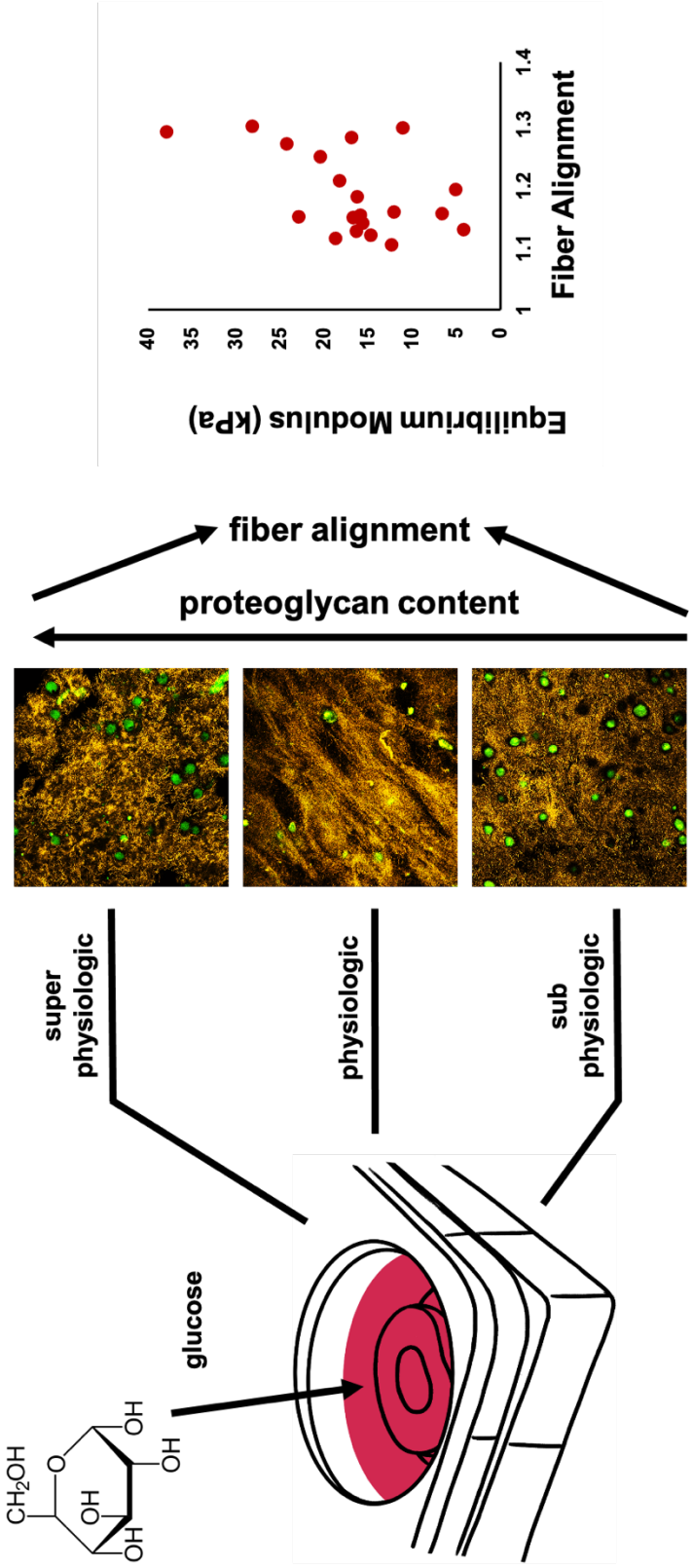

Introduction

Intervertebral disc (IVD) degeneration is often implicated as a primary contributor to lower back pain (LBP), one of the leading causes of disability in the United States[1-3]. While the process is multi-factorial and not fully understood, degeneration is characterized by alterations to the disc composition, structure, and cellular content[4,5]. These ultimately lead to loss of hydration and an inability of the disc to sustain loads, as well as deterioration of the complex fibrous structure leading to tears and then bulging or rupture. Current surgical standards for treatment of disc degeneration are (i) spinal fusion, whereby the entire disc is removed and the adjacent vertebrae are fused together and (ii) total disc replacement (TDR), involving the introduction of a prosthetic disc device to maintain some mobility in the motion segment[6-9]. However, studies have determined that both treatments have a high rate of additional surgeries due to an increased risk of adjacent segment disease[10-12]. Ultimately, these surgical interventions do not provide long-term solutions, as they fail to recapitulate the native structure of the disc as well as restore the depleted endogenous cell population, leaving the underlying cause of disease untreated.

Tissue engineered strategies for repairing and replacing degenerated discs by addressing these shortcomings have been proposed by multiple groups for the better part of the last two decades[13-33]. The resulting composite cell-laden scaffolds contain both a fibrous annulus fibrosus (AF) and soft gelatinous nucleus pulposus (NP) region and aim to restore function by recapitulating structure with a variety of material choices and a cellular population comprised of either primary IVD cells or mesenchymal stem cells (MSCs). In 2010 our group developed a composite TE-IVD seeded with ovine AF and NP cells[18], utilizing cellular contractile forces to drive self-alignment of a type I collagen AF boundary around an alginate NP core. We chose to work with collagen for the engineered AF due to the native annulus' composition as well as its ability to promote

self-assembly and reorganization of the material. Alginate meanwhile was chosen for the nucleus as it is isotropic and hydrophilic, possesses high swelling capabilities, and encapsulates cells to promote chondrocyte-like phenotypes much like in the native NP[34-36]. Both natural materials were additionally chosen for their being nontoxic and better correlating to native tissue structure and matrix composition, though they are mechanically weaker than their synthetic counterparts.

Since we first demonstrated the feasibility of our engineered system, we have published multiple *in vitro* and *in vivo* studies detailing its use and optimization[19-21,27-31]. Our early studies pointed to the tunable nature of this system, where altering parameters such as initial collagen concentration and cell seeding densities impacted the final structure and composition of these constructs, highlighting how the AF architecture could be manipulated prior to contraction-induced remodeling[18]. Despite initial mechanical weakness, pilot *in vivo* studies utilizing a rat model indicated that stably implanted constructs were able to successfully integrate with native tissue, restoring native function as well as maintaining disc height and hydration in caudal and lumbar spines (16 weeks and 8 months, respectively)[20,21]. Post-sacrificial analysis also showed that the engineered discs, though mechanically inferior prior to implantation, achieved comparable mechanical and biochemical properties to native discs. These same results were seen when scaled up for use in a large animal model and implanted in the cervical spines of beagles for up to 16 weeks[26]. Dynamic loading *in vitro* was also explored as a tool for pre-conditioning constructs prior to implantation, with biochemical and mechanical properties increasing in a dose-dependent manner when subjected to dynamic unconfined compressive loading[27]. Cell sources for the aforementioned studies include MSCs as well as primary IVD cells, given their appeal in a wide range of tissue engineering applications as a robust and readily available population from which to draw[37-39].

Recapitulating the complex fiber organization of the AF, however, is an enduring challenge for tissue engineering of the IVD, where poor fiber organization contributes to inferior mechanical performance. As a result there is a need for optimization of existing tissue engineering techniques to promote mechanical and therefore structural stability. In the native AF fiber formation is initiated during development and is thought to proceed from the immature notochord[40], with matrix assembly largely guided by the involvement of proteoglycans[41-43]. Some of the prime players in mediating formation belong to a family of proteoglycans which play a critical role in tissue growth[44-48]. Small leucine rich proteoglycans (SLRPs) such as fibromodulin and decorin drive AF assembly and organization[40] and cartilage development in the regions surrounding the disc, respectively. However, there has been little attempt to manipulate proteoglycans as a way of achieving desired fiber organization.

Glucose proves to be an interesting tool to optimize proteoglycan production *in vitro*, as it plays a key role in the maintenance of some tissues. Specifically, glucose provides the cell with the energy necessary for proteoglycan synthesis, where they are utilized as substrates during the transcription stage to generate core proteins[49,50]. Typically, IVD cells and MSCs are cultured in media containing 1000 or 4500 mg/L glucose[18,20,51]. As physiologic levels of glucose tend to average around 500-1000 mg/L for healthy adults[52,53], these concentrations are the higher range of physiologic and super-physiologic, respectively. The above observations motivated previous work from our group, where we demonstrated that fiber formation can be controlled by altering glucose concentration in culture media[54,55]. Fiber formation in engineered menisci was enhanced by contraction of the extracellular matrix (ECM) but limited by glycosaminoglycan (GAG) deposition, leading to optimal formation at glucose concentrations lower than used for cell culture. Although such phenomena have been

explored in the formation of meniscal fibrocartilage, the extent to which they extend to other types of fibrocartilage such as the AF has never been examined.

The purpose of this study was to determine the extent to which alterations in media glucose concentration and in turn GAG content impact fiber organization in the AF portion of engineered constructs, and ultimately how the mechanics of these composite discs would be affected. Utilizing our established self-aligning TE-IVD model, we implemented a range of glucose concentrations from sub-physiologic (125, 250 mg/L) to physiologic (500, 1000 mg/L) and super-physiologic (4500 mg/L) in the culture of MSC-seeded composite discs. The resulting glucose metabolism, fiber organization, and mechanical properties were examined for each group to determine the impact of structure and composition on mechanical stability.

Materials and Methods

Cell Isolation and Culture

MSCs were isolated as previously described from the trabecular bone marrow of 2-3 year old Finn-Dorset sheep femurs[56,57]. Trilineage potential of this cellular population was determined as per previous studies[56]. After 48 hours the resulting cell population was expanded in 2D culture to second passage in growth media composed of: Dulbecco's modified Eagle's medium (DMEM), 10% fetal bovine serum (FBS, Gemini Bio, West Sacramento, CA), 100 µg/ml penicillin and streptomycin, 0.25 µg/ml amphotericin B (Corning, NY), and 1 ng/mL basic fibroblast growth factor (bFGF, Corning). Cells were cultured to confluence at 37°C, 5% CO_2, and normoxia with media replenished three times a week.

Construct Fabrication and Culture

At confluence cells were removed from flasks with 0.05% trypsin (Gibco BRL) in preparation for seeding. 3% (wt/vol) low viscosity grade alginate (NovaMatrix, Wilmington, DE) was mixed with 0.02 g/mL $CaSO_4$ (Sigma-Aldrich, St. Louis, MO) and set in 12-well plates in $CaCl_2$ (Sigma-Aldrich) to crosslink the alginate plugs. 3mm-diameter alginate NPs were then cut from the gels using a biopsy punch and set in the well centers of a 12-well plate. Collagen I was obtained from rat-tail tendons (BioIVT, Westbury, NY) according to established protocol[18-21]. A 10 mg/ml collagen gel was seeded with 10 x 10^6 cells/ml and the suspension was pipetted around the NP core and allowed to gel, forming the AF[18]. Constructs were cultured for 4 weeks with varying glucose concentrations (125, 250, 500, 1000, and 4500 mg/L) while the AF contracted around the NP to final dimensions.

Multiphoton Microscopy

Following each culture period, constructs from each glucose group were halved and placed in 10% buffered formalin for 48 hours before transfer to 70% ethanol. A Zeiss LSM i-880 confocal microscope was used with a 40x/1.2 C-Apochromat water immersion objective to image into the bottom portions of the constructs as previously described[54,55]. Collagen fiber architecture was captured using second harmonic generation (SHG), with reflectance between 437-464 nm, and cell morphology using autofluorescence between 495-580 nm. Fiber organization was determined through degree of alignment, obtained using a previously described custom MATLAB code[18,58,59] where a series of Fast Fourier Transforms (FFT) was used to calculate a fiber alignment (FA) index as the ratio of major to minor axis.

Biochemical Assays

Biochemical content was measured for each remaining half of the samples collected for imaging, as previously described[18-21,54]. Samples were weighed and lyophilized for 48 hours, weighed again and then digested overnight in a papain digest buffer. A Hoescht DNA assay[60], modified 1,9-dimethylmethylene blue (DMMB) assay[61], and hydroxyproline (hypro) assay[62] were used to measure DNA, sulfated GAG (s-GAG), and collagen content, respectively. These values were then normalized to the corresponding samples' dry weights.

Media Glucose Assay

Media samples were collected following each media change during the 4-week culture period. Glucose concentration was measured using an Amplex Red glucose assay kit (Invitrogen, Eugene, OR) according to manufacturer instructions[54]. Fraction of glucose consumed was determined by subtracting glucose collected from media change from total glucose available, then dividing by total available.

Mechanical Testing

Construct samples were collected following each culture group and subjected to multi-step stress-relaxation tests to determine biomechanical response. Samples underwent unconfined uniaxial compression between two nonporous surfaces at strains up to 50%, with incremental steps of 5% applied over the course of the tests utilizing ElectroForce (ELF) 5500 mechanical testing frame (TA Instruments, New Castle, DE). The time-dependent load response was measured at each of the steps, and effective equilibrium and instantaneous moduli, as well as hydraulic permeability, were calculated for the different experimental groups using a previously described poroelastic model[18,20,21,63].

Statistics

Fiber alignment, glucose consumption, and GAG content were analyzed using a two-way ANOVA with Tukey's test for post-hoc analysis. The relationship between FA index, GAG content, and equilibrium modulus was determined via Pearson correlation using Matlab/Excel. Data are presented as mean ± standard deviation, with significance determined at $p<0.05$.

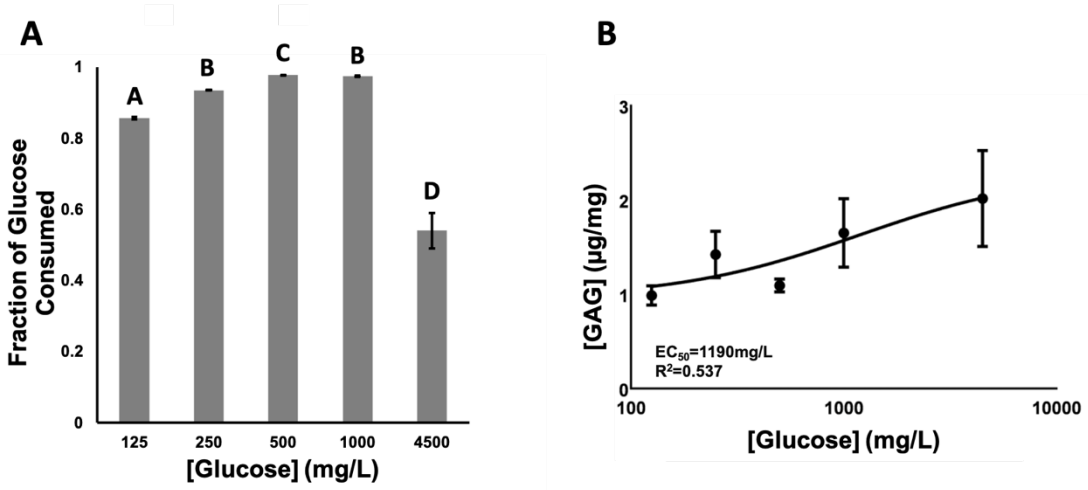

Figure 2.1. A) Fraction of glucose consumed and **B)** GAG concentration at 4 weeks for each glucose group. Lines represent logistic 4P sigmoid. Error bars represent standard deviation. Different letters between groups indicate significant differences ($p<0.05$) using two-way ANOVA and Tukey's test. (n=3-5)

Results

Similar trends in glucose consumption were observed in all culture groups at the 2- and 4-week timepoints (Fig. 1A). Constructs in the 4500 mg/L group consumed between 50-60% of the available glucose during the incubation period, indicating a media glucose surplus throughout culture. In contrast, the remaining groups saw a majority (85-100%) of media glucose consumed and therefore a limitation in the available supply.

At the conclusion of culture, constructs contracted to approximately 46-58% of their initial area, measured as the surface area of an individual well in the 12-well plate,

though no significant differences in final dimensions were observed between the various groups. Comparisons between the culture groups can be found in graphical form in the supplemental materials (Fig. S1).

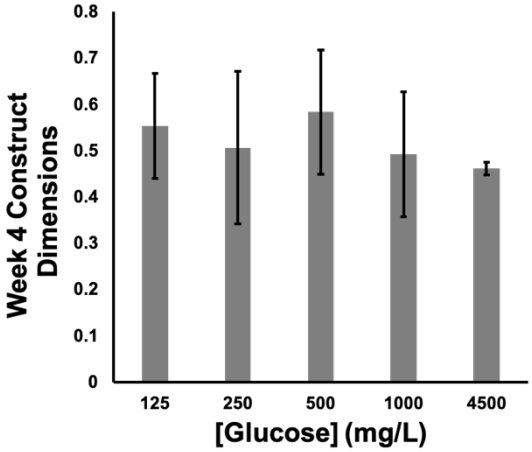

Supplemental Figure 2.1. Final dimensions of the constructs at 4 weeks, reported as current surface area normalized to initial surface area. Error bars represent standard deviation. (n=4)

Increasing media glucose concentrations corresponded to an increase in the s-GAG content of IVD constructs at 4 weeks (Fig. 1B). Constructs in the 125 mg/L group were at the lower end of the range with an average concentration of 0.99 μg/mg, while the 4500 mg/L group averaged 2.02 μg/mg ($p<0.05$). GAG content showed a dose-dependent response with an EC_{50} at ~1190 mg/L ($R^2=0.537$), although it did not appear that saturation was been achieved by 4500 mg/L. Hypro and DNA content were also measured but did not change appreciatively with either time or glucose concentration.

Fiber organization as visualized by SHG microscopy was most pronounced in the 500 mg/L constructs at the conclusion of culture (Fig. 2A). Immediately after fabrication all groups appeared as identical soft gels with no distinct fiber organization. Constructs at Week 1 showed a slight increase in alignment, although with no discernable difference between the groups (data not shown). Imaging at the 2-week

timepoint revealed a noticeable though non-significant change in architecture, with increased alignment occurring in the higher glucose groups, and a modest peak at 500 mg/L which persisted throughout the duration of the experiment. At the conclusion of culture, fibers at 500 mg/L demonstrated greater organization and alignment at Week 4 as compared to the other groups, with continuous bundles of longitudinally-oriented fibers and an average FA index of 1.30. Directionality decreased both with lower and higher glucose concentrations, with the 125, 250, and 4500 mg/L groups showing comparable alignment indices and the 1000 mg/L group slightly more aligned (Fig. 2B, $p<0.05$).

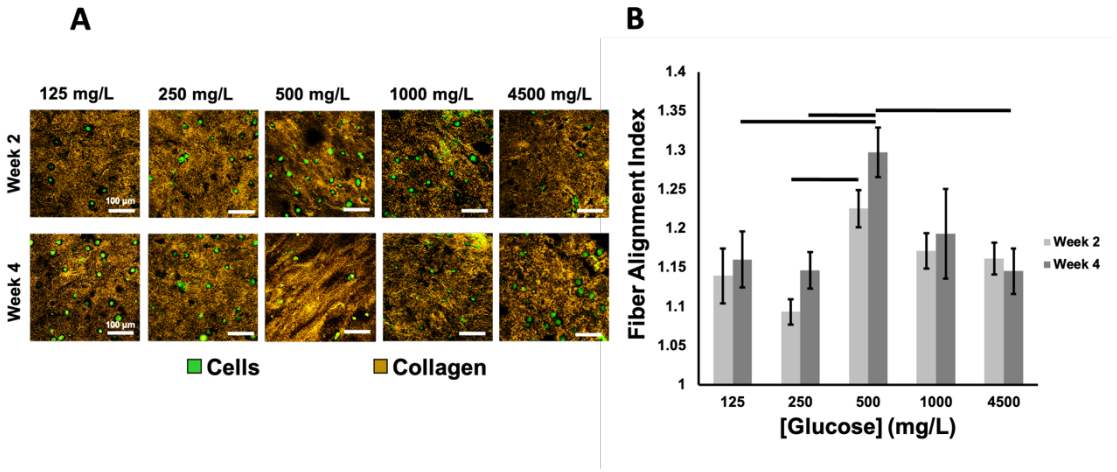

Figure 2.2. A) Representative SHG images of constructs at 2 and 4 weeks. **B)** Fiber alignment index at 2 and 4 weeks for each glucose group. Error bars represent standard deviation. Significant differences ($p<0.05$) using two-way ANOVA and Tukey's test are indicated using bars. (n=4)

Constructs in the 500 mg/L group showed the largest degree of mechanical stability by the end of the culture period as compared to the other groups (Fig. 3 and 4). At the start of culture, all samples had equilibrium moduli of 2.86 ± 1.17 kPa. At Week 4 of culture, construct stiffness increased compared to Week 0, but was dependent on the concentration of glucose in the culture media. The peak in equilibrium modulus occurred at 500 mg/L at a value of 27.3 kPa (Fig. 3A, $p<0.05$), with moduli of 10.9 kPa

and 15.8 kPa at 125 mg/L and 4500 mg/L respectively. A similar trend was observed with instantaneous moduli (Fig. 4A, $p<0.05$) peaking at 192.47 kPa again at 500 mg/L, with values of 137.11 kPa (125 mg/l) and 146.28 kPa (4500 mg/L) at the extremes. Hydraulic permeability meanwhile observed an inverse trend, with the lowest value occurring for the 500 mg/L at 2.11 x 10^{-12} m^2/Pa·s while the 125 and 4500 mg/L groups saw values at 3.22 x 10^{-12} m^2/Pa·s and 3.1 x 10^{-12} m^2/Pa·s, respectively (Fig. 4B, $p<0.05$).

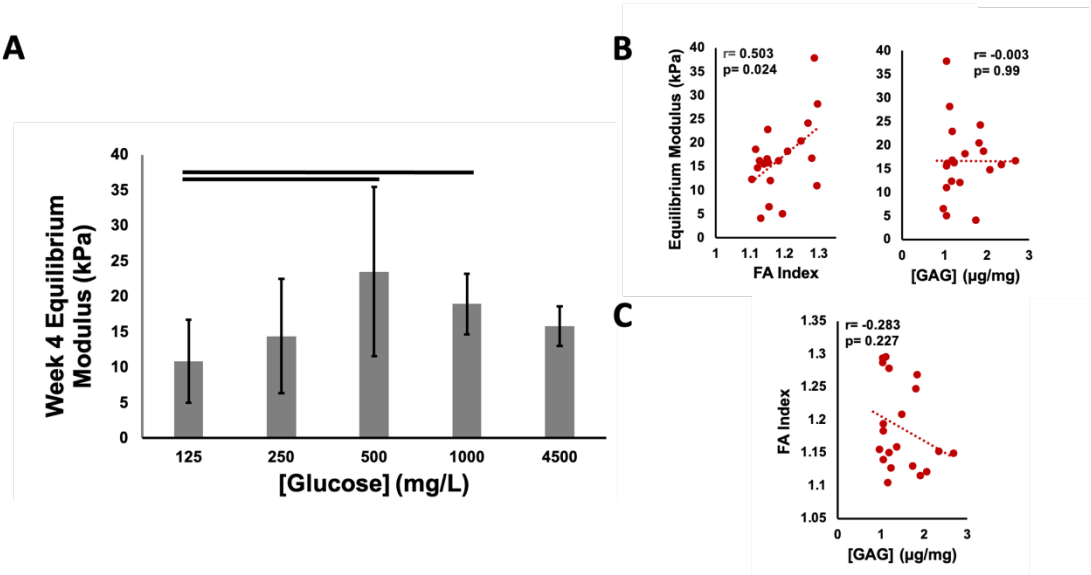

Figure 2.3. A) Equilibrium modulus for each glucose group at week 4. Dependence of **B)** equilibrium modulus on fiber alignment index and GAG concentration and **C)** fiber alignment index on GAG concentration. Error bars represent standard deviation. Significant differences ($p<0.05$) using two-way ANOVA and Tukey's test are indicated using bars. (n=4)

Analysis of the relationships between FA index, GAG content, and equilibrium modulus revealed a strong positive correlation between equilibrium modulus and FA index with $r(20) = 0.503$, $p<0.05$. Equilibrium modulus and GAG content showed a weak negative correlation with $r(20) = -0.003$, $p>0.05$ while FA index and GAG content showed a moderate negative correlation with $r(20) = -0.283$, $p>0.05$.

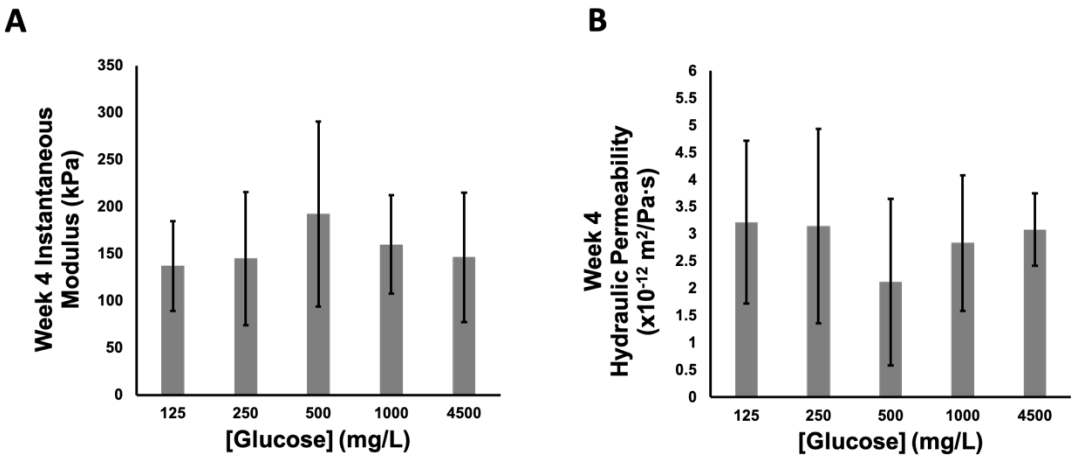

Figure 2.4. A) Instantaneous modulus for each glucose group at week 4. **B)** Hydraulic permeability for each glucose group at week 4. Error bars represent standard deviation. (n=4)

Discussion

The goal of this study was to determine the effect of media glucose concentration on the fiber architecture and mechanics of tissue-engineered IVD constructs. We hypothesized that high levels of glucose would increase matrix components and proteoglycan content while decreasing fiber alignment and organization. We found that culture in concentrations of glucose typical of chondrocyte culture (i.e. either 1000 or 4500 mg/L) resulted in increased s-GAG content but ultimately led to a disorganized fiber network in the AF portion of the constructs. In turn, this disorganized fiber network led to inferior mechanics. A large number of studies focusing on culture of MSCs and IVD cells/constructs have high glucose media formulations (~4500 mg/L), however even those using commercial formulations of low-glucose media appear to contain more glucose than is optimal for fiber formation (~1000 mg/L)[14,15,19-21,24,33,51,54,56,57,64,65].

Following construct fabrication, fiber organization was controlled via GAG production through changes to media glucose content. Bulk GAG content in these constructs increased with increasing glucose concentration while the alignment index

was highest in the 500 mg/L constructs as early as Week 2 and remained consistent throughout the 4 week culture period. These data are consistent with previous studies of meniscus tissue engineering, in which 500 mg/L glucose also produced the most highly organized collagen network[54,55]. In both the current work on AF and previous work on meniscus, either decreasing or increasing glucose media content resulted in significantly decreased alignment indices. Interestingly, this glucose concentration corresponds to the lower end of what is considered a healthy physiologic level in serum[67,68]. IVD constructs seeded with MSCs are often cultured in 4500 mg/L, which corresponds to super-physiologic levels of glucose at 4.5x the higher end of physiologic blood glucose level[52,53] and in this study resulted in a highly disorganized matrix. Constructs in this group consumed only half of their available glucose supply over the two-day incubation period while the remaining groups consumed the majority of their supply in the same amount of time. At the same time, there were no significant effects on cellular DNA content or contraction rates by glucose concentration in any of the groups. When taken with the observation that constructs in all groups contracted throughout culture, indicating consistent cellular activity through remodeling, these results suggest no large negative effects to the cell population during the 4-week culture period. Our previous glucose studies support this conclusion, as neither DNA content nor viability measured through Alamar blue content was affected by glucose concentration[54]. It is important to note, however, that the detrimental effects of excessive glucose levels have been well documented. Studies have shown that prolonged exposure to hyperglycemic environments can impede cell proliferation and result in reduced growth and eventually apoptosis[69,70], suggesting that care must be taken for longer periods of culture. While super-physiologic levels of glucose in short-term culture therefore a) do not detrimentally affect cell viability and b) result in enhanced GAG production—a typical hallmark of healthy tissue in articular cartilage and the reasoning behind high glucose

media in cell culture[68,71]—saturating self-assembling constructs with glucose may in fact lead to a prioritization of GAG deposition over fiber maintenance. These findings appear to be consistent with previous literature on the role of GAG content in the maintenance of engineered and native fibrocartilage[72,73]. Studies have indicated that while GAGs do play a beneficial role in the development and mechanical function of fibrocartilaginous tissues, they also can accumulate to a pathologic level in aging or tendinopathic tissues and ultimately interfere with the tissues' load-bearing capacities[7-77]. Taken together, these data point to a highly sensitive balance between compositional and structural changes, where additional mechanisms may need to be taken into consideration when culturing tissue engineered structures in isolation.

Mechanical testing revealed a corresponding peak in effective construct stiffness at 500 mg/L glucose concentrations, which decreased both with increasing and decreasing media glucose content, with the 125 mg/L and 4500 mg/L groups yielding the lowest stiffness values. Historically, the mechanical stability of viable IVD constructs has been thought to depend more on GAG content. Thus, studies have focused on driving composition over structure[38,39,78]. Analysis conducted in this study, however, indicates that the variations in construct mechanics observed during the experiment were explained more by structure rather than composition. An increase in equilibrium modulus was strongly correlated to an increase in corresponding FA index but weakly correlated to a decrease in GAG content. Alignment index was simultaneously found to moderately correlate to GAG content, ultimately indicating that increased fiber alignment independently of GAG content corresponds to enhanced mechanics in this tissue-engineered system.

Cells were harvested from sheep spines specifically due to their detailed use as an established large animal model of disc disease and regeneration[79,80]. Sheep, like humans, are chondrodystrophic animals and lose their notochordal cell population with

age[81-83] and can therefore function as an analog to the human healing process in disc injury. Ovine discs also resemble human discs with respect to geometry, composition, cellular phenotype, and mechanics. Despite being quadrupedal, sheep spines demonstrate a similar range of motion to that reported for human specimens and have been found biomechanically comparable, thus validating their use as a large animal model for spine repair[83]. For these reasons our group has used an ovine model extensively in our IVD regeneration efforts; these include *in vitro* and *in vivo* annular repair applications[84-86].

We chose to use MSCs in this study in place of primary IVD cells to replicate the results from the previous glucose studies conducted by our group on this same cell type[54,55]; they present an attractive alternative to cells taken directly from the IVD regions due to their versatility as well as reported immunosuppressive capabilities and have been used in various IVD therapies[14,15,23,25], including the creation of composite discs since Nesti et al. and Nerurkar et al. generated their TE-IVD composites in 2008 and 2009, respectively[14,15]. MSCs are particularly attractive for applications in IVD regeneration given a) the largely avascular disc is considered immunoprivileged and b) different stages in the degenerative cascade may result in senescence of the endogenous cell population[86-93]. Given their availability, multipotency, and capacity for self-repair the rationale for using them in place of AF/NP cells lies with their potential to repair the disc by replacing damaged disc cells with a new population of viable tissue-specific cells, promoting regeneration through the secretion of factors aimed at matrix generation while mitigating an inflammatory response. Additionally, straightforward techniques such as trilineage assays have demonstrated how MSC phenotype is dictated by cues from their environment; alterations to media content or additional growth factors guide the cells to differentiate and commit to different lineages[94,95]. *In vivo* studies have further investigated these effects by delivering MSCs into the IVD either via injection or

engineered constructs[89-91,93,96] and concluded that these cells do differentiate into disc-like cells[89-91] and subsequently increase production of proteoglycans and type II collagen[96]: elongated fibroblast-like cells were found in the AF and rounded chondrocyte-like cells in the NP[93], indicating that two distinct phenotypes arise from the same cell source in the different regions of the disc. Kim et al. recently directly compared the effect of delivering MSCs or primary IVD cells via an engineered construct into a rat caudal model[25], concluding that following 5 weeks of implantation both cell types behaved similarly and maintained the structural integrity of the implants for the duration of the study.

Despite the aforementioned rationale behind the selection of our cell source for this study, certain considerations and limitations must be kept in mind. While we saw similar effects from alterations to media glucose levels in our previous experiments with TE-menisci seeded with bovine MSCs, further characterization may be required before transitioning glucose-altered systems in different animal models to *in vivo* use. Not only has cellular heterogeneity in MSCs been reported between species with respect to parameters such as immunosuppression[97], evidence exists that this heterogeneity extends across cellular populations derived from the same host organism[98]. Previous work from our group determined that TE-IVDs seeded with MSCs elicited a mild immune response when implanted in the rat caudal spine for an 8 week duration[93], with a greater reaction marked by the presence of leukocyte marker CD45 at the earlier timepoints (i.e. 2 weeks) than the later. While the constructs successfully integrated with the host tissue regardless of immune response, these results suggest that MSC differentiation may trigger an immune response and that the cells should potentially be screened (immunophenotyping, etc.[93]) prior to use in tissue engineering applications for *in vivo* use. Future studies should assess whether the results observed here extend to IVD-derived AF cells in engineered constructs as well.

One of the limitations of this study is the mechanical stiffness of the engineered constructs following 4 weeks of culture. The average equilibrium moduli for the constructs tested were approximately an order of magnitude weaker than those of native discs (238 kPa)[19,20] in all experimental groups. Notably, IVD constructs of similar stiffness have been implanted in canine cervical spine, and rat caudal and lumbar spine *in vivo* models[19-21]. Post-sacrifice, constructs were found to successfully integrate with the host tissue at 6 week and 9 months, and mechanical testing showed that integration enabled the discs to achieve native stiffness values (~235 kPa)[20]. Though sub-physiologic glucose culture does not yield native mechanical properties following the 4-week culture period, therefore, these previous experiments indicate that with *in vivo* implantation these values can be achieved. As we have shown successful integration with host tissue has allowed soft constructs to reach appropriate mechanical properties, these results suggest that enhancing the fiber architecture of these self-assembling discs may provide a technique for *in vitro* pre-conditioning and ultimately yield a template for tissue engineering approaches.

In conclusion, we found that culturing IVD constructs in media glucose concentrations at the lower end of physiologic levels *in vitro* led to increased fiber alignment and effective stiffness. The peak in both parameters occurred at 500 mg/L, with concentrations on either side of this peak yielding unaligned fibers and weaker mechanical properties. Of notable interest, culture media with 4500 mg/L glucose resulted in constructs with enhanced composition but inferior alignment and mechanics. Ultimately, changes in mechanics were explained more by variations in fiber architecture and were largely independent of biochemical composition, mimicking the native IVD's dependence on structure and demonstrating the necessity for carefully regulated culture in a system highly sensitive to manipulation of these factors.

Acknowledgments

The authors would like to thank Ellaine Chou and Jongkil Kim for their help with culture and biochemistry, as well as the Colman Family Foundation for stipend support. This work was supported by the following funding sources: the Colin MacDonald Fund, the Daedalus Innovation Fund, and the Center for Advanced Technology from the New York State Advanced Research Fund (NYSTAR).

REFERENCES

[1] Luoma K., Riihimäki H., Luukkonen R., Raininko R., Viikari-Juntura E., Lamminen A. (2000). Low back pain in relation to lumbar disc degeneration. *Spine*, 25(4):487–92.

[2] Urban J.P.G., Roberts S. (2003). Degeneration of the intervertebral disc. *Arthritis Research and Therapy*, 5(3):120-30.

[3] Molinos M., Almeida C.R., Caldeira J., Cunha C., Gonçalves R.M., Barbosa M.A. (2015). Inflammation in intervertebral disc degeneration and regeneration. *Journal of the Royal Society Interface*, 12(104): 20141191.

[4] Buckwalter J.A. (1995). Spine update: Aging and degeneration of the human intervertebral disc. *Spine*, 20(11):1307–14.

[5] Lyons G., Eisenstein S.M., Sweet M.B.E. (1981). Biochemical changes in intervertebral disc degeneration. *BBA - General Subjects*, 673(C):443–53.

[6] Phillips F.M., Garfin S.R. (2005). Cervical Disc Replacement. *Spine*, 30(17 Suppl.):S27–S33.

[7] Dower A., Chatterji R., Swart A., Winder M.J. (2016). Surgical management of recurrent lumbar disc herniation and the role of fusion. *Journal of Clinical Neuroscience*, 23:44–50.

[8] Petersilge C.A. (2006). Lumbar disc replacement. *Seminars in Musculoskeletal Radiology*, 10:22-9.

[9] MacDowall A., Skeppholm M., Lindhagen L., Robinson Y., Löfgren H., Michaëlsson K.,Olerud C. (2019). Artificial disc replacement versus fusion in patients with cervical degenerative disc disease with radiculopathy: 5-year outcomes from the National Swedish Spine Register. *Journal Of Neurosurgery*, 30(2):149–297.

[10] Setton L.A., Bonassar L.J., Masuda K. (2007). Regeneration and Replacement of the Intervertebral Disc. In *Principles of Tissue Engineering* (pp. 877-96).

[11] Wu T.K., Wang B.Y., Meng Y., Ding C., Yang Y., Lou J.G., Liu H. (2017). Multilevel cervical disc replacement versus multilevel anterior discectomy and fusion: A meta-analysis. *Medicine*, 96(16):e6503.

[12] Salzmann S.N., Plais N., Shue J., Girardi F.P. (2017). Lumbar disc replacement surgery—successes and obstacles to widespread adoption. *Current Reviews in Musculoskeletal Medicine*, 10(2):153–9.

[13] Mizuno H., Roy A.K., Vacanti C.A., Kojima K., Ueda M., Bonassar, L.J. (2004).

Tissue-Engineered Composites of Anulus Fibrosus and Nucleus Pulposus for Intervertebral Disc Replacement. *Spine*, 29(12):1290–7.

[14] Nesti L.J., Li W.J., Shanti R.M., Jiang Y.J., Jackson W., Freedman B.A., Kuklo T.R., Giuliani J.R., Tuan R.S. (2008). Intervertebral disc tissue engineering using a novel hyaluronic acid-nanofibrous scaffold (HANFS) amalgam. In *Tissue Engineering - Part A.*, 14(9):1527–37.

[15] Nerurkar N.L., Sen S., Huang A.H., Elliott D.M., Mauck R.L. (2010). Engineered disc-like angle-ply structures for intervertebral disc replacement. *Spine*, 35(8):867–873.

[16] Zhuang Y., Huang B., Li C.Q., Liu L.T., Pan Y., Zheng W.J., Luo G., Zhou Y. (2011). Construction of tissue-engineered composite intervertebral disc and preliminary morphological and biochemical evaluation. *Biochemical and Biophysical Research Communications*, 407(2):327–32.

[17] Park S.H., Gil E.S., Cho H., Mandal B.B., Tien L.W., Min B.H., Kaplan D.L. (2012). Intervertebral disk tissue engineering using biphasic silk composite scaffolds. *Tissue Engineering - Part A*, 18(5–6):447–58.

[18] Bowles R.D., Williams R.M., Zipfel W.R., Bonassar L.J. (2010). Self-Assembly of Aligned Tissue-Engineered Annulus Fibrosus and Intervertebral Disc Composite Via Collagen Gel Contraction. *Tissue Engineering - Part A*, 16(4):1339–48.

[19] Moriguchi Y., Mojica-Santiago J., Grunert P., Pennicooke B., Berlin C., Khair T., Navarro-Ramirez R., Arbona R.J.R., Nguyen J., Härtl R., Bonassar L.J. (2017). Total disc replacement using tissue-engineered intervertebral discs in the canine cervical spine. *PLoS ONE*, 12(10).

[20] Bowles R.D., Gebhard H.H., Härtl R., Bonassar L.J. (2011). Tissue-engineered intervertebral discs produce new matrix, maintain disc height, and restore biomechanical function to the rodent spine. *Proceedings of the National Academy of Sciences of the United States of America*, 108(32):13106–11.

[21] Bowles R.D., Gebhard H.H., Dyke J.P., Ballon D.J., Tomasino A., Cunningham M.E., Härtl R., Bonassar, L.J. (2012). Image-based tissue engineering of a total intervertebral disc implant for restoration of function to the rat lumbar spine. *NMR in Biomedicine*, 25(3):443–51.

[22] Chang, G., Kim, H. J., Kaplan, D., Vunjak-Novakovic, G., & Kandel, R. A. (2007). Porous silk scaffolds can be used for tissue engineering annulus fibrosus. *European spine journal : official publication of the European Spine Society, the European Spinal Deformity Society, and the European Section of the Cervical Spine Research Society*, *16*(11), 1848–1857.

[23] Martin, J. T., Milby, A. H., Chiaro, J. A., Kim, D. H., Hebela, N. M., Smith, L. J., Elliott, D. M., & Mauck, R. L. (2014). Translation of an engineered nanofibrous disc-like angle-ply structure for intervertebral disc replacement in a small animal model. *Acta biomaterialia*, *10*(6), 2473–2481.

[24] Gullbrand, S. E., Kim, D. H., Bonnevie, E., Ashinsky, B. G., Smith, L. J., Elliott, D. M., Mauck, R. L., & Smith, H. E. (2018). Towards the scale up of tissue engineered intervertebral discs for clinical application. *Acta biomaterialia*, *70*, 154–164.

[25] Kim, D. H., Martin, J. T., Gullbrand, S. E., Elliott, D. M., Smith, L. J., Smith, H. E., & Mauck, R. L. (2020). Fabrication, maturation, and implantation of composite tissue-engineered total discs formed from native and mesenchymal stem cell combinations. *Acta biomaterialia*, *114*, 53–62.

[26] Mojica-Santiago, J. A., Lang, G. M., Navarro-Ramirez, R., Hussain, I., Härtl, R., & Bonassar, L. J. (2018). Resorbable plating system stabilizes tissue-engineered intervertebral discs implanted ex vivo in canine cervical spines. *JOR spine*, *1*(3), e1031.

[27] Hudson, K. D., Mozia, R. I., & Bonassar, L. J. (2015). Dose-dependent response of tissue-engineered intervertebral discs to dynamic unconfined compressive loading. *Tissue engineering. Part A*, *21*(3-4), 564–572.

[28] Hudson, K. D., & Bonassar, L. J. (2017). Hypoxic Expansion of Human Mesenchymal Stem Cells Enhances Three-Dimensional Maturation of Tissue-Engineered Intervertebral Discs. *Tissue engineering. Part A*, *23*(7-8), 293–300.

[29] Gebhard, H., Bowles, R., Dyke, J., Saleh, T., Doty, S., Bonassar, L., & Härtl, R. (2010). Total disc replacement using a tissue-engineered intervertebral disc in vivo: new animal model and initial results. *Evidence-based spine-care journal*, *1*(2), 62–66.

[30] Grunert, P., Borde, B. H., Hudson, K. D., Macielak, M. R., Bonassar, L. J., & Härtl, R. (2014). Annular repair using high-density collagen gel: a rat-tail in vivo model. *Spine*, *39*(3), 198–206.

[31] James, A. R., Bowles, R. D., Gebhard, H. H., Bonassar, L. J., & Härtl, R. (2011). Tissue-engineered total disc replacement: final outcomes of a murine caudal disc in vivo study. *Evidence-based spine-care journal*, *2*(4), 55–56.

[32] Yang, F., Xiao, D., Zhao, Q., Chen, Z., Liu, K., Chen, S., Sun, X., Yue, Q., Zhang, R., & Feng, G. (2018). Fabrication of a novel whole tissue-engineered intervertebral disc for intervertebral disc regeneration in the porcine lumbar spine. *RSC Advances*, *8*(68), 39013–39021.

[33] Lazebnik, M., Singh, M., Glatt, P., Friis, L. A., Berkland, C. J., & Detamore, M. S. (2011). Biomimetic method for combining the nucleus pulposus and annulus fibrosus

for intervertebral disc tissue engineering. *Journal of tissue engineering and regenerative medicine*, *5*(8), e179–e187.

[34] Leone, G., Torricelli, P., Chiumiento, A., Facchini, A., & Barbucci, R. (2008). Amidic alginate hydrogel for nucleus pulposus replacement. *Journal of biomedical materials research. Part A*, *84*(2), 391–401.

[35] Marsich, E., Borgogna, M., Donati, I., Mozetic, P., Strand, B. L., Salvador, S. G., Vittur, F., & Paoletti, S. (2008). Alginate/lactose-modified chitosan hydrogels: a bioactive biomaterial for chondrocyte encapsulation. *Journal of biomedical materials research. Part A*, *84*(2), 364–376.

[36] Chou, A. I., & Nicoll, S. B. (2009). Characterization of photocrosslinked alginate hydrogels for nucleus pulposus cell encapsulation. *Journal of biomedical materials research. Part A*, *91*(1), 187–194.

[37] van Uden S., Silva-Correia J., Oliveira J.M., Reis R.L. (2017). Current strategies for treatment of intervertebral disc degeneration: Substitution and regeneration possibilities. *Biomaterials Research*, 21(1):22.

[38] Stergar J., Gradisnik L., Velnar T., Maver U. (2019). Intervertebral disc tissue engineering: A brief review. *Bosnian Journal of Basic Medical Sciences*, 19(2):130–7.

[39] Kandel R., Roberts S., Urban J.P.G. (2008). Tissue engineering and the intervertebral disc: The challenges. *European Spine Journal*, 17(4):480–491.

[40] Aszódi A., Chan D., Hunziker E., Bateman J.F., Fässler R. (1998). Collagen II is essential for the removal of the notochord and the formation of intervertebral discs. *Journal of Cell Biology*, 143(5):1399–412.

[41] Hayes A.J., Isaacs M.D., Hughes C., Caterson B., Ralphs, J.R. (2011). Collagen fibrillogenesis in the development of the annulus fibrosus of the intervertebral disc. *European Cells and Materials*, 22:226–41.

[42] Lawson L.Y., Harfe B.D. (2017). Developmental mechanisms of intervertebral disc and vertebral column formation. *Wiley Interdisciplinary Reviews: Developmental Biology*, 6(6): e283.

[43] Colombier P., Clouet J., Hamel O., Lescaudron L., Guicheux J. (2014). The lumbar intervertebral disc: From embryonic development to degeneration. *Joint Bone Spine*, 81(2):125–9.

[44] Kelleher C.M., McLean S.E., Mecham R.P. (2004). Vascular Extracellular Matrix and Aortic Development. *Current Topics in Developmental Biology*, 62:153–88.

[45] Iozzo R.V., Schaefer L. (2015). Proteoglycan form and function: A comprehensive nomenclature of proteoglycans. *Matrix Biology*, 42:11–55.

[46] Iozzo, R.V, Murdoch, A.D. (1996). *Proteoglycans of the extracellular environment: clues from the gene and protein side offer novel perspectives in molecular diversity and function* (Vol. 10).

[47] Banos C.C., Thomas A.H., Kuo C.K. (2008). Collagen fibrillogenesis in tendon development: Current models and regulation of fibril assembly. *Birth Defects Research Part C - Embryo Today: Reviews*, 84(3):228-44.

[48] Kalamajski S., Oldberg A. (2010). The role of small leucine-rich proteoglycans in collagen fibrillogenesis. *Matrix Biology*, 29(4):248–53.

[49] Mobasheri A., Vannucci S.J., Bondy C.A., Carter S.D., Innes J.F., Arteaga M.F., Shakibaei M., Martín-Vasallo, P. (2002). Glucose transport and metabolism in chondrocytes: A key to understanding chondrogenesis, skeletal development and cartilage degradation in osteoarthritis. *Histology and Histopathology*, 17(4):1239–67.

[50] Prydz K., Dalen K.T. (2000). Synthesis and sorting of proteoglycans. *Journal of Cell Science*, 113(2):193–205.

[51] Puetzer J.L., Bonassar L.J. (2016). Physiologically Distributed Loading Patterns Drive the Formation of Zonally Organized Collagen Structures in Tissue-Engineered Meniscus. *Tissue Engineering - Part A*, 22(13–14):907–16.

[52] Otte P. (1991). Basic cell metabolism of articular cartilage. Manometric studies. Rheumatol, 50(5):304–12.

[53] Polakof S., Mommsen T.P., Soengas, J.L. (2011). Glucosensing and glucose homeostasis: From fish to mammals. *Comparative Biochemistry and Physiology - B Biochemistry and Molecular Biology*, 160(4):123–49.

[54] McCorry M.C., Kim J., Springer N.L., Sandy J., Plaas A., Bonassar L.J. (2019). Regulation of proteoglycan production by varying glucose concentrations controls fiber formation in tissue engineered menisci. *Acta Biomaterialia*, 100:173–83.

[55] Kim J, Boys AJ, Estroff LA, Bonassar LJ. Combining TGF-β1 and Mechanical Anchoring to Enhance Collagen Fiber Formation and Alignment in Tissue-Engineered Menisci. *ACS Biomater Sci Eng*. 2021;7(4):1608-1620.

[56] McCorry M.C., Puetzer J.L., Bonassar L.J. (2016). Characterization of mesenchymal stem cells and fibrochondrocytes in three-dimensional co-culture: Analysis of cell shape, matrix production, and mechanical performance. *Stem Cell Research and Therapy*, 7(1):39.

[57] McCorry M.C., Bonassar, L.J. (2017). Fiber development and matrix production in tissue-engineered menisci using bovine mesenchymal stem cells and fibrochondrocytes. *Connective Tissue Research*, 58(3–4):329–41.

[58] Puetzer J.L., Koo E., Bonassar L.J. (2015). Induction of fiber alignment and mechanical anisotropy in tissue engineered menisci with mechanical anchoring. *Journal of Biomechanics*, 48(8):1436–43.

[59] Boys A.J., Kunitake J.A.M.R., Henak C.R., Cohen I., Estroff L.A., Bonassar L.J. (2019). Understanding the Stiff-to-Compliant Transition of the Meniscal Attachments by Spatial Correlation of Composition, Structure, and Mechanics. *ACS Applied Materials and Interfaces*, 11(30):26559–70.

[60] Kim Y.J., Sah R.L.Y., Doong J.Y.H., Grodzinsky A.J. (1988). Fluorometric assay of DNA in cartilage explants using Hoechst 33258. *Analytical Biochemistry*, 174(1):168–176.

[61] Enobakhare B.O., Bader D.L., Lee D.A. (1996). Quantification of sulfated glycosaminoglycans in chondrocyte/alginate cultures, by use of 1,9-dimethylmethylene blue. *Analytical Biochemistry*, 243(1):189–91.

[62] Neuman R., Logan M. (1949). The determination of hydroxyproline. *Journal of Biological Chemistry*, 184(1):299-306.

[63] Kim Y.J., Bonassar L.J., Grodzinsky A.J. (1995). The role of cartilage streaming potential, fluid flow and pressure in the stimulation of chondrocyte biosynthesis during dynamic compression. *Journal of Biomechanics*, 28(9):1055–66.

[64] Schubert A.K., Smink J.J., Pumberger M., Putzier M., Sittinger M., Ringe, J. (2018). Standardisation of basal medium for reproducible culture of human annulus fibrosus and nucleus pulposus cells. *Journal of Orthopaedic Surgery and Research*, 13(1):209.

[65] Mauck R L., Yuan X., Tuan R.S. (2006). Chondrogenic differentiation and functional maturation of bovine mesenchymal stem cells in long-term agarose culture. *Osteoarthritis and Cartilage*, 14(2):179–89.

[66] Güemes M., Rahman S.A., Hussain K. (2016). What is a normal blood glucose? *Archives of Disease in Childhood*, 101(6):569–74.

[67] Liakat S., Bors K.A., Huang T.Y., Michel A.P.M., Zanghi E., Gmachl C.F. (2013). In vitro measurements of physiological glucose concentrations in biological fluids using mid-infrared spectroscopy. In *2013 Conference on Lasers and Electro-Optics, CLEO 2013*, 4:1083.

[68] Fakunle E.S., Lane J.G. (2017). Cell culture approaches for articular cartilage: Repair and regeneration. In *Bio-orthopaedics: A New Approach* (pp. 161–72).

[69] Liu, Y., Li, Y., Nan, L., Wang, F., Zhou, S., Wang, J., Feng, X., & Zhang, L. (2020). The effect of high glucose on the biological characteristics of nucleus pulposus-derived mesenchymal stem cells. *Cell Biochemistry and Function*, *38*(2), 130–140.

[70] Chang, T. C., Hsu, M. F., & Wu, K. K. (2015). High glucose induces bone marrow-derived mesenchymal stem cell senescence by upregulating autophagy. *PloS one*, *10*(5), e0126537.

[71] Connelly J.T., Wilson C.G., Levenston M.E. (2008). Characterization of proteoglycan production and processing by chondrocytes and BMSCs in tissue engineered constructs. *Osteoarthritis and Cartilage*, 16(9):1092–100.

[72] MacBarb R.F., Makris E.A., Hu J.C., Athanasiou K.A. (2013). A chondroitinase-ABC and TGF-β1 treatment regimen for enhancing the mechanical properties of tissue-engineered fibrocartilage. *Acta Biomaterialia*, 9(1):4626–34.

[73] Ryan C.N.M., Sorushanova A., Lomas A.J., Mullen A.M., Pandit A., Zeugolis D.I. (2015). Glycosaminoglycans in Tendon Physiology, Pathophysiology, and Therapy. *Bioconjugate Chemistry*, 26(7):1237–51.

[74] Attia M., Scott A., Carpentier G., Lian Ø., Van Kuppevelt T., Gossard C., Papy-Garcia D., Tassoni M., Martelly I. (2014). Greater glycosaminoglycan content in human patellar tendon biopsies is associated with more pain and a lower VISA score. *British Journal of Sports Medicine*, 48(6):469–75.

[75] Wang V.M., Bell R.M., Thakore R., Eyre D.R., Galante J.O., Li J., Sandy J.D., Plaas A. (2012). Murine tendon function is adversely affected by aggrecan accumulation due to the knockout of ADAMTS5. *Journal of Orthopaedic Research*, 30(4):620–6.

[76] Plaas A., Sandy J.D., Liu H., Diaz M.A., Schenkman D., Magnus R.P., Bolam-Bretl C., Kopesky P.W., Wang V.M., Galante J.O. (2011). Biochemical identification and immunolocalizaton of aggrecan, ADAMTS5 and inter-alpha-trypsin-inhibitor in equine degenerative suspensory ligament desmitis. *Journal of Orthopaedic Research*, 29(6):900–6.

[77] Parkinson J., Samiric T., Ilic M.Z., Cook J., Handley C.J. (2011). Involvement of proteoglycans in tendinopathy. *Journal of Musculoskeletal and Neuronal Interactions*, 11(2):86-93.

[78] Mizuno H., Roy A.K., Zaporojan V., Vacanti C.A., Ueda M., Bonassar L.J. (2006). Biomechanical and biochemical characterization of composite tissue-engineered intervertebral discs. *Biomaterials*, 27(3): 362–370.

[79] Daly, C., Ghosh, P., Jenkin, G., Oehme, D., & Goldschlager, T. (2016). A Review of Animal Models of Intervertebral Disc Degeneration: Pathophysiology, Regeneration, and Translation to the Clinic. *BioMed research international*, *2016*, 5952165.

[80] Daly, C. D., Ghosh, P., Badal, T., Shimmon, R., Jenkin, G., Oehme, D., Cooper-White, J., Sher, I., Chandra, R. V., & Goldschlager, T. (2018). A Comparison of Two Ovine Lumbar Intervertebral Disc Injury Models for the Evaluation and Development of Novel Regenerative Therapies. *Global spine journal*, *8*(8), 847–859. https://doi.org/10.1177/2192568218779988

[81] Melrose, J., Burkhardt, D., Taylor, T. K., Dillon, C. T., Read, R., Cake, M., & Little, C. B. (2009). Calcification in the ovine intervertebral disc: a model of hydroxyapatite deposition disease. *European spine journal : official publication of the European Spine Society, the European Spinal Deformity Society, and the European Section of the Cervical Spine Research Society*, *18*(4), 479–489.

[82] Hunter, C. J., Matyas, J. R., & Duncan, N. A. (2004). Cytomorphology of notochordal and chondrocytic cells from the nucleus pulposus: a species comparison. *Journal of anatomy*, *205*(5), 357–362.

[83] Wilke, H. J., Kettler, A., & Claes, L. E. (1997). Are sheep spines a valid biomechanical model for human spines?. *Spine*, *22*(20), 2365–2374.

[84] Sloan, S. R., Jr, Wipplinger, C., Kirnaz, S., Navarro-Ramirez, R., Schmidt, F., McCloskey, D., Pannellini, T., Schiavinato, A., Härtl, R., & Bonassar, L. J. (2020). Combined nucleus pulposus augmentation and annulus fibrosus repair prevents acute intervertebral disc degeneration after discectomy. *Science translational medicine*, *12*(534), eaay2380.

[85] Jiang, E. Y., Sloan, S. R., Jr, Wipplinger, C., Kirnaz, S., Härtl, R., & Bonassar, L. J. (2019). Proteoglycan removal by chondroitinase ABC improves injectable collagen gel adhesion to annulus fibrosus. *Acta biomaterialia*, *97*, 428–436.

[86] Wei, A., Shen, B., Williams, L., & Diwan, A. (2014). Mesenchymal stem cells: potential application in intervertebral disc regeneration. *Translational pediatrics*, *3*(2), 71–90.

[87] Acosta, F. L., Jr, Metz, L., Adkisson, H. D., Liu, J., Carruthers-Liebenberg, E., Milliman, C., Maloney, M., & Lotz, J. C. (2011). Porcine intervertebral disc repair using allogeneic juvenile articular chondrocytes or mesenchymal stem cells. *Tissue engineering. Part A*, *17*(23-24), 3045–3055.

[88] Crevensten, G., Walsh, A. J., Ananthakrishnan, D., Page, P., Wahba, G. M., Lotz, J. C., & Berven, S. (2004). Intervertebral disc cell therapy for regeneration:

mesenchymal stem cell implantation in rat intervertebral discs. *Annals of biomedical engineering*, *32*(3), 430–434.

[89] Sakai, D., Mochida, J., Yamamoto, Y., Nomura, T., Okuma, M., Nishimura, K., Nakai, T., Ando, K., & Hotta, T. (2003). Transplantation of mesenchymal stem cells embedded in Atelocollagen gel to the intervertebral disc: a potential therapeutic model for disc degeneration. *Biomaterials*, *24*(20), 3531–3541.

[90] Sakai, D., Mochida, J., Iwashina, T., Watanabe, T., Nakai, T., Ando, K., & Hotta, T. (2005). Differentiation of mesenchymal stem cells transplanted to a rabbit degenerative disc model: potential and limitations for stem cell therapy in disc regeneration. *Spine*, *30*(21), 2379–2387.

[91] Sakai, D., Mochida, J., Iwashina, T., Hiyama, A., Omi, H., Imai, M., Nakai, T., Ando, K., & Hotta, T. (2006). Regenerative effects of transplanting mesenchymal stem cells embedded in atelocollagen to the degenerated intervertebral disc. *Biomaterials*, *27*(3), 335–345.

[92] Hiyama, A., Mochida, J., Iwashina, T., Omi, H., Watanabe, T., Serigano, K., Tamura, F., & Sakai, D. (2008). Transplantation of mesenchymal stem cells in a canine disc degeneration model. *Journal of orthopaedic research : official publication of the Orthopaedic Research Society*, *26*(5), 589–600.

[93] Hudson, K.D. (2016). Tissue Engineering of the Intervertebral Disc Using Chemical and Mechanical Stimulation of Mesenchymal Stem Cells. Retrieved from Cornell University's Institutional Repository.

[94] Bernacki, S. H., Wall, M. E., & Loboa, E. G. (2008). Isolation of human mesenchymal stem cells from bone and adipose tissue. *Methods in cell biology*, *86*, 257–278.

[95] Pittenger, M. F., Mackay, A. M., Beck, S. C., Jaiswal, R. K., Douglas, R., Mosca, J. D., Moorman, M. A., Simonetti, D. W., Craig, S., & Marshak, D. R. (1999). Multilineage potential of adult human mesenchymal stem cells. *Science (New York, N.Y.)*, *284*(5411), 143–147.

[96] Zhang, Y. G., Guo, X., Xu, P., Kang, L. L., & Li, J. (2005). Bone mesenchymal stem cells transplanted into rabbit intervertebral discs can increase proteoglycans. *Clinical orthopaedics and related research*, (430), 219–226.

[97] Ren, G., Su, J., Zhang, L., Zhao, X., Ling, W., L'huillie, A., Zhang, J., Lu, Y., Roberts, A. I., Ji, W., Zhang, H., Rabson, A. B., & Shi, Y. (2009). Species variation in the mechanisms of mesenchymal stem cell-mediated immunosuppression. *Stem cells (Dayton, Ohio)*, *27*(8), 1954–1962.

[98] O'Connor K. C. (2019). Molecular Profiles of Cell-to-Cell Variation in the Regenerative Potential of Mesenchymal Stromal Cells. *Stem cells international*, *2019*, 5924878.

CHAPTER 3

The Degenerative Impact of Hyperglycemia on the Structure and Mechanics of Developing Murine Intervertebral Discs[2]

Abstract

Diabetes has long been implicated as a major risk factor for intervertebral disc (IVD) degeneration, interfering with molecular and biochemical signaling pathways that ultimately aggravate the progression of the disease. Glucose content has been previously shown to influence structural and compositional changes in engineered discs *in vitro*, impeding fiber formation and mechanical stability. In this study, we investigated the impact of diabetic hyperglycemia on the developing IVD by assessing biochemical composition, collagen fiber architecture, and mechanical behavior of discs harvested from 3-4 month old db/db mouse caudal spines. We found that discs taken from diabetic mice demonstrated elevated blood glucose levels as well an increase in glycosaminoglycan (GAG) and collagen content, but with comparable advanced glycation end products (AGE) levels to wild type discs. Diabetic discs also contained ill-defined boundaries between the nucleus pulposus (NP) and annulus fibrosis (AF), with the latter showing a disorganized and unaligned collagen fiber network at this same boundary. These compositional and structural changes had a detrimental effect on function, as the diabetic discs were twice as stiff as their wild type counterparts and demonstrated a significant resistance to deformation. These results indicate that diabetes may predispose the young disc to DDD later in life by altering patterns of extracellular matrix (ECM) deposition, fiber formation, and motion segment mechanics independently of AGE accumulation.

[2] This chapter will be submitted to JOR Spine: Lintz M, Walk RE, Tang SY, Bonassar LJ. The Degenerative Impact of Hyperglycemia on the Structure and Mechanics of Developing Murine Intervertebral Discs. 2021

Introduction

Lower back pain (LBP) is an extremely prevalent disorder and one of the leading causes of disability worldwide, with approximately 50-80% of the adult population experiencing symptoms at least once in their lifetime[1,2]. Although a variety of risk factors are attributed to its onset, degeneration of the intervertebral disc (IVD) is implicated as a major contributor to its advancement[3-5]. Disc degeneration is a complex, multifactorial process characterized by deterioration of the disc's composition and structure, as well as irreversible changes to its endogenous cell population[3-7]. As the disease progresses the highly hydrated nucleus pulposus (NP) loses water content and is rendered unable to sustain loads, while the complex fiber network of the surrounding annulus fibrosus (AF) becomes increasingly disorganized, eventually leading to rupture or herniation of the disc. The accumulation of damage to the AF triggers a degenerative cascade, favoring catabolism and upregulating matrix metalloproteases (MMPs) and other factors contributing to extracellular matrix (ECM) degeneration[8-14], which the cell population is no longer able to repair.

Diabetes is a collection of chronic metabolic illnesses with varying etiologies, but common symptoms characterized by improper production, and in some cases resistance, to the hormone insulin which in turn results in heightened blood glucose levels or hyperglycemia[15-18]. With time, diabetes and its associated symptoms result in additional comorbidities such as cardiovascular disease, loss of vision or total blindness, musculoskeletal disorders, nerve damage, impaired wound healing, etc., all of which can lead to decreased quality of life or even death[16,18-22].

Diabetes is also a common comorbidity for degenerative disc disease[23-33]. Clinical studies have indicated that patients receiving surgical intervention for lumbar disc disease demonstrate a higher incidence of diabetes[28-30]. Additionally, diabetic patients have been found to be significantly more likely to receive surgical treatments

for lumbar disc disease than non-diabetics, and while they experience higher initial benefit from surgery[29] they are 7 times more likely to require additional surgical intervention[32]. Laboratory studies meanwhile have attempted to elucidate the mechanisms under which diabetes contributes to DDD, finding strong evidence suggesting that diabetes has a degenerative effect on the disc and may interfere with molecular pathways associated with disc disease[24,26,33-35]. However, it can be difficult to discern which changes arise as a direct consequence of diabetes from those associated with typical degeneration, as both diseases are time-dependent and DDD is only diagnosed following reports of painful symptoms, and the damage is discovered once they are well established.

While the connections between diabetes and DDD have been reported clinically, the mechanism behind this connection is still not fully understood, particularly at the molecular level. Previous studies have investigated the effect of glucose on the formation of collagen fibers in fibrocartilaginous tissues, similar to the annulus fibrosus of the intervertebral disc[36-38]. High levels of glucose drove contractile forces and increased proteoglycan, which ultimately had a negative effect on the formation of the collagen network. Fiber organization was maximal at low physiologic levels of glucose (500 mg/L), while the higher range of physiologic and super-physiologic concentrations (4500 mg/L) resulted in the formation of unaligned and disorganized fiber networks. Utilizing self-assembling tissue engineered IVD (TE-IVD) constructs[39-44] to investigate the impact of glucose on the formation of the engineered disc, we showed that these super-physiologic levels of glucose also had a detrimental effect on mechanics: TE-IVDs with elevated proteoglycan content and diminished fiber alignment in the AF region demonstrated lower equilibrium moduli when subjected to mechanical testing[38]. Mechanical integrity was ultimately found to correlate most with fiber alignment rather

than proteoglycan content, highlighting the importance of structure over composition on the function of the disc.

Interestingly, diabetics are reported to have fasting blood glucose levels greater than 1250 mg/L, while hyperglycemia occurs around 1800 mg/L[17]. Taken together this evidence suggests that diabetes may not only aggravate the progression of DDD but may in fact play a detrimental role in the developing disc by impeding fiber formation, leading to a highly disorganized and ultimately mechanically inferior matrix. The purpose of this study, therefore, was to investigate effect of hyperglycemia on the structure and mechanical function of developing intervertebral discs. Using discs collected from mouse caudal spines, we assessed biochemical composition, fiber structure, and mechanical response to find that diabetic animals demonstrated noticeable detrimental changes to the disc as compared to non-diabetics.

Materials and Methods

Sample Preparation

Whole tails were harvested from 3-4 month old female db/db (n=8) and db/+ (n=9) mice post-mortem as described previously[45]. Caudal spines were then collected from the tails per existing protocol[39,40].

Diabetic Characterization

Whole blood samples were collected at time of euthanasia following 6 hours of fasting, and fasting blood glucose levels were measured using a GLUCOCARD Vital blood glucose meter (ARKRAY, Edina, MN). A hemoglobin A1C (HbA1c) (Crystal Chem, Elk Grove Village, IL) assay was used to quantify glycemic control in these blood samples over the previous 2-3 months. Caudal discs were hydrolyzed in 12 N HCl for 3 hours to assay advanced glycation end product (AGE) content as previously

described[46]. Fluorescence was measured against a quinine standard and normalized to hydroxyproline.

Biochemical Assays

Discs were extracted from the CA9/10 space and lyophilized for 48 hours prior to overnight digestion in a papain digest buffer. Biochemical content was then measured for each whole disc, NP and AF regions included, as previously described[38,40,43]. A Hoescht DNA assay[47], modified 1,9-dimethylmethylene blue (DMMB) assay[48], and hydroxyproline (hypro) assay[49] were used to measure DNA, sulfated GAG (s-GAG), and collagen content, respectively. These values were then normalized to wet weights.

Mechanical Testing

Motion segments were collected from the CA7/8 disc space and adjacent vertebrae, then potted in polymethyl methacrylate (PMMA) (COE Tray Plastic, GC America, Alsip, IL) to prevent slippage during testing. To maintain hydration during mechanical tests, samples were wrapped in gauze soaked in PBS (Dulbecco's 1x PBS, Corning, NY) with added protease inhibitor (ThermoFisher Scientific, Waltham, MA). Segments were clamped at the potted ends and subjected to unconfined mechanical tests utilizing an ElectroForce (ELF) 5500 mechanical testing frame (TA Instruments, New Castle, DE) to determine biomechanical behavior.

Dynamic compressive responses were measured by applying a cyclic uniaxial loading protocol. A dynamic amplitude of 8% sinusoidal strain was imposed about the neutral position at 13 frequencies from 1 mHz to 1 Hz with 3 cycles per frequency. Time-dependent load response was measured at each of the frequencies. Effective equilibrium moduli and hydraulic permeability were calculated for wild type and

diabetic samples using previously described fiber-reinforced poroelastic models and custom MATLAB codes[50].

Following these tests a uniaxial stress-relaxation protocol consisting of 10 incremental steps of 5% strain each up to 50% total strain was imposed on each sample. Time-dependent load response was measured at each of the steps. Effective compressive moduli and hydraulic permeability were calculated for wild type and diabetic samples using previously described poroelastic models and custom MATLAB codes[40,51].

Histology

Motion segments from the aforementioned mechanical tests were prepared for histological assessment as previously described[40,43,52,53]. Segments were removed from the PMMA pots and cut closer to the endplates, then fixed in 10% buffered formalin for 48 hours prior to transfer to 70% ethanol. The segments were then decalcified, cut parallel to the sagittal plane, and sliced to 5-μm thick sections. Sections were stained with either Safranin-O and a fast green counterstain for proteoglycan content, or picrosirius red for collagen network visualization. Safranin-O and picrosirius red stained sections were imaged using brightfield microscopy, and picrosirus red stained sections were additionally imaged with polarized light microscopy to qualitatively assess collagen alignment through birefringent intensity.

Multiphoton Microscopy

Motion segments were generated using the CA8/9 disc and adjacent vertebrae, then placed in 10% buffered formalin and transferred to 70% ethanol after 48 hours. Samples were sliced down the sagittal axis prior to imaging with a Zeiss LSM i-880 confocal microscope. 10x/0.45 C-Apochromat water immersion and 20x/0.75 Fluor DICII objectives were used as previously described[36-38], and collagen fiber architecture

was captured using second harmonic generation (SHG), with reflectance between 437-464 nm.

Image Processing and Quantitative Assessment

Safranin-O images of the whole disc were processed using ImageJ for quantitative staining assessment. Images were deconvolved in ImageJ and split into red, green, and blue color channels, after which intensity normalization and background subtraction were performed on the red. Depth of stain was subsequently calculated as the ratio of the number of pixels in the stained region over the number of pixels in the whole disc. The relative dimensions of the NP were also quantified by taking the ratio of pixels in the NP region and dividing by the pixels in the whole disc.

SHG images of the AF regions at 20x magnitude were processed using ImageJ as previously described[54] for quantitative fiber orientation assessment. Briefly, initial processing steps include intensity normalization, sharpening, background subtraction (sliding paraboloid / rolling ball), and smoothing. Images were then converted to 8-bit greyscale before a final noise removal (despeckle) step was applied. Fiber orientation in the AF region was determined for wild type and diabetic samples using the OrientationJ plugin[55-57]. The resulting orientation angle distributions from 0 to +90° were filtered to remove baseline noise and then normalized to total number of samples for each experimental group. The distributions were assumed to be symmetric and were mirrored to generate histograms for -90° to +90° orientations.

Statistics

Dynamic stiffness was analyzed using a two-way ANOVA with repeated measures, followed by Tukey's test for post-hoc analysis in R Studio. Differences in fiber orientation angle distributions were assessed using a χ^2 test for independence in R

Studio. All other parameters were analyzed using a t-test in Matlab/Excel. Data are presented as mean ± standard deviation, with significance determined at $p<0.05$.

Results

db/db mice had an average fasting blood glucose level of 263.6 ± 37.0 mg/dL (Fig. 1a) and body mass of 53.34 ± 2.79 g (Fig 1c), and developed diabetes at 4-8 weeks of age. db/+ mice meanwhile had an average fasting blood glucose level of 52.1 ± 8.8 mg/dL (Fig. 1a) and body mass of 23.32 ± 2.03 g (Fig. 1c). Diabetic animals also had an average HbA1c level of 8.5 ± 1.3% compared to wild type mice at 4.0 ± 0.8% ($p<0.05$), with levels of 6.5% and higher indicative of diabetes (Fig. 1b). s-GAG content was higher in the diabetic discs, averaging at 34.0 ± 12.7 μg/mg compared to 27.8 ± 9.2 μg/mg in the wild type (Fig. 2a). Average collagen content as approximated from hydroxyproline concentration was also higher in the diabetic samples, with 300 ± 166 μg/mg present in the diabetic and 233 ± 134 μg/mg in the wild type discs (Fig. 2b). Wild type discs showed significantly higher cell content than their diabetic counterparts (Fig. 2c), with an average of 9.93 ± 4.46 μg/mg DNA content as compared to 7.02 ± 1.68 μg/mg in the diabetic discs ($p<0.05$). No significant differences in AGE content were detected between db/db (0.017 ± 0.005 μg quinine/μg hydroxyproline) and db/+ (0.016 ± 0.005 μg quinine/μg hydroxyproline) animals (Fig. 2D).

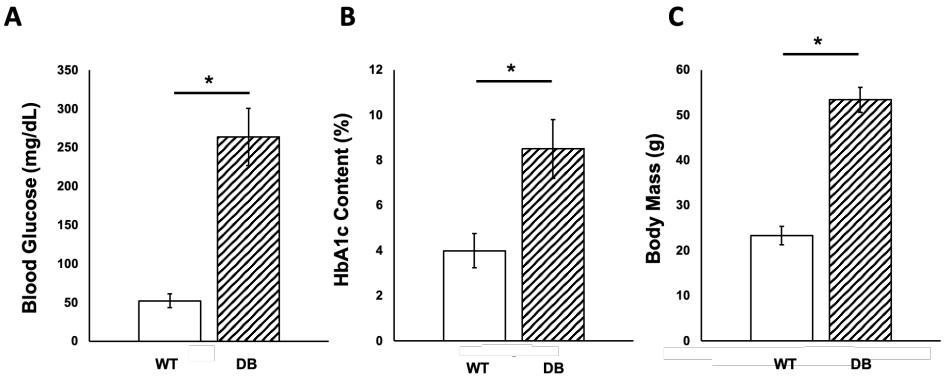

Figure 3.1. A) Fasting blood glucose level, **B)** percent HbA1c content, and **C)** body mass measured for each group. Significant differences ($p<0.05$) are indicated using (*) and bars. Error bars represent standard deviation. (n=8-9)

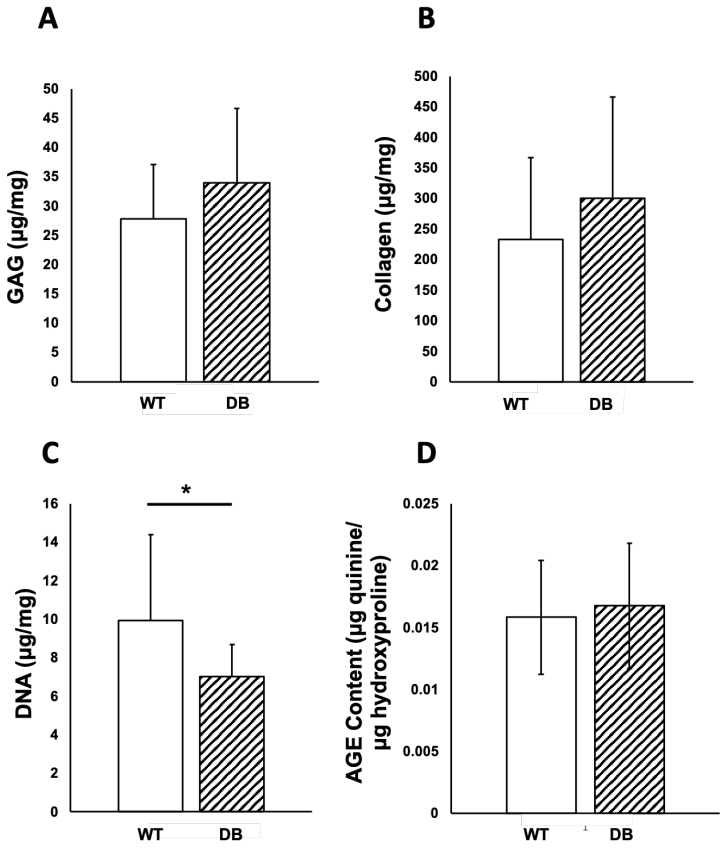

Figure 3.2. A) Whole disc sGAG concentration, **B)** whole disc collagen content, and **C)** whole disc DNA content normalized to wet weight for each group. **D)** AGE content normalized to hydroxyproline for each group. Significant differences ($p<0.05$) are indicated using (*) and bars. Error bars represent standard deviation. (n=8-9)

Gross histological images revealed morphological differences between the diabetic and wild type IVDs. The NP regions in the diabetic discs appeared more oval than their wild type counterparts, extending further into the disc with an irregular AF/NP boundary (Fig. 3). They were also significantly larger, accounting for approximately 41.8% of the whole disc area as compared to 35.1% in the wild type discs (Fig. S1a, $p<0.05$). Safranin-O staining for proteoglycan content also extended further past the NP boundary and into the inner AF for the diabetic discs as compared to the wild type, occupying 65.8% of the whole disc area in the former and 55.0% in the latter (Fig. S1b, $p<0.05$).

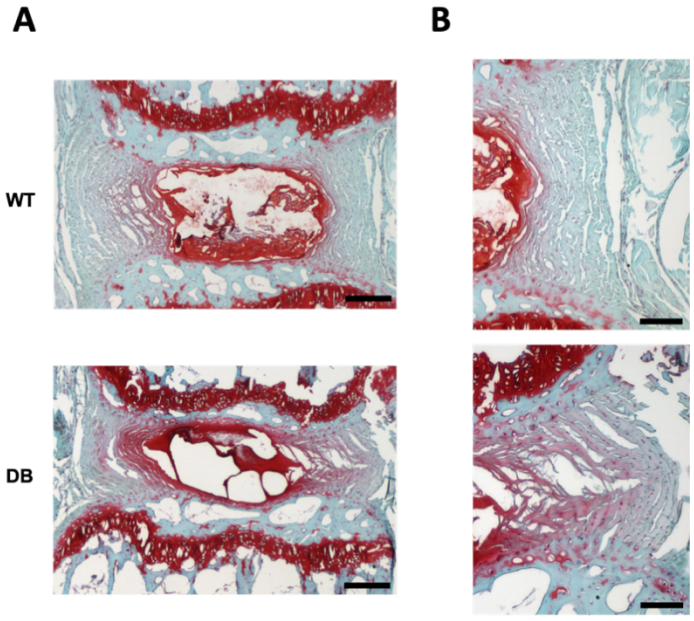

Figure 3.3. Representative histological images for Safranin-O staining of wild type (top) and diabetic (bottom) discs of **A)** the entire disc at 40x and **B)** the inner AF at 100x magnification. Significant differences ($p<0.05$) are indicated using (*) and bars. Error bars represent standard deviation while scale bars indicate 0.15 mm. (n=5-6)

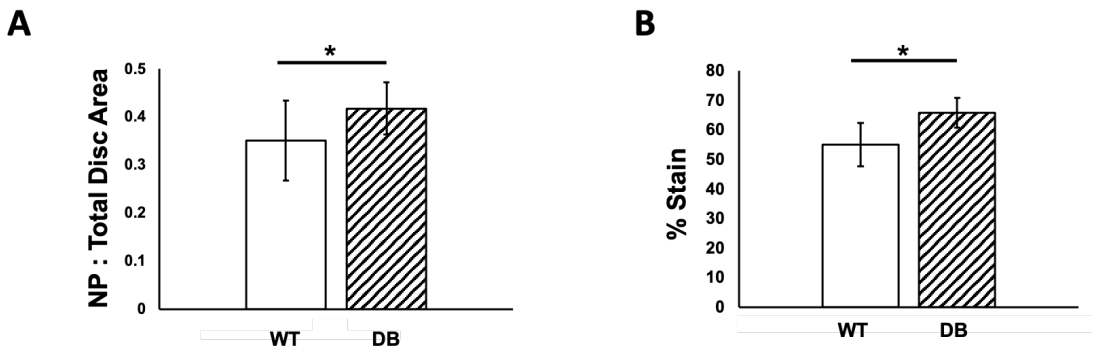

Supplemental Figure 3.1. A) Fraction of total disc area occupied by the NP for each group. **B)** Percent of total disc area occupied by Safranin-O staining. Significant differences ($p<0.05$) are indicated using (*) and bars. Error bars represent standard deviation while scale bars indicate 0.15 mm. (n=5-6)

SHG microscopy also revealed subtle qualitative differences in the collagen fiber architecture at the inner AF between the two groups. Collagen fibers at the AF/NP border in diabetic discs appeared more disorganized and less aligned than in the wild type samples, with larger gaps present between fiber bundles as well as bundles arranged at a wider variety of angles (Fig. 4). The fiber bundles in wild type IVDs were more tightly packed and oriented in a more parallel fashion. Quantitative analysis indicated two primary peaks in fiber orientation distribution for wild type discs, centered around $\pm$30° (Fig. 4c). These peaks were also present for the diabetic discs, though the peaks were less prominent than in the wild type and the overall curve flatter to indicate a wider range of angles (Fig. 4c). Approximately 10% and 13.3% of fibers lie within $\pm$5° of the main peaks for the diabetic and wild type discs, respectively. This trend of greater fiber organization in wild type IVDs continues as the range of angles increases, with $\pm$10° range yielding 20.0 and 26.4%; a $\pm$15°range yielding 29.9 and 39.2%; and a $\pm$20° range

yielding 39.9 and 51.4%, for example. Of the aforementioned values the groups were statistically distinct at the ±20° range alone (χ^2=121.89, p<0.05).

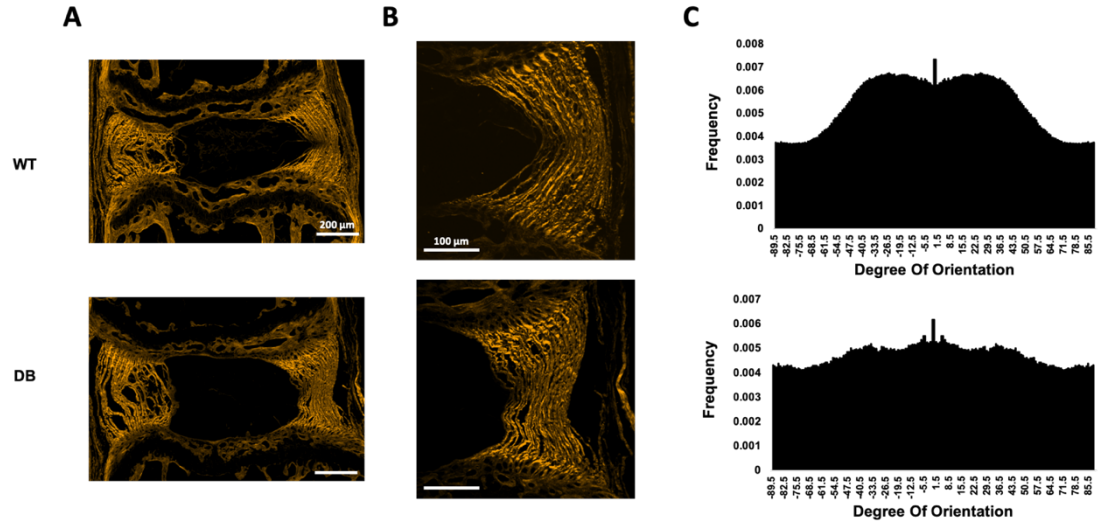

Figure 3.4. Representative SHG images for wild type (top) and diabetic (bottom) discs of **A)** the entire disc and **B)** the inner AF. **C)** Normalized fiber orientation distributions for wild type (top) and diabetic (bottom) discs. Scale bars indicate 200 (**A**) or 100 µm (**B**). (n=6-7)

In order to assess mechanical response, samples were subjected to a two-part mechanical testing protocol consisting of a) dynamic tension/compression about the neutral position and b) compressive stress-relaxation. Both diabetic and wild type discs demonstrated time- and frequency-dependent behavior in response to loading. Following cyclic testing, average dynamic stiffness increased from 518 MPa at 1 mHz to 998 kPa at 1 Hz for the diabetic samples, while the wild type demonstrated an average stiffness of 367 and 551 kPa at 1 mHz and 1 Hz, respectively (Fig. 5a, p<0.05). The dynamic stiffness data fit well to a poroelastic model (R^2 ranged from 0.84 to 0.99), enabling the calculation of an average equilibrium modulus of 232 kPa and hydraulic permeability of $1.1x10^{-14}$ m^2/Pa*s was calculated for the wild type segments, while the diabetic averaged 451 kPa and $0.761x10^{-14}$ m^2/Pa*s in comparison (Fig. 5b, 5c, p<0.05).

Stress relaxation data were also fit to a poroelastic model for calculation of material properties, with wild type samples having an average compressive modulus of 130 kPa and hydraulic permeability of $2.71x10^{-14}$ $m^2/Pa*s$ while their diabetic counterparts averaged 278 kPa and $0.981x10^{-14}$ $m^2/Pa*s$. (Fig. 5d, 5e, $p<0.05$).

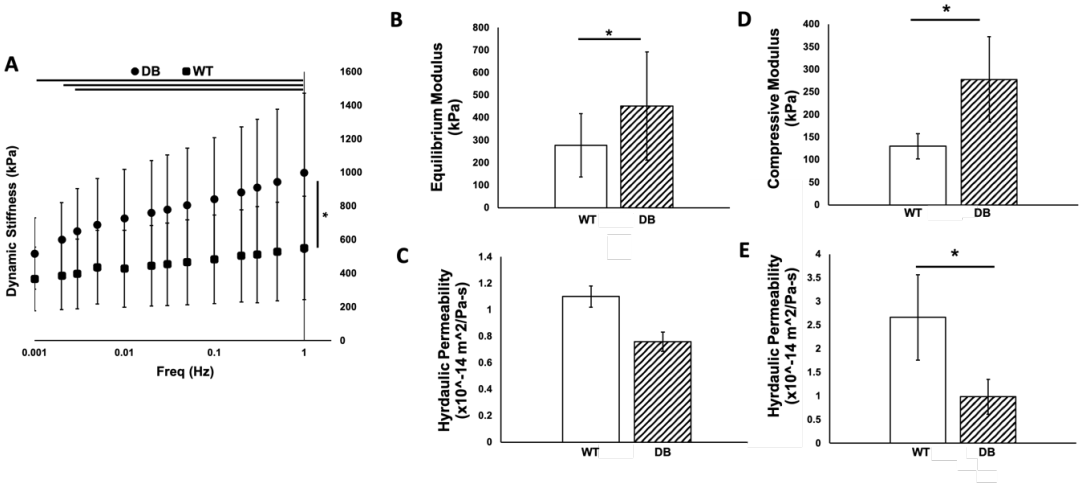

Figure 3.5. A) Dynamic stiffness for each group over 13 frequencies. **B)** Equilibrium modulus and **C)** hydraulic permeability determined from stiffness and phase angle values following cyclic tests for each group. **D)** Compressive modulus and **E)** hydraulic permeability determined from stress/relaxation tests for each group. Significant differences ($p<0.05$) are indicated using (*) and/or bars. Error bars represent standard deviation. (n=7-9)

Discussion

The objective of this study was to determine whether diabetes, a major risk factor for the development of DDD later in life, can generate significant degenerative changes to the developing IVD. Using caudal spines collected from 3-4-month-old db/db and db/+ mice, we quantified the structural and mechanical characteristics of the discs to determine if there were any major functional differences between diabetic and healthy animals. Our results indicate that increased levels of glucose appeared to impact the formation and deposition of fibers in the AF to produce an unaligned, disorganized matrix with biochemical and mechanical properties distinct from those present in physiologic or healthy levels of glucose.

In assessing ECM composition, we found that both s-GAG and collagen content were higher in the diabetic discs: the former demonstrated an average value approximately 22.1% larger than the wild type, the latter 29.0% larger. Assessment of the microscopy and histology images helped contribute to a better understanding of the trends in proteoglycan content. In the healthy disc, proteoglycans are primarily contained in the NP; they comprise 35-65% of the NP dry weight as opposed to 15-20% in the AF[6,58-63]. This is consistent with our wild type samples, where the NP had a regular cross-section and was contained by a defined inner AF. The boundary between these regions was distinct and the Safranin-O staining was limited to the NP; it did not appear to encroach beyond the NP border into the inner AF. In diabetic animals, however, a large and distorted NP occupied more space in the disc: the NP regions were larger than the wild type by 10.7%. The NP/AF boundary was ill-defined compared to the wild type discs, with a disorganized fiber network in the inner AF allowing for deeper penetration of the Safranin-O stain further into the annulus, with 6.7% greater staining, indicating a higher proteoglycan content than in healthy animals.

Analysis of the collagen structure of AF showed significant differences between diabetic and wild type mice. SHG microscopy revealed that the inner AF of the diabetic animals was structurally distinct from their wild type counterparts, and appeared more disorganized, similar to what is seen in degeneration[64]. Compiling quantitative fiber orientation data supported this observation, showing that healthy fiber networks demonstrated clean peaks in orientation at $\pm 30^{o}$, producing a bimodal distribution, while the those in diabetic IVDs ranged across a broader distribution with less defined peaks. Taken together these data point to a disruption in the structure of the disc that is associated with changes in biochemical components. Collectively, these data indicate that in diabetic animals, hyperglycemic levels of glucose were associated with an increase in proteoglycan production and a disruption in collagen organization.

Assessment of mechanical properties provided insight into the functional consequences of biochemical and structural changes in IVD from diabetic animals. During cyclic testing, diabetic discs demonstrated almost twice the dynamic stiffness of their wild type counterparts. When the dynamic stiffness and phase angle data from the cyclic tests were fit to a poroelastic model, the resulting equilibrium modulus and hydraulic permeability values observed the same trends: diabetic discs had approximately twice the moduli of their wild type counterparts and half the permeability. Analysis of the stress-relaxation data had comparable differences between the experimental groups, with diabetic discs demonstrating an approximately two-fold increase in compressive modulus over the wild type as well as about half the hydraulic permeability. Both the wild type and diabetic groups demonstrated dynamic moduli that were almost twice their stress-relaxation counterparts, likely explained by the differences between the tests. While stress-relaxation consists of solely compression, dynamic testing has an aspect of tension, and this incorporation may explain the two-fold increase in dynamic modulus over stress-relaxation modulus. Despite these differences, the measured moduli are comparable to what has been seen in previous rodent *in vivo* studies. Rat tail IVDs extracted from the caudal spine demonstrated an average compressive modulus of 238 kPa following the same stress-relaxation loading protocol used in this study[40]. Mouse caudal IVDs have been shown to range from 160 kPa to 2.48 MPa as compared to the 430 kPa – 3.65 MPa range seen in lumbar IVDs when exposed to a variety of testing regimes[65]. These results indicate that the diabetic discs were significantly stiffer than the wild type and had a greater resistance to deformation as well as taking markedly longer to recover from deformation, as seen in previous studies[33,66].

Numerous studies have determined a strong correlation between diabetes and DDD, as well as investigated the mechanisms by which diabetes and its comorbidities

aggravate disc degeneration. As a consequence of long-term hyperglycemia the formation of AGEs is accelerated, the accumulation of which severely damages tissues on their own as well as stimulates the production of biologic mechanisms and other byproducts, such as oxidative species, which further degeneration[67]. For example activation of MMP-13, one of the main metalloproteinases associated with increased catabolism in DDD, is found to be stimulated by the presence of reactive oxygen species (ROS)[34,67-69]. Hyperglycemia has also been found to promote the expression of factors which trigger apoptosis or senescence in discogenic cells, accelerating the progression of DDD in diabetic animals[26,35]. Additionally, the receptor for AGE (RAGE) has been implicated as a trigger for further inflammatory responses in the disc[70-72]. Increases in RAGE content via AGE accumulation, for example, has been shown to directly impact AF structure, resulting in increased collagen disruption and degeneration[69,70]. The structural changes brought about by early onset diabetes on developing discs, however, is less understood.

A striking feature of this model is the lack of AGE accumulation in these young animals. Despite this lack of accumulation, there are clear changes to the ECM in the diabetic animals, notably significant deposition of proteoglycans in the inner AF. Interestingly, higher levels of AGEs present in diabetic animals have been shown to correlate with decreased proteoglycan content[73-75]. Our findings demonstrate that diabetic animals show distinct detrimental changes even at a young age and in the absence of AGE accumulation. These data indicate that the disease affects the manner in which the immature disc is formed via an imbalance in its composition. Ultimately this imbalance results in structural changes to the complex fiber architecture of the AF and the distinct AF/NP boundary which serves to contain the NP, consequences of an inferior matrix deposited by cells with altered metabolism. It has been established that the IVD's structure is fundamental to its function[58,76,77] , evident here where the disc's

ability to resist deformation is significantly impaired under diabetic conditions. Collectively our data suggests that while diabetes accelerates the progression of DDD later in life through the accumulation of AGEs, hyperglycemia associated with diabetes predisposes the disc to the disease during developmental stages by producing an ECM that is too rich in proteoglycans and deficient in fiber formation.

This deficiency in fiber formation is consistent with previous *in vitro* studies examining the effect of glucose media content on engineered fibrocartilage[36-38]. In general, many of the same trends we observed *in vitro* in the development of TE-IVDs were reflected in this *in vivo* study. Wild type mice in our cohort averaged a fasting blood glucose level of 52.1 mg/dl (or 521 mg/L), in line with the *in vitro* optimal glucose concentration (500 mg/L) that yielded both the highest degree of fiber alignment[36-38] and the highest effective stiffness[38]. db/db mice in our cohort meanwhile averaged a hyperglycemic blood glucose concentration of 263.6 mg/dL (2636 mg/L) when tested. This value lies between the two high glucose concentrations examined *in vitro*: 1000 mg/L (high physiologic) and 4500 mg/L (super-physiologic)[36-38]. The 4500 mg/L engineered group demonstrated the most dramatic response to increased glucose, with reduced fiber alignment and impaired mechanics; in fact, these parameters were comparable to what was seen in the sub-physiologic culture groups. The 1000 mg/L group, while not as drastic, saw a substantial decrease in these parameters as compared to the 500 mg/L group, indicating that glucose levels at the cusp of the physiologic limit will already affect the disc cell population and alter their metabolism, impacting their ability to effectively produce and maintain matrix.

In these engineered discs, media glucose directly affected biochemical composition as higher glucose content yielded higher proteoglycan content. These elevated proteoglycan levels in turn negatively impacted the disc's collagen network, generating a disorganized and ultimately inferior matrix. Constructs in this study

averaged an order of magnitude lower modulus than native discs even with the increased mechanical stability of the 500 mg/L group. In this current study, however, the diabetic discs were significantly stiffer than what is normally expected in healthy mice[66,78-80]. Hyperglycemia, then, led to a higher modulus *in vitro* but a lower modulus *in vivo*. A potential explanation for this discrepancy is that the engineered discs had an average sGAG concentration ranging from 0.99 µg/mg at 125 mg/L glucose to 2.02 µg/mg at 500 mg/L[38] while murine discs averaged 27.8 µg/mg (wild type) to 34.0 µg/mg (diabetic). As the engineered discs contain approximately an order of magnitude less sGAG than the harvested discs, they may not contain sufficient amounts of proteoglycans to appreciably influence the mechanics as compared to the *in vivo* discs. Changes in the *in vivo* mechanics, then, appear to be driven primarily by the increase in proteoglycan content and NP size. In combination with these observations, collagen content as indicated from the biochemical assay likely also influenced disc mechanics, as diabetic discs contained 29.0% more collagen than the wild type, while in our *in vitro* study there was no appreciable difference in collagen content between discs. In DDD, increased stiffness in the disc and in the calcified cartilaginous end plates (CEPs) results in an impaired ability to swell and recover from compressive loading[4-6,64,78,81,82]: when subjected to loads, disc height and water content decrease at a higher rate and an equilibrium state is achieved more slowly than in healthy discs. Continued loading leads to the propagation of damage as cracks or tears throughout the AF, further disrupting its integrity and potentially resulting in bulging, herniation, or eventual destabilization of the entire motion segment[6].

One of the potential limitations of this study is that the db/db mutation in mice not only results in diabetes but also leads to additional phenotypical changes such as obesity. The db/+ mice in our cohort had an average body mass of 23.32 g while the db/db mice averaged a significantly higher body mass of 53.34 g (Fig. S1b, $p<0.05$).

Obesity has been implicated as a major risk factor for DDD as well as a common comorbidity for diabetes[28,33,83,84] and as such the effects may be difficult to divorce from those arising as a result of diabetic hyperglycemia alone. However as the discs were extracted from the tails of the animals, any loading effects resulting from obesity are likely minimal. We also note that while the mice used here are 3-4 months of age and are therefore young animals, not infants, db/db mice at this age are not yet fully grown[85,86]. As a result, the discs are likely still maturing along with the organism and may yet provide interesting insight into the mechanisms by which the diabetic disc arises. Finally, due to the small size of murine caudal discs, NP and AF regions could not be separated for biochemical analysis. Given the histological assessments here indicated significant structural alterations to both the NP and inner AF sections of the diabetic disc, further analysis of the compositional changes associated with these observations could provide additional insight into the mechanisms responsible.

In conclusion, we found that diabetes and its associated hyperglycemia impact matrix formation in the IVD prior to the onset of DDD and independently of the accumulation of AGEs. Diabetic discs with super-physiologic glucose levels displayed elevated proteoglycan content as compared to the wild type mice; these trends corresponded to a greater degree of disorganization in the AF, ill-defined AF/NP boundaries, and impaired mechanical response to deformation. Ultimately these observations indicate that diabetes impacts discogenic cells' ability to effectively produce and maintain matrix in development, altering the disc's basic structure and biomechanical function in such a manner that the disc is now primed for DDD later in life.

Acknowledgments

The authors would like to thank Drs. Eliot Frank and Alan Grodzinsky for

generously providing their MATLAB code for fiber-reinforced poroelastic fits, as well as Leigh Slyker for his immense help with MATLAB, and the Anna K. Cunningham and Mary E. Cunningham Trust for stipend support. This work was supported by the following funding sources: the Colin MacDonald Fund, the Daedalus Innovation Fund, and the Center for Advanced Technology from the New York State Advanced Research Fund (NYSTAR).

REFERENCES

[1] Fatoye F, Gebrye T, Odeyemi I. Real-world incidence and prevalence of low back pain using routinely collected data. *Rheumatol Int*. 2019;39(4):619-626.

[2] Rubin DI. Epidemiology and risk factors for spine pain. *Neurol Clin*. 2007;25(2):353-371.

[3] Luoma K, Riihimäki H, Luukkonen R, Raininko R, Viikari-Juntura E, Lamminen A. Low back pain in relation to lumbar disc degeneration. *Spine (Phila Pa 1976)*. 2000;25(4):487-492.

[4] Urban JP, Roberts S. Degeneration of the intervertebral disc. *Arthritis Res Ther*. 2003;5(3):120-130.

[5] Molinos M, Almeida CR, Caldeira J, Cunha C, Gonçalves RM, Barbosa MA. Inflammation in intervertebral disc degeneration and regeneration. *J R Soc Interface*. 2015;12(108):20150429.

[6] Buckwalter JA. Aging and degeneration of the human intervertebral disc. *Spine (Phila Pa 1976)*. 1995;20(11):1307-1314.

[7] Lyons G, Eisenstein SM, Sweet MB. Biochemical changes in intervertebral disc degeneration. *Biochim Biophys Acta*. 1981;673(4):443-453.

[8] Freemont AJ, Watkins A, Le Maitre C, Jeziorska M, Hoyland JA. Current understanding of cellular and molecular events in intervertebral disc degeneration: implications for therapy. *J Pathol*. 2002;196(4):374-379.

[9] Liu J, Roughley PJ, Mort JS. Identification of human intervertebral disc stromelysin and its involvement in matrix degradation. *J Orthop Res*. 1991;9(4):568-575.

[10] Liu MH, Sun C, Yao Y, Fan X, Liu H, Cui YH, Bian XW, Huang B, Zhou Y. Matrix stiffness promotes cartilage endplate chondrocyte calcification in disc degeneration via miR-20a targeting ANKH expression. *Sci Rep*. 2016;6:25401.

[11] Kanemoto M, Hukuda S, Komiya Y, Katsuura A, Nishioka J. Immunohistochemical study of matrix metalloproteinase-3 and tissue inhibitor of metalloproteinase-1 human intervertebral discs. *Spine (Phila Pa 1976)*. 1996;21(1):1-8.

[12] Nemoto O, Yamagishi M, Yamada H, Kikuchi T, Takaishi H. Matrix metalloproteinase-3 production by human degenerated intervertebral disc. *Journal of Spinal Disorders*. 1997;10(6):493-498.

[13] Kang JD, Georgescu HI, McIntyre-Larkin L, Stefanovic-Racic M, Evans CH. Herniated cervical intervertebral discs spontaneously produce matrix metalloproteinases, nitric oxide, interleukin-6, and prostaglandin E2. *Spine (Phila Pa 1976)*. 1995;20(22):2373-2378.

[14] Kang JD, Georgescu HI, McIntyre-Larkin L, Stefanovic-Racic M, Donaldson WF 3rd, Evans CH. (1996). Herniated lumbar intervertebral discs spontaneously produce matrix metalloproteinases, nitric oxide, interleukin-6, and prostaglandin E2. *Spine (Phila Pa 1976)*. 1996;21(3):271-277.

[15] Guthrie RA, Guthrie DW. Pathophysiology of diabetes mellitus. *Crit Care Nurs Q*. 2004;27(2):113-125.

[16] Schmidt AM. Highlighting Diabetes Mellitus: The Epidemic Continues. *Arterioscler Thromb Vasc Biol*. 2018;38(1):e1-e8.

[17] American Diabetes Association. 2. Classification and diagnosis of diabetes. *Diabetes Care*. 2015;38(Supplement 1): S8-S16.

[18] Lascar N, Brown J, Pattison H, Barnett AH, Bailey CJ, Bellary S. Type 2 diabetes in adolescents and young adults. *Lancet Diabetes Endocrinol*. 2018;6(1):69-80.

[19] International Diabetes Federation. *IDF Diabetes Atlas, 9th edn.* 2019.

[20] Gaiz A, Mosawy S, Colson N, Singh I. Thrombotic and cardiovascular risks in type two diabetes; Role of platelet hyperactivity. Biomed Pharmacother. 2017 Oct;94:679-686.

[21] Cole JB, Florez JC. Genetics of diabetes mellitus and diabetes complications. *Nat Rev Nephrol*. 2020;16(7):377-390.

[22] Zheng Y, Ley SH, Hu FB. Global aetiology and epidemiology of type 2 diabetes mellitus and its complications. *Nat Rev Endocrinol*. 2018;14(2):88-98.

[23] Cannata F, Vadalà G, Ambrosio L, Fallucca S, Napoli N, Papalia R, Pozzilli P, Denaro V. Intervertebral disc degeneration: A focus on obesity and type 2 diabetes. *Diabetes Metab Res Rev*. 2020;36(1):e3224.

[24] Alpantaki K, Kampouroglou A, Koutserimpas C, Effraimidis G, Hadjipavlou A. Diabetes mellitus as a risk factor for intervertebral disc degeneration: a critical review. *Eur Spine J*. 2019;28(9):2129-2144.

[25] Li X, Liu X, Wang Y, Cao F, Chen Z, Hu Z, Yu B, Feng H, Ba Z, Liu T, Li H, Jiang B, Huang Y, Li L, Wu D. Intervertebral disc degeneration in mice with type II

diabetes induced by leptin receptor deficiency. *BMC Musculoskelet Disord*. 2020;21(1):77.

[26] Zhang Y, Proenca R, Maffei M, Barone M, Leopold L, Friedman JM. Positional cloning of the mouse obese gene and its human homologue [published correction appears in Nature 1995 Mar 30;374(6521):479]. *Nature*. 1994;372(6505):425-432.

[27] Kivimäki M, Virtanen M, Kawachi I, Nyberg ST, Alfredsson L, Batty GD, Bjorner JB, Borritz M, Brunner EJ, Burr H, Dragano N, Ferrie JE, Fransson EI, Hamer M, Heikkilä K, Knutsson A, Koskenvuo M, Madsen IEH, Nielsen ML, Nordin M, Oksanen T, Pejtersen JH, Pentti J, Rugulies R, Salo P, Siegrist J, Steptoe A, Suominen S, Theorell T, Vahtera J, Westerholm PJM, Westerlund H, Singh-Manoux A, Jokela M. Long working hours, socioeconomic status, and the risk of incident type 2 diabetes: a meta-analysis of published and unpublished data from 222 120 individuals. *Lancet Diabetes Endocrinol*. 2015;3(1):27-34.

[28] Jakoi AM, Pannu G, D'Oro A, Buser Z, Pham MH, Patel NN, Hsieh PC, Liu JC, Acosta FL, Hah R, Wang JC. The Clinical Correlations between Diabetes, Cigarette Smoking and Obesity on Intervertebral Degenerative Disc Disease of the Lumbar Spine. *Asian Spine J*. 2017;11(3):337-347.

[29] Sakellaridis N. The influence of diabetes mellitus on lumbar intervertebral disk herniation. *Surg Neurol*. 2006;66(2):152-154.

[30] Anekstein Y, Smorgick Y, Lotan R, Agar G, Shalmon E, Floman Y, Mirovsky Y. Diabetes mellitus as a risk factor for the development of lumbar spinal stenosis. *Isr Med Assoc J*. 2010;12(1):16-20.

[31] Teraguchi M, Yoshimura N, Hashizume H, Muraki S, Yamada H, Minamide A, Oka H, Ishimoto Y, Nagata K, Kagotani R, Takiguchi N, Akune T, Kawaguchi H, Nakamura K, Yoshida M. Prevalence and distribution of intervertebral disc degeneration over the entire spine in a population-based cohort: the Wakayama Spine Study. *Osteoarthritis Cartilage*. 2014;22(1):104-110.

[32] Mobbs RJ, Newcombe RL, Chandran KN. Lumbar discectomy and the diabetic patient: incidence and outcome. J Clin Neurosci. 2001;8(1):10-13

[33] Mahmoud M, Kokozidou M, Auffarth A, Schulze-Tanzil G. The Relationship between Diabetes Mellitus Type II and Intervertebral Disc Degeneration in Diabetic Rodent Models: A Systematic and Comprehensive Review. *Cells*. 2020;9(10):2208.

[34] Wang J, Hu J, Chen X, Huang C, Lin J, Shao Z, Gu M, Wu Y, Tian N, Gao W, Zhou Y, Wang X, Zhang X. BRD4 inhibition regulates MAPK, NF-κB signals, and autophagy to suppress MMP-13 expression in diabetic intervertebral disc degeneration. *FASEB J*. 2019;33(10):11555-11566.

[35] Jiang L, Zhang X, Zheng X, Ru A, Ni X, Wu Y, Tian N, Huang Y, Xue E, Wang X, Xu H.. Apoptosis, senescence, and autophagy in rat nucleus pulposus cells: Implications for diabetic intervertebral disc degeneration. *J Orthop Res*. 2013;31(5):692-702.

[36] McCorry MC, Kim J, Springer NL, Sandy J, Plaas A, Bonassar LJ. Regulation of proteoglycan production by varying glucose concentrations controls fiber formation in tissue engineered menisci. *Acta Biomater*. 2019;100:173-183.

[37] Kim J, Boys AJ, Estroff LA, Bonassar LJ. Combining TGF-β1 and Mechanical Anchoring to Enhance Collagen Fiber Formation and Alignment in Tissue-Engineered Menisci. *ACS Biomater Sci Eng*. 2021;7(4):1608-1620.

[38] Lintz ML, Bonassar LJ. Physiologic Levels of Glucose Drive Fiber Alignment in Tissue-Engineered Intervertebral Discs. In preparation 2021.

[39] Bowles RD, Williams RM, Zipfel WR, Bonassar LJ. Self-assembly of aligned tissue-engineered annulus fibrosus and intervertebral disc composite via collagen gel contraction. *Tissue Eng Part A*. 2010;16(4):1339-1348.

[40] Bowles RD, Gebhard HH, Härtl R, Bonassar LJ. Tissue-engineered intervertebral discs produce new matrix, maintain disc height, and restore biomechanical function to the rodent spine. *Proc Natl Acad Sci U S A*. 2011;108(32):13106-13111.

[41] Bowles RD, Gebhard HH, Dyke JP, Ballon DJ, Tomasino A, Cunningham ME, Härtl R, Bonassar, LJ. Image-based tissue engineering of a total intervertebral disc implant for restoration of function to the rat lumbar spine. *NMR Biomed*. 2012;25(3):443-451.

[42] Hudson KD, Mozia RI, Bonassar LJ. Dose-dependent response of tissue-engineered intervertebral discs to dynamic unconfined compressive loading. *Tissue Eng Part A*. 2015;21(3-4):564-572.

[43] Moriguchi Y, Mojica-Santiago J, Grunert P, Pennicooke B, Berlin C, Khair T, Navarro-Ramirez R, Arbona RJR, Nguyen J, Härtl R, Bonassar LJ. Total disc replacement using tissue-engineered intervertebral discs in the canine cervical spine. *PLoS One*. 2017;12(10):e0185716.

[44] Mojica-Santiago JA, Lang GM, Navarro-Ramirez R, Hussain I, Härtl R, Bonassar LJ. Resorbable plating system stabilizes tissue-engineered intervertebral discs implanted ex vivo in canine cervical spines. *JOR Spine*. 2018;1(3):e1031.

[45] Walk RE, Tang SY. In vivo contrast-enhanced microCT for the monitoring of mouse thoracic, lumbar, and coccygeal intervertebral discs. *JOR Spine*. 2019;2(2):e1058.

[46] Tang SY, Zeenath U, Vashishth D. Effects of non-enzymatic glycation on cancellous bone fragility. *Bone*. 2007;40(4):1144-1151.

[47] Kim YJ, Sah RL, Doong JY, Grodzinsky AJ. Fluorometric assay of DNA in cartilage explants using Hoechst 33258. *Anal Biochem*. 1988;174(1):168-176.

[48] Enobakhare BO, Bader DL, Lee DA. Quantification of sulfated glycosaminoglycans in chondrocyte/alginate cultures, by use of 1,9-dimethylmethylene blue. *Anal Biochem*. 1996;243(1):189-191.

[49] Neuman R, Logan M. The determination of hydroxyproline. *J Biol Chem*. 1950;184(1):299-306.

[50] Frank EH, Grodzinsky AJ. Cartilage electromechanics--II. A continuum model of cartilage electrokinetics and correlation with experiments. *J Biomech*. 1987;20(6):629-639.

[51] Kim YJ, Bonassar LJ, Grodzinsky AJ. The role of cartilage streaming potential, fluid flow and pressure in the stimulation of chondrocyte biosynthesis during dynamic compression. *J Biomech*. 1995;28(9):1055-1066.

[52] Sloan SR Jr, Wipplinger C, Kirnaz S, Navarro-Ramirez R, Schmidt F, McCloskey D, Pannellini T, Schiavinato A, Härtl R, Bonassar LJ.. Combined nucleus pulposus augmentation and annulus fibrosus repair prevents acute intervertebral disc degeneration after discectomy. *Sci Transl Med*. 2020;12(534):eaay2380.

[53] Hussain I, Sloan SR, Wipplinger C, Navarro-Ramirez R, Zubkov M, Kim E, Kirnaz S, Bonassar LJ, Härtl R. Mesenchymal Stem Cell-Seeded High-Density Collagen Gel for Annular Repair: 6-Week Results From In Vivo Sheep Models. *Neurosurgery*. 2019;85(2):E350-E359.

[54] Morrill EE, Tulepbergenov AN, Stender CJ, Lamichhane R, Brown RJ, Lujan TJ. A validated software application to measure fiber organization in soft tissue. *Biomech Model Mechanobiol*. 2016;15(6):1467-1478.

[55] Püspöki Z, Storath M, Sage D, Unser M. Transforms and Operators for Directional Bioimage Analysis: A Survey. *Adv Anat Embryol Cell Biol*. 2016;219:69-93.

[56] Rezakhaniha R, Agianniotis A, Schrauwen JT, et al. Experimental investigation of collagen waviness and orientation in the arterial adventitia using confocal laser scanning microscopy. *Biomech Model Mechanobiol*. 2012;11(3-4):461-473.

[57] Fonck E, Feigl GG, Fasel J, Sage D, Unser M, Rüfenacht DA, Stergiopulos N. Effect of aging on elastin functionality in human cerebral arteries. *Stroke*. 2009;40(7):2552-2556.

[58] Newell N, Little JP, Christou A, Adams MA, Adam CJ, Masouros SD. Biomechanics of the human intervertebral disc: A review of testing techniques and results. *J Mech Behav Biomed Mater*. 2017;69:420-434.

[59] Dickson IR, Happey F, Pearson CH, Naylor A, Turner RL. Variations in the protein components of human intervertebral disk with age. *Nature*. 1967;215(5096):52-53.

[60] Iatridis JC, Weidenbaum M, Setton LA, Mow VC. Is the nucleus pulposus a solid or a fluid? Mechanical behaviors of the nucleus pulposus of the human intervertebral disc. *Spine (Phila Pa 1976)*. 1996;21(10):1174-1184.

[61] McDevitt, Cahir A. "Proteoglycans of the intervertebral disc." *The Biology of the Intervertebral Disc. Boca Raton, Fla* (1988).

[62] Eyre DR, Muir H. Types I and II collagens in intervertebral disc. Interchanging radial distributions in annulus fibrosus. *Biochem J*. 1976;157(1):267-270.

[63] Eyre, David R. "Collagens of the disc." *Biology of* (1988).

[64] Dowdell J, Erwin M, Choma T, Vaccaro A, Iatridis J, Cho SK. Intervertebral Disk Degeneration and Repair. *Neurosurgery*. 2017;80(3S):S46-S54.

[65] Sarver JJ, Elliott DM. Mechanical differences between lumbar and tail discs in the mouse. *J Orthop Res*. 2005;23(1):150-155.

[66] Krishnamoorthy D, Hoy RC, Natelson DM, Torre OM, Laudier DM, Iatridis JC, Illien-Jünger S. Dietary advanced glycation end-product consumption leads to mechanical stiffening of murine intervertebral discs. *Dis Model Mech*. 2018;11(12):dmm036012.

[67] Waldron AL, Schroder PA, Bourgon KL, Bolduc JK, Miller JL, Pellegrini AD, Dubois AL, Blaszkiewicz M, Townsend KL, Rieger S. Oxidative stress-dependent MMP-13 activity underlies glucose neurotoxicity. *J Diabetes Complications*. 2018;32(3):249-257.

[68] Chen YJ, Chan DC, Lan KC, Wang CC, Chen CM, Chao SC, Tsai KS, Yang RS, Liu SH. PPARγ is involved in the hyperglycemia-induced inflammatory responses and collagen degradation in human chondrocytes and diabetic mouse cartilages. *J Orthop Res*. 2015;33(3):373-381.

[69] Chen YJ, Chan DC, Chiang CK, Wang CC, Yang TH, Lan KC, Chao SC, Tsai KS, Yang RS, Liu SH. Advanced glycation end-products induced VEGF production and inflammatory responses in human synoviocytes via RAGE-NF-κB pathway activation. *J Orthop Res*. 2016;34(5):791-800.

[70] Hoy RC, D'Erminio DN, Krishnamoorthy D, Natelson DM, Laudier DM, Illien-Jünger S, Iatridis JC. Advanced glycation end products cause RAGE-dependent annulus fibrosus collagen disruption and loss identified using in situ second harmonic generation imaging in mice intervertebral disk in vivo and in organ culture models. *JOR Spine*. 2020;3(4):e1126.

[71] Illien-Jünger S, Palacio-Mancheno P, Kindschuh WF, Chen X, Sroga GE, Vashishth D, Iatridis JC. Dietary Advanced Glycation End Products Have Sex- and Age-Dependent Effects on Vertebral Bone Microstructure and Mechanical Function in Mice. *J Bone Miner Res*. 2018;33(3):437-448.

[72] Nerlich AG, Bachmeier BE, Schleicher E, Rohrbach H, Paesold G, Boos N. Immunomorphological analysis of RAGE receptor expression and NF-kappaB activation in tissue samples from normal and degenerated intervertebral discs of various ages. *Ann N Y Acad Sci*. 2007;1096:239-248.

[73] Yokosuka K, Park JS, Jimbo K, Yamada K, Sato K, Tsuru M, Takeuchi M, Yamagishi S, Nagata K. Advanced glycation end-products downregulating intervertebral disc cell production of proteoglycans in vitro. *J Neurosurg Spine*. 2006:324-329.

[74] Fields AJ, Berg-Johansen B, Metz LN, Miller S, La B, Liebenberg EC, Coughlin DG, Graham JL, Stanhope KL, Havel PJ, Lotz JC. Alterations in intervertebral disc composition, matrix homeostasis and biomechanical behavior in the UCD-T2DM rat model of type 2 diabetes. *J Orthop Res*. 2015;33(5):738-746.

[75] Illien-Jünger S, Grosjean F, Laudier DM, Vlassara H, Striker GE, Iatridis JC. Combined anti-inflammatory and anti-AGE drug treatments have a protective effect on intervertebral discs in mice with diabetes. *PLoS One*. 2013;8(5):e64302.

[76] Humzah MD, Soames RW. Human intervertebral disc: structure and function. *Anat Rec*. 1988;220(4):337-356.

[77] Adams MA, Roughley PJ. What is intervertebral disc degeneration, and what causes it? *Spine (Phila Pa 1976)*. 2006;31(18):2151-2161.

[78] Liu JW, Abraham AC, Tang SY. The high-throughput phenotyping of the viscoelastic behavior of whole mouse intervertebral discs using a novel method of dynamic mechanical testing. *J Biomech*. 2015;48(10):2189-2194.

[79] Walter BA, Korecki CL, Purmessur D, Roughley PJ, Michalek AJ, Iatridis JC. Complex loading affects intervertebral disc mechanics and biology. *Osteoarthritis Cartilage*. 2011;19(8):1011-1018.

[80] Iatridis JC, Nicoll SB, Michalek AJ, Walter BA, Gupta MS. Role of biomechanics in intervertebral disc degeneration and regenerative therapies: what needs repairing in the disc and what are promising biomaterials for its repair?. *Spine J*. 2013;13(3):243-262.

[81] Antoniou J, Steffen T, Nelson F, Winterbottom N, Hollander AP, Poole RA, Aebi M, Alini M. The human lumbar intervertebral disc: evidence for changes in the biosynthesis and denaturation of the extracellular matrix with growth, maturation, ageing, and degeneration. *J Clin Invest*. 1996;98(4):996-1003.

[82] Colombini A, Lombardi G, Corsi MM, Banfi G. Pathophysiology of the human intervertebral disc. *Int J Biochem Cell Biol*. 2008;40(5):837-842.

[83] Coppock JA, Danyluk ST, Englander ZA, Spritzer CE, Goode AP, DeFrate LE. Increasing BMI increases lumbar intervertebral disc deformation following a treadmill walking stress test [published online ahead of print, 2021 Mar 20]. *J Biomech*. 2021;121:110392.

[84] Parenteau CS, Lau EC, Campbell IC, Courtney A. Prevalence of spine degeneration diagnosis by type, age, gender, and obesity using Medicare data. *Sci Rep*. 2021;11(1):5389.

[85] Srinivasan K, Ramarao P. Animal models in type 2 diabetes research: an overview. *Indian J Med Res*. 2007;125(3):451-472.

[86] Lindström P. The physiology of obese-hyperglycemic mice [ob/ob mice]. *Scientific World Journal*. 2007;7:666-685.

CHAPTER 4

In Vivo Assessment of Biodegradable Support Structures for Total Disc Replacement in the Minipig Cervical Spine [3]

Abstract

In recent years, there has been an increase in efforts to translate tissue engineered strategies for total disc repair (TDR) to large animal models. Previous work in an *in vivo* canine cervical spine model demonstrated that at 6 weeks post-implantation, constructs resembled native intervertebral discs (IVDs) with respect to biochemical and biomechanical behavior after successful tissue integration. However, additional surgical techniques were deemed necessary to overcome geometrical constraints imposed by the curvature of the canine spine and prevent implant displacement. To address the complex loading profiles imposed by large animal spines and move the work to a more clinically relevant animal model, we developed a resorbable delivery vehicle to provide mechanical support to soft engineered constructs delivered to the Göttingen minipig cervical spine. Two- and one-piece cage designs were found to be mechanically sufficient under uniform compressive loading, however all cages experienced structural failure during the 4 week study. Post-sacrificial analysis revealed consistent failure at the posterior region regardless of design or experimental level, revealing an irregular endplate geometry with bony processes which likely provide the repeated, concentrated loading responsible for structural failure. These results contribute to better understanding the anatomical constraints imposed by the minipig spine, providing a template upon which to build more robust cages to ensure successful tissue integration.

[3] This work was presented at the ORS 2021 Annual Meeting and is in preparation for publication: Lintz M, Kim B, Kirnaz S, Goldberg J, Härtl R, Bonassar LJ. *In Vivo Assessment of Biodegradable Support Structures for Total Disc Replacement in the Minipig Cervical Spine.* Poster presented at the ORS 2021 Annual Meeting; February 12-16, 2021; Virtual Conference.

Introduction

Lower back pain (LBP), which refers to a range of painful symptoms of varying degrees of severity, affects about 10% of the global population in some form and is therefore considered the leading cause of disability worldwide[1,2]. In the United States alone during the years 2012-2014, direct medical costs for the treatment of back-related health conditions totaled approximately $315 billion per year[2], with cost and prevalence only expected to rise in the coming years. Intervertebral disc (IVD) degeneration is implicated as one of the major contributors to LBP, characterized by irreversible detrimental changes to the disc's structure, composition, and native cell population which in turn impede its mechanical function in the spine[3-7]. There are currently few options to address degenerative disc disease (DDD) apart from surgical intervention, particularly for end-stage disease.

Standard surgical interventions involve removal of the damaged disc followed by either spinal fusion or total disc replacement (TDR) with an artificial disc. Though fusion has been utilized as the gold standard for many years, common side effects such as pseudoarthrosis and graft site pain continue to be observed[8,9]. TDR meanwhile is not widely used due to high surgery costs and difficult surgeries[10]. More importantly, these strategies traditionally involve the introduction of mechanical implants and therefore do not possess comparable structural or biomechanical properties to native discs. Both treatments ultimately focus on restricting range of motion, potentially forcing the spine to compensate for abnormal loading patterns and stress distributions, and may therefore increase the risk of reoperation due to adjacent segment disease[9,11]. Ultimately, then, both options treat the symptoms of the disease rather than the underlying causes of the disease itself[11], failing to repair the damaged disc.

To address the concerns present in the aforementioned approaches, researchers have explored biologic approaches for the treatment of DDD, focusing on a) repairing

or replacing the damaged endogenous cell population and b) recreating the complex fiber architecture of the AF. Following the development of the first composite tissue-engineered (TE) disc in 2004, consisting of a cell-laden alginate gel core at the center of a cellular poly(lactic acid) (PLA) / poly(glycolic acid) (PGA) scaffold[12], several investigators have proposed their own alternate material combinations and approaches[12-22]. The majority of these studies have explored composite disc constructs *in vitro*, with few focused on transitioning these strategies to *in vivo* use. Of the *in vivo* studies published, most utilize small animals such as rodents to assess the feasibility of different approaches. Though helpful as high-throughput validation systems, there are significant anatomical and mechanical differences between the rodent and human spine which prevent successful translation to clinical use[18,23-26].

More recently, large animals such as dogs and goats have been successfully implemented in an attempt to address some of the challenges in translating to human models[19-21]. In our group's efforts to scale up from the rat caudal spine model, we have investigated the feasibility of applying our self-assembling TE-IVD technique to a beagle cervical spine model for a duration of 16 weeks[20]. Following successful integration into the host tissue, discs maintained height and hydration as well as deposited new extracellular matrix (ECM). Goats meanwhile were chosen for use in other studies due to their relatively upright posture and the comparable size of their discs[21]. 8 weeks of culture following implantation in the cervical spine revealed tissue integration as well as biochemical and biomechanical values on the same order as those observed in native discs[19,21].

Although these models demonstrate significant progress in scaling up from small animal work, there are still hurdles to proper clinical translation. While human cervical spines display a lordotic curvature, the canine spine demonstrates primarily kyphotic curvature[27]. As a consequence of this curvature, implants at certain

experimental levels demonstrated significant displacement issues[20,28] in response to a more complex loading profile in canines as opposed to rodents. To address these shortcomings, we propose a new minipig cervical spine model for use in TDR application, as Göttingen minipig cervical spines have been found anatomically and physiologically similar to those of humans; of note, the kyphotic curvature is reduced[29]. Despite this reduced curvature, minipig IVDs are still subject to high stress in response to loading, which may potentially result in damage to our soft engineered constructs due to their mechanically compliant nature. To provide mechanical support and protection prior to tissue integration in this new environment, then, we developed a resorbable support and delivery vehicle for our TE-IVDs. We assessed the durability of these "cages" in different levels of the spine as well as their ability to maintain disc height, and modified our TE-IVD manufacturing protocol to produce engineered discs held stably inside of the cages for ease of delivery.

Materials and Methods

Cage Fabrication

Micro-computed tomography (μCT) scans of the C3/4 and C5/6 levels in the minipig spine were obtained and used to determine disc dimensions as previously described[18,20]. One- and two-piece cage models, both at 100% scale, were drafted in Inventor Professional 2020 using the aforementioned dimensions. These were then 3D-printed on a Prusa i3 MK3S+ 3D printer (Prusa3D, Prague, Czech Republic) using biodegradable poly(lactic acid) polymer (PLA) filaments with a 1.75 mm diameter and 100% infill (Prusa3D).

Mechanical Testing and Design Validation

Cages were subjected to mechanical testing using an FM-20 screw-drive uniaxial tension/compression frame (United Testing Systems, Huntington Beach, CA). A testing protocol consisting of continuous compression at a constant strain rate (50 Hz, 0.1 mm/s) was implemented to assess mode of failure.

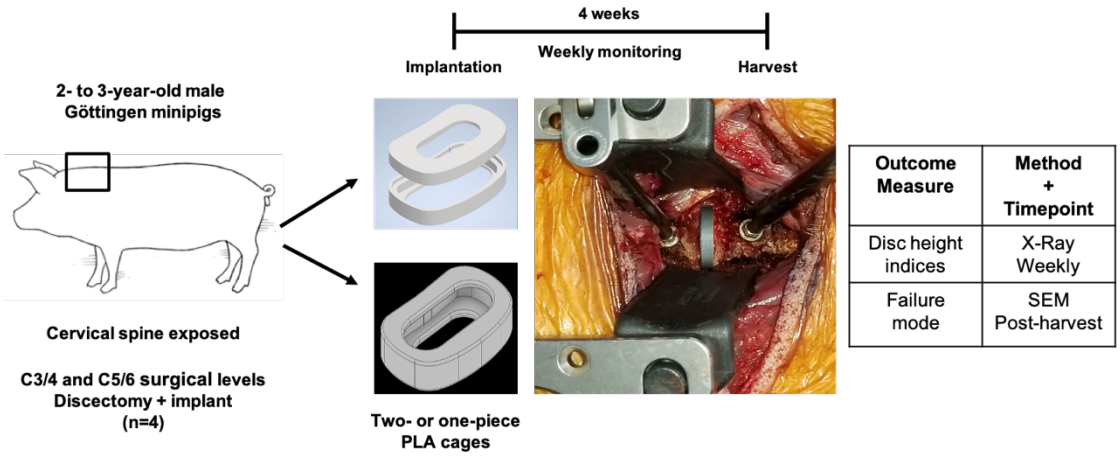

Figure 4.1. Schematic outlining surgical procedure for implantation of one-and two-piece cages into the minipig cervical spine. Implantation photograph as well as outcome measures collected during the 4 week study timeline are presented.

Surgical Procedure

All procedures were reviewed and approved by the appropriate Institutional Animal Care and Use Committee (IACUC). 2-3 year old skeletally mature Göttingen minipigs (Marshall BioResources, North Rose, NY) underwent discectomy followed by implantation of the empty support structure at levels C3/4 and C5/6 (n=4) (Fig. 1). These were divided into two groups that received either a two-piece or one-piece design for a period of 4 weeks.

Animals were anesthetized following appropriate fasting, then underwent endotracheal intubation prior to being attached to the anesthesia and ventilator units. General anesthesia was maintained throughout the procedure using anesthetic agents,

and the animal's vital signs (heart and respiration rate, oxygenation, body temperature, and invasive blood pressure when needed) continuously monitored. Upon obtaining proper depth of anesthesia, the ventral neck was prepared for surgery using povidone iodine followed by 70% isopropyl alcohol.

All surgical procedures followed spinal cord injury (SPI) guidelines for large animal surgery, including sterilization, pre- and post-operative care, and surgical procedures, and were carried out as previously described[20]. Animals were placed on their backs with the neck hyperextended and secured to the table. A 3-4 inch ventral midline incision was made from the base of the larynx to the sternum in each animal, after which the paired sternocleidomastoideus and sternohyoideus muscles were separated with blunt dissection, exposing the trachea. The paired longus colli muscles were exposed, allowing for the experimental levels to be identified and marked by cauterizing of the anterior ligaments. Small curved hemostats were used to separate the long colli muscle overlying the ventral AF.

The following steps were carried out microscopically: after incision of the ventral annulus with a scalpel, the inner AF and NP were extracted using a small tartar scraper or 3-0 to 4-0 bone curette. The outer annulus was left intact. Experimental groups received cage constructs in the disc space followed by outer annulus closure with suture material. Bipolar cauterization was used for homeostasis, the wounds closed with absorbable subcutaneous and cutaneous sutures. Incision sites were dressed in accordance with standard veterinary practices and in consultation with an SCI veterinarian. Once gag reflex returned, animals were extubated and anesthesia discontinued. Animals received antibiotics peri-operatively and were recovered in SCI large animal housing by veterinary staff. As surgery may cause neck pain, post-operative pain management was administered as prescribed by an SCI veterinarian. Orthopedic and neurologic exams were performed at least once daily for the first three

post-operative days by an SCI veterinarian, who was available for consultation for additional examinations.

Imaging Acquisition and Analysis

Interim imaging was performed weekly to assess cage placement and positioning. At these timepoints, animals were anesthetized as described above. X-rays were collected to monitor implants preoperatively, immediately postoperatively, and at weekly intervals (Fig. 2a) by assessing disc height and cage position. Adjacent discs were used as healthy controls for comparison in each animal. IVD height was determined using disc height index (DHI) (Fig. 2b), or the ratio of disc height by adjacent vertebral body height, as previously described[30].

SEM Imaging and Analysis

Constructs were collected upon sacrifice (Fig. 2c) and post-mortem imaging analysis was conducted to determine mode of failure. Directly prior to imaging, samples were fixed to 18 mm aluminum specimen mounts with double sided copper tape and sputter-coated with gold/palladium alloy for 20 seconds at a target current of 20 mA. Samples were then imaged on a Mira3 scanning electron microscope (SEM) (TESCAN, Brno, Czechia) at an accelerating voltage of 5 kV and 5-15 mm working distance.

Cell Isolation and Culture

Whole IVDs were dissected as previously described[20,28] from the cervical spines of 2-3 year old Göttingen minpigs. Tissue was then washed in PBS (Dulbecco's 1x PBS, Corning, NY) and separated into AF and NP sections, then cut into smaller pieces. AF and NP tissue fragments were digested overnight in 200 and 150 ml of 0.3% wt/vol collagenase type II (Worthington Biochemical Corporation, Lakewood, NJ),

respectively, at 37°C. Cells were then collected from the digested tissue using 100 µm nylon filters (Corning, NY), and the resulting cell population was expanded in 2D culture to second passage in growth media composed of: Ham's F-12 (Corning, NY), 10% fetal bovine serum (FBS, Gemini Bio, West Sacramento, CA), 100 µg/ml penicillin and streptomycin, 0.25 µg/ml amphotericin B (Corning, NY), and 25 µg/mL ascorbic acid (Sigma-Aldrich, St. Louis, MO). Cells were cultured to confluence at 37°C with 5% CO_2 and under normoxic conditions, with media replenished three times a week.

Mesenchymal stem cells (MSCs) were also isolated as previously described from the trabecular bone marrow of 2-3 year old Göttingen minipig femurs[44,45]. Cells were then expanded to second passage after 48 hours and cultured in growth media composed of: Dulbecco's modified Eagle's medium (DMEM), 10% fetal bovine serum (FBS, Gemini Bio, West Sacramento, CA), 100 µg/ml penicillin and streptomycin, 0.25 µg/ml amphotericin B (Corning, NY), and 1 ng/mL basic fibroblast growth factor (bFGF, Corning). Cells were cultured to confluence at 37°C and 5% CO_2 under normoxic conditions. Media changes were performed three times a week.

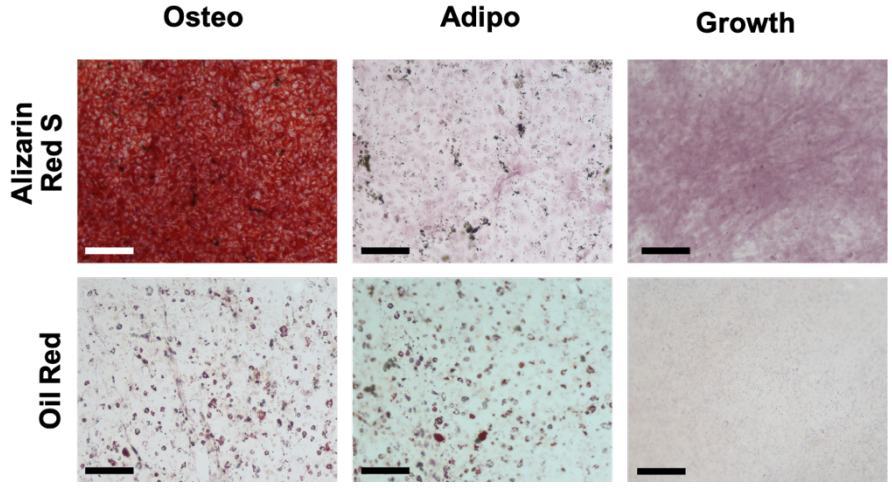

Supplemental Figure 4.1. Trilineage differentiation potential for MSCs cultured in **A)** osteogenic, **B)** adipogenic, and **C)** growth media. Samples were stained with either Alizarin Red S (top) or Oil Red O (bottom). Scale bars indicate 0.15 mm.

Trilineage differentiation assays were performed as per previous studies to assess osteogenic, adipogenic, and chondrogenic potential of the MSC population (Fig. S1)[44,46,47].

Construct Fabrication and Culture

In preparation for seeding, confluent cells were removed from culture flasks using 0.05% trypsin (Gibco BRL). NP cells were encapsulated in 3% (wt/vol) low viscosity grade alginate (NovaMatrix, Wilmington, DE) mixed in a 2:1 ratio with 0.02 g/mL $CaSO_4$ (Sigma-Aldrich, St. Louis, MO). The resulting $25x10^6$ cells/mL alginate solution was set in 12-well plates in $CaCl_2$ (Sigma-Aldrich) to crosslink for one hour. Meanwhile the different cage constructs were placed individually in 6-well plates. A 3mm biopsy punch was used to generate NP plugs, which were then set in the center of each cage. A collagen solution was created by mixing type I collagen obtained from rat-tail tendons (BioIVT, Westbury, NY)[18,20] with a basic working solution (10x PBS, 1x PBS, 1N NaOH). The neutralized collagen solution was seeded with 10 x 10^6 AF cells/ml to obtain a final concentration of 10 mg/ml, then pipetted around each NP in the cage constructs to form the AF. Implants were then cultured at 37°C for 1 hour to allow for gelation, after which 3 ml of the previously described media were added to each well. Media was replenished three times a week over a culture period of 5 weeks.

Statistics

Data are presented as mean $\pm$ standard deviation, with significance determined at $p<0.05$.

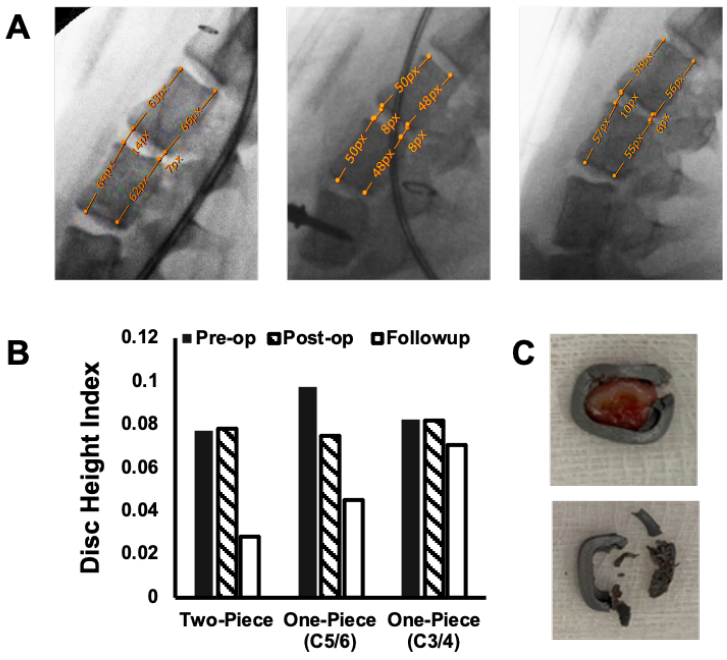

Figure 4.2. A) X-ray monitoring of controls and implants at pre-op, immediately post-op, and 4 week followup timepoints. **B)** Disc height indices in surgically-treated levels at different timepoints. **C)** One-piece implants recovered post-sacrifice from the C3/4 (top) and C5/6 (bottom) experimental levels.

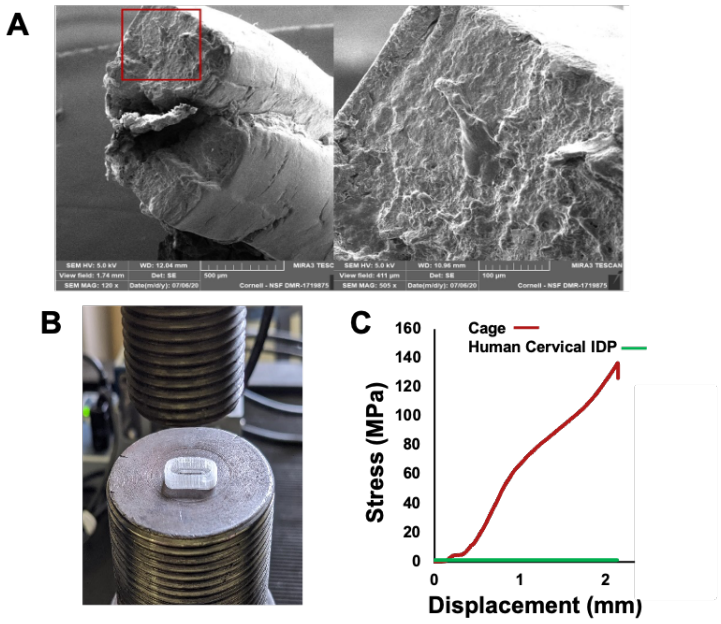

Figure 4.3. A) Representative SEM images taken at implant failure site. **B)** Experimental set up for unconfined compression mechanical tests. **C)** Stress vs. displacement plot of cage construct as compared to human intradiscal pressure (IDP).

Results

In response to compressive loading (Fig. 3b), the one-piece design demonstrated a nearly linear increase in stress, culminating to approximately 134 MPa at a displacement of 2 mm (Fig. 3c). The stress profile demonstrated no apparent point of failure, and upon collection cages were confirmed to be structurally intact following mechanical testing. Both cage designs were therefore deemed appropriate for *in vivo* implantation.

Immediate post-operative X-ray assessment following implantation indicated cages were stable at experimental levels in all pigs. No adverse neurological symptoms were present at this assessment, and animals remained neurologically normal at all weekly follow-ups. At the first weekly follow-up post-implantation, X-rays revealed one-piece designs were still stable in the cervical spine and remained so until harvest at 4 weeks. Pigs implanted with the initial two-piece design, however, demonstrated complete collapse of the disc space upon assessment at week 1.

Quantification of disc height from collected X-rays revealed stably implanted one-piece structures experienced a slight decrease in DHI from pre-op to immediate post-op (0.0824 to 0.0816 at C3/4 and 0.0972 to 0.0746 at C5/6). At 4 weeks the cages maintained their position in the disc space while DHI values decreased to 0.0705 and 0.045 at C3/4 and C5/6, respectively. In contrast, two-piece structures maintained disc height from pre-op to immediately post-op with DHI values of 0.077 and 0.078, respectively, while DHI decreased dramatically to 0.028 at the 1 week follow-up.

At sacrifice all implants were revealed to have structural damage of varying degrees. When retrieved from the collapsed disc space, the top and bottom portions of the two-piece implants were found separated and broken into smaller fragments, with bending evident at the broken edges. One-piece implants from the C3/4 level were shown to have been damaged but remained largely intact, whereas those at C5/6 showed

more overall damage with a higher incidence of smaller crushed fragments. For all implants, damage appeared to be localized to the posterior end of the cages.

Follow-up SEM analysis confirmed that failure sites remained consistent throughout the trials, both for cage design and experimental level, and was concentrated at two locations in the posterior region (Fig. 3a). At these locations the cages demonstrated clean breaks, with the edges bent inwards, regardless of the extent of damage to the cage.

TE-IVDs cultured in one-piece cages demonstrated moderate contraction over the duration of the culture period so that a small gap was present between the constructs and surrounding walls. While the AF portion did not adhere to the cage walls, constructs still remained stable within cages and no floating was observed during culture.

Discussion

The goal of this study was to develop a biodegradable delivery vehicle for the *in vivo* application of our TE-IVD constructs into a new large animal model. We hypothesized that the cages would have sufficient mechanical strength to maintain disc height, stabilizing the motion segment and allowing the soft implant sufficient time to integrate with the host tissue. We found that while the cages on their own appeared sufficiently stiff to prevent segment collapse *in vitro*, this was not the case *in vivo*. Additional design considerations must therefore be taken into account to ensure proper protection and integration of the implants. Nonetheless, we successfully adapted our culture methods to allow our engineered constructs to mature within the cages and achieve optimal final dimensions prior to implantation.

Due to its biocompatible and biodegradable nature, PLA has been utilized in a variety of medical applications in forms ranging from screws, plates, etc. in various parts of the body[31]. As a result of its rate of degradation due to hydrolysis[31,32], the load

experienced by the implant is gradually transferred to the surrounding body part. This gradual transfer of load is attractive to our work, as our intent was to create a temporary support for the TE-IVD implants until they mature and are mechanically robust enough to maintain disc height on their own. While to our knowledge the ability of a PLA construct to facilitate the delivery of a TE-IVD implant into the spine has not been investigated, resorbable structures composed of various PLA copolymer formulations have been used in spinal fusion applications[33-40]. These studies utilized rectangular or cylindrical constructs in conjunction with bone grafts in sheep, goat, and pig models for study durations ranging from 12 weeks to 48 months, recording the immune response as well as extent of cage absorption. Biocompatibility was generally favorable across all studies, though the copolymer formulations with reduced degradation times yielded more extensive foreign body response[36,38] while the longer studies resulted in mild to moderate immune responses[34,35,37,39,40]. Though microcracks were observed in multiple studies, the majority retained their mechanical integrity for sufficient time to maintain segment stability and allow for proper fusion.

Following material selection, we varied cage model parameters such as wall thickness, percent of disc volume, curvature, and others before arriving at final one- and two-piece design prototypes for testing. Both were intended to maximize mechanical support while minimizing contact area with the vertebral bodies in order to support the implant while simultaneously enabling it to remodel and mature through mechanical stimulation. One-piece structures were designed to facilitate surgical implantation while two-piece structures were intended to ease insertion of the engineered constructs following culture. Both designs were mechanically tested to determine point of failure, however neither demonstrated any disruption of structure following the tests. In fact, measured stress in the one-piece designs reached up to 134 MPa, approximately two orders of magnitude higher than what is observed *in vivo*: in the human cervical spine,

intradiscal pressure averages 1-2 MPa[41]. These results indicate that, given uniform distribution of loads evenly across the surface, cage constructs are capable of withstanding loads imposed by the cervical spine.

Following surgery, however, imaging revealed collapse of the disc space as early as the first week for the two-piece cage, with DHI decreasing 63.67%, indicating that this design would not be sufficient to stabilize implants until integration with host tissue. Experimental levels receiving one-piece designs meanwhile remained stable, with quantitative DHI measurements supporting qualitative observations that one-piece designs maintained disc height throughout study duration while two-piece designs destabilized by the first follow-up. Post-sacrificial assessment using SEM imaging suggests the halves either slid against each other in the disc space and separated, resulting in collapse, or greater mechanical loading on the posterior region led to separation and then collapse. The one-piece prototype appeared to address these shortcomings, and while the implants maintained their place in the disc space following 4 weeks *in vivo*, those in C5/6 saw a 39.7% decrease in post-op to 4 week follow-up DHI as well as significant damage to the overall structure. Implants at the C3/4 level meanwhile were more structurally intact upon retrieval than their C5/6 counterparts, with DHI decreasing only 13.6% in comparison. Our previous research[20,28] has indicated that the C5/6 level is mechanically complex, as constructs implanted at this level in the canine spine were displaced nearly 100% of the time. Anatomical differences between endplate geometries have also been reported in human cervical spines between different levels, further indicating care must be taken when comparing the different experimental levels[42,43]. From the post-operative analyses we also observed that in all implants, regardless of design or experimental level, damage occurred at the same locations. Structural failure from repetitive mechanical loading, then, is a more likely explanation than initial cage degradation due to hydrolysis: localized compressive stresses account

for consistent mechanism of failure across iterations. Because concentrated high stresses at the posterior region resulted in failure regardless of design, there is likely an anatomic or geometric component contributing to failure. Cages were shown to withstand uniform loading magnitudes drastically higher than what is seen *in vivo*. Failure, however, indicates that implants *in vivo* are not being loaded uniformly, fracturing consistently in the posterior region. Reconstruction of the vertebrae (Fig. 4) reveals that the endplate surface, not structural integrity, accounts for mechanical failure. Bony processes at the posterior region of the vertebrae are the most likely cause of concentrated stress on the implants, fracturing them after repeated and localized loading.

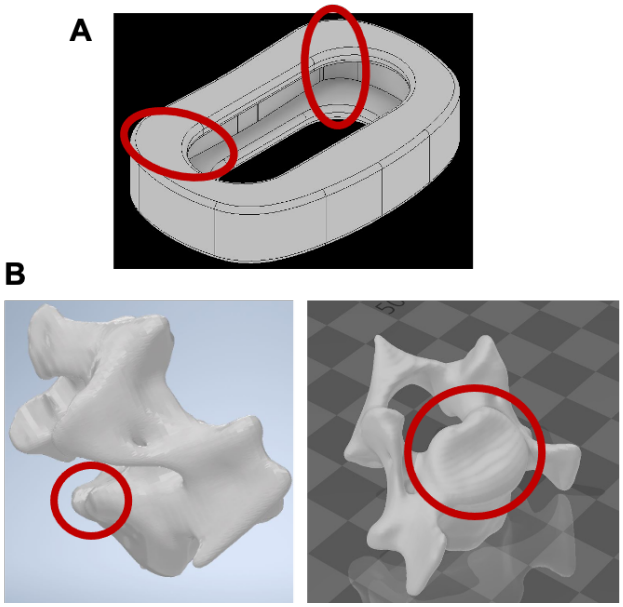

Figure 4.4. A) Failure locations in the cage based on post-mortem assessment. **B)** Reconstructed 3D model of a minipig cervical vertebrae showing presence of posterior bony extrusion.

Figure 4.5. Photographs of composite TE-IVDs cultured in cages between media changes. Scale bars represent 17.5 mm while the red arrow indicates the location of the NP within the construct.

TE-IVDs cultured within the cage constructs (Fig. 5) demonstrated slight contraction over the culture period, though rate of contraction leveled off early in culture, suggesting that a smaller initial surface area requires less time in culture to achieve final dimensions. While all constructs remained in place throughout culture and retained cage geometry despite contraction, there is still a potential risk of floating free of the cage. Should TE-IVDs contract sufficiently to risk floating, a reinforcing ring of collagen may be pipetted around the constructs to fill in the gaps and hold them in place for the remainder of culture. It is also crucial to note that PLA degrades via hydrolysis: extended culture in media at 37°C did not cause any noticeable damage to the cages but did soften the material, weakening their mechanical integrity. To prevent premature failure and ensure ideal material properties, cage designs should be converted to molds, guiding appropriate construct geometry during culture. Discs should then be transferred to freshly printed cage constructs following culture and immediately prior to implantation, ensuring that any degradation or loss of integrity occurs only after the implant has been secured in the disc space. MSC multipotency was also confirmed (Fig. S1), indicating that this cellular population can be used for TE-IVD populations alongside or in place of the IVD population.

A range of limitations exist for this study that must be addressed before continuing forward. First, our cage prototypes were tested solely under uniaxial loading, which does not encompass the full range of complex loading regimes that occur in the spine. However, given the upright posture and bending of the head and neck, quadrupedal cervical spines are in fact primarily subjected to uniaxial loading[39]. Incorporation of the bony processes is a necessity, though, potentially through the use of motion segments to replicate the high stress damage we observed in samples collected post-operatively. Although the TE-IVD results are promising, testing of our next-generation prototypes likely requires additional modeling analysis to iteratively assess prototype potential before delivery is possible. A detailed degradation study should be incorporated into this screening process with an attempt to parse out details on kinetics, to determine how rate of degradation impacts structural integrity.

In the field, it is imperative that implants must be delivered with a mechanical support system. However, in this study our designs screened with uniform mechanical loading still experienced structural failure, ultimately a result of geometry rather than material properties. Therefore, additional measures should be taken to further strengthen the structure and prolong stabilization of the implant until integration is achieved. Despite the limitations, this study facilitates further investigation of disc regeneration in large animal models, specifically enhancing the biologic TDR approach by providing a mechanically robust delivery and support vehicle for ease of implantation. In this manner we will more thoroughly be able to assess the feasibility of the Göttingen minipig as a new, relevant model system to assist in moving the technology closer to clinical application.

Acknowledgments

The authors would like to thank the Anna K. Cunningham and Mary E.

Cunningham Trust for stipend support. This work was supported by the following funding sources: the Colin MacDonald Fund, the Daedalus Innovation Fund, and the Center for Advanced Technology from the New York State Advanced Research Fund (NYSTAR).

REFERENCES

[1] Murray CJ, Lopez AD. Measuring the global burden of disease. *N Engl J Med*. 2013; 369(5):448-457.

[2] Collaborators US Burden of Disease. *United States Bone and Joint Initiative: The Burden of Musculoskeletal Diseases in the United States United States.* Second. Rosemont, IL: American Academy of Orthopaedic Surgeons; 2020.

[3] Buckwalter JA. Aging and degeneration of the human intervertebral disc. *Spine (Phila Pa 1976)*. 1995;20(11):1307-1314.

[4] Antoniou J, Steffen T, Nelson F, Winterbottom N, Hollander AP, Poole RA, Aebi M, Alini M. The human lumbar intervertebral disc: evidence for changes in the biosynthesis and denaturation of the extracellular matrix with growth, maturation, ageing, and degeneration. *J Clin Invest*. 1996;98(4):996-1003.

[5] Urban JP, Roberts S. Degeneration of the intervertebral disc. *Arthritis Res Ther*. 2003;5(3):120-130.

[6] Lyons G, Eisenstein SM, Sweet MB. Biochemical changes in intervertebral disc degeneration. *Biochim Biophys Acta*. 1981;673(4):443-453.

[7] Colombini A, Lombardi G, Corsi MM, Banfi G. Pathophysiology of the human intervertebral disc. *Int J Biochem Cell Biol*. 2008;40(5):837-842.

[8] Frelinghuysen P, Huang RC, Girardi FP, Cammisa FP Jr. Lumbar total disc replacement part I: rationale, biomechanics, and implant types. *Orthop Clin North Am*. 2005;36(3):293-299.

[9] Lee YC, Zotti MG, Osti OL. Operative Management of Lumbar Degenerative Disc Disease. *Asian Spine J*. 2016;10(4):801-819.

[10] Salzmann SN, Plais N, Shue J, Girardi FP. Lumbar disc replacement surgery-successes and obstacles to widespread adoption. *Curr Rev Musculoskelet Med*. 2017;10(2):153-159.

[11] Setton LA, Bonassar LJ, Masuda K. Regeneration and replacement of the intervertebral disc. In: Robert L, Robert L, Joseph V, eds. *Principles of Tissue Engineering*. 3rd ed. Boston: Elsevier Academic Press. 2007;877-96.

[12] Mizuno H, Roy AK, Vacanti CA, Kojima K, Ueda M, Bonassar LJ. Tissue-engineered composites of anulus fibrosus and nucleus pulposus for intervertebral disc replacement. *Spine (Phila Pa 1976)*. 2004;29(12):1290-1298.

[13] Nesti LJ, Li WJ, Shanti RM, Jiang YJ, Jackson W, Freedman BA, Kuklo TR, Giuliani JR, Tuan RS. Intervertebral disc tissue engineering using a novel hyaluronic acid-nanofibrous scaffold (HANFS) amalgam. *Tissue Eng Part A*. 2008;14(9):1527-1537.

[14] Nerurkar NL, Sen S, Huang AH, Elliott DM, Mauck RL. Engineered disc-like angle-ply structures for intervertebral disc replacement. *Spine (Phila Pa 1976)*. 2010;35(8):867-873.

[15] Park SH, Gil ES, Cho H, Mandal BB, Tien LW, Min BH, Kaplan DL. Intervertebral disk tissue engineering using biphasic silk composite scaffolds. *Tissue Eng Part A*. 2012;18(5-6):447-458.

[16] Chang G, Kim HJ, Kaplan D, Vunjak-Novakovic G, Kandel RA. Porous silk scaffolds can be used for tissue engineering annulus fibrosus. *Eur Spine J*. 2007;16(11):1848-1857.

[17] Zhuang Y, Huang B, Li CQ, Liu LT, Pan Y, Zheng WJ, Luo G, Zhou Y. Construction of tissue-engineered composite intervertebral disc and preliminary morphological and biochemical evaluation. *Biochem Biophys Res Commun*. 2011;407(2):327-332.

[18] Bowles RD, Gebhard HH, Härtl R, Bonassar LJ. Tissue-engineered intervertebral discs produce new matrix, maintain disc height, and restore biomechanical function to the rodent spine. *Proc Natl Acad Sci U S A*. 2011;108(32):13106-13111.

[19] Martin JT, Milby AH, Chiaro JA, Kim DH, Hebela NM, Smith LJ, Elliott DM, Mauck RL. Translation of an engineered nanofibrous disc-like angle-ply structure for intervertebral disc replacement in a small animal model. *Acta Biomater*. 2014;10(6):2473-2481.

[20] Moriguchi Y, Mojica-Santiago J, Grunert P, Pennicooke B, Berlin C, Khair T, Navarro-Ramirez R, Ricart Arbona RJ, Nguyen J, Härtl R, Bonassar LJ. otal disc replacement using tissue-engineered intervertebral discs in the canine cervical spine. *PLoS One*. 2017;12(10):e0185716.

[21] Gullbrand SE, Kim DH, Bonnevie E, Ashinsky BG, Smith LJ, Elliott DM, Mauck RL, Smith HE. Towards the scale up of tissue engineered intervertebral discs for clinical application. *Acta Biomater*. 2018;70:154-164.

[22] Kim DH, Martin JT, Gullbrand SE, Elliott DM, Smith LJ, Smith HE, Mauck RL. Fabrication, Maturation, and Implantation of Composite Tissue-Engineered Total Discs Formed from Native and Mesenchymal Stem Cell Combinations [published online ahead of print, 2020 Jun 4]. *Acta Biomater*. 2020;S1742-7061(20)30318-4.

[23] Lotz JC. Animal models of intervertebral disc degeneration: lessons learned. *Spine (Phila Pa 1976)*. 2004; 29 (23):2742–50.

[24] O'Connell GD, Vresilovic EJ, Elliott DM. Comparison of animals used in disc research to human lumbar disc geometry. *Spine (Phila Pa 1976)*. 2007; 32(3):328–33.

[25] Showalter BL, Beckstein JC, Martin JT, Beattie EE, Espinoza Orias AA, Schaer TP, et al. Comparison of animal discs used in disc research to human lumbar disc: torsion mechanics and collagen content. *Spine (Phila Pa 1976)*. 2012; 37(15): E900–7.

[26] Navarro R, Juhas S, Keshavarzi S, Juhasova J, Motlik J, Johe K, Marsala S, Scadeng M, Lazar P, Tomori Z, Schulteis G, Beattie M, Ciacci JD, Marsala M. Chronic spinal compression model in minipigs: a systematic behavioral, qualitative, and quantitative neuropathological study. *J Neurotrauma*. 2012;29(3):499-513.

[27] Sheng SR, Wang XY, Xu HZ, Zhu GQ, Zhou YF. Anatomy of large animal spines and its comparison to the human spine: a systematic review. *Eur Spine J*. 2010;19(1):46-56.

[28] Mojica-Santiago JA, Lang GM, Navarro-Ramirez R, Hussain I, Härtl R, Bonassar LJ. Resorbable plating system stabilizes tissue-engineered intervertebral discs implanted ex vivo in canine cervical spines. *JOR Spine*. 2018;1(3):e1031.

[29] Foditsch EE, Miclaus G, Patras I, Foditsch EE, Miclaus G, Patras I, Hutu I, Roider K, Bauer S, Janetschek G, Aigner L, Zimmermann R. A new technique for minimal invasive complete spinal cord injury in minipigs. *Acta Neurochir (Wien)*. 2018;160(3):459-465.

[30] Lu DS, Shono Y, Oda I, Abumi K, Kaneda K. Effects of chondroitinase ABC and chymopapain on spinal motion segment biomechanics. An in vivo biomechanical, radiologic, and histologic canine study. *Spine (Phila Pa 1976)*. 1997; 22(16):1828– 34; discussion 34–5.

[31] Auras R, Lim L-T, Selke SEM, Tsuji H, eds. *Poly(Lactic Acid): Synthesis, Structures, Properties, Processing, and Applications.* Wiley Series on Polymer Engineering and Technology; 2010.

[32] Nazre A, Lin S. Theoretical Strength Comparison of Bioabsorbable (PLLA) Plates and Conventional Stainless Steel and Titanium Plates Used in Internal Fracture Fixation. In: Harvey JP, Games RF, eds. *Clinical and Laboratory Performance of Bone Plates*. ASTM International; 1994:53-64.

[33] van Dijk M, Smit TH, Sugihara S, Burger EH, Wuisman PI. The effect of cage stiffness on the rate of lumbar interbody fusion: an in vivo model using poly(l-lactic Acid) and titanium cages. *Spine (Phila Pa 1976)*. 2002;27(7):682-688.

[34] Wuisman PI, van Dijk M, Smit TH. Resorbable cages for spinal fusion: an experimental goat model. *J Neurosurg*. 2002;97(4 Suppl):433-439.

[35] Toth JM, Wang M, Scifert JL, et al. Evaluation of 70/30 D,L-PLa for use as a resorbable interbody fusion cage. *Orthopedics*. 2002;25(10 Suppl):s1131-s1140.

[36] Cahill DW, Martin GJ Jr, Hajjar MV, Sonstein W, Graham LB, Engelman RW. Suitability of bioresorbable cages for anterior cervical fusion. *J Neurosurg*. 2003;98(2 Suppl):195-201.

[37] Krijnen MR, Smit TH, Strijkers GJ, Nicolay K, Pouwels PJ, Wuisman PI. The use of high-resolution magnetic resonance imaging for monitoring interbody fusion and bioabsorbable cages: an ex vivo pilot study. *Neurosurg Focus*. 2004;16(3):E3.

[38] Pflugmacher R, Schleicher P, Gumnior S, Turan O, Scholz M, Eindorf T, Haas NP, Kandziora F. Biomechanical comparison of bioabsorbable cervical spine interbody fusion cages. *Spine (Phila Pa 1976)*. 2004;29(16):1717-1722.

[39] Smit TH, Krijnen MR, van Dijk M, Wuisman PI. Application of polylactides in spinal cages: studies in a goat model. *J Mater Sci Mater Med*. 2006;17(12):1237-1244.

[40] Abbah SA, Lam CX, Ramruttun AK, Goh JC, Wong HK. Fusion performance of low-dose recombinant human bone morphogenetic protein 2 and bone marrow-derived multipotent stromal cells in biodegradable scaffolds: a comparative study in a large animal model of anterior lumbar interbody fusion. *Spine (Phila Pa 1976)*. 2011;36(21):1752-1759.

[41] Bell KM, Yan Y, Hartman RA, Lee JY. Influence of follower load application on moment-rotation parameters and intradiscal pressure in the cervical spine. *J Biomech*. 2018;76:167-172.

[42] Chen H, Zhong J, Tan J, Wu D, Jiang D. Sagittal geometry of the middle and lower cervical endplates. *Eur Spine J*. 2013;22(7):1570-1575.

[43] Lou J, Liu H, Rong X, Li H, Wang B, Gong Q. Geometry of inferior endplates of the cervical spine. *Clin Neurol Neurosurg*. 2016;142:132-136.

[44] McCorry MC, Bonassar LJ. Fiber development and matrix production in tissue-engineered menisci using bovine mesenchymal stem cells and fibrochondrocytes. *Connect Tissue Res*. 2017;58(3-4):329-341.

[45] McCorry MC, Puetzer JL, Bonassar LJ. Characterization of mesenchymal stem cells and fibrochondrocytes in three-dimensional co-culture: analysis of cell shape, matrix production, and mechanical performance. *Stem Cell Res Ther*. 2016;7:39.

[46] Bernacki SH, Wall ME, and Loboa EG. Isolation of human mesenchymal stem cells from bone and adipose tissue. *Methods Cell Biol*. 2008; 86(8):257-278.

[47] Pittenger MF, Mackay AM, Beck SC, Jaiswal RK, Douglas R, Msca JD, Moorman MA, Simonetti DW, Craig S, and Marshak DR. Multilineage Potential of Adult Human Mesenchymal Stem Cells. *Science*. 1999; 284(5411):143-147.

CHAPTER 5

Conclusions and Future Directions

Conclusions

The goals of this dissertation were to investigate the mechanisms behind glucose-driven fiber formation in the developing IVD as a means to augment mechanical behavior in engineered constructs and bring biologic TDR options closer to clinical translation. First, glucose was used as an *in vitro* tool for controlling proteoglycan content and in turn fiber alignment in TE-IVD constructs, with optimal fiber organization corresponding to enhanced mechanics (Chapter 2). Then, the effects of hyperglycemic levels of glucose on matrix organization and mechanical behavior were examined in discs taken from a diabetic mouse model (Chapter 3). Finally, a resorbable cage was designed and investigated as a delivery vehicle to provide mechanical support and facilitate TE-IVD implantation in a new large animal model for *in vivo* TDR applications (Chapter 4). This chapter examines the findings from each aim in the context of previous work in the field and presents potential future directions in which it may continue.

Specific Aim 1

In Chapter 2, we investigated the effects of altering media glucose concentrations for *in vitro* culture of TE-IVD constructs, focusing on the relationship between composition, structure, and mechanical function. We reported that a glucose concentration of 500 mg/L yielded the most organized fiber network in the AF as well as the highest effective stiffness, while this effect decreased with both higher and lower levels of media glucose. The 4500 mg/L group demonstrated disorganized, unaligned fibers and weaker mechanics, comparable to the 125 mg/L group, despite having the

highest measured proteoglycan content. Of note, 4500 mg/L represents the glucose concentration that is commonly used in the culture of MSCs and fibrocartilage, indicating that standard culture techniques are likely prioritizing GAG deposition and matrix composition over fiber structure and integrity, resulting in enhanced levels of proteoglycans but inferior organization and mechanics.

Previous studies have indicated that proteoglycans play a critical role in the development of fibrocartilage such as the AF[1-8], driving proper matrix assembly and maintenance during embryogenesis. Despite directly influencing fiber formation, however, manipulation of proteoglycan content has not to our knowledge been widely utilized to control fiber organization in engineered cartilage. These observations motivated recent work in our group in engineered meniscal constructs where we demonstrated that glucose can be used as a tool to regulate proteoglycan production[9,10] as glucose plays a key role in proteoglycan synthesis and the production of core proteins for tissue maintenance[11,12]. Our combined studies in the meniscus and disc indicate that the media glucose formulations utilized for fibrocartilage culture are almost 10 times higher than the ideal 500 mg/L concentration we reported. As GAG deposition is considered a hallmark of healthy articular cartilage, culture techniques are aimed at stimulating production to achieve elevated GAG concentrations in engineered cartilaginous tissue, hence the high glucose media. However, even media formulations taken from tendon engineering with the goal of enhancing fiber production may contain higher levels of glucose (1000 mg/L) than optimal for tissue engineering. Our findings indicate that due to the sensitive nature of the constructs and the manner in which they are cultured, lower glucose media should be utilized to ensure a balance between composition and structure, ultimately driving fiber organization to promote enhanced mechanical properties. These findings also served as the primary motivation for the work carried out in the following summary.

Specific Aim 2

In the aforementioned chapter, we reported interesting observations regarding the effect of glucose on fiber organization and mechanics in an engineered disc model. Given the range of glucose concentrations utilized in the study, we sought to determine whether super-physiologic levels of glucose had comparable effects on the developing disc *in vivo*. The focus of Chapter 3, then, was to investigate whether hyperglycemia in young mice would alter fiber formation, ECM composition, and mechanical behavior in diabetic discs as compared to wild type. Diabetic mice showed increased s-GAG and collagen content over their wild type counterparts, as well as significant structural changes to the NP and inner AF regions. Diabetic NPs were larger, extending further into the inner AF and contained by an irregular, unaligned AF/NP border. In response to both dynamic and compressive mechanical loading, diabetic discs demonstrated a two-fold increase in stiffness over the wild type discs, as well as a nearly doubled recovery time following deformation.

Multiple studies have examined the relationship between diabetes and DDD, particularly to understand how diabetes aggravates the progression of the disease. The molecular mechanisms by which this occurs, however, are not fully understood. Long-term hyperglycemia results in the accumulation of AGEs and over-production of ROS which may contribute to the transition from primarily anabolic processes to catabolism, as well as triggering apoptosis in the endogenous cell population[13-17]. The work presented in Chapter 3 indicates that diabetes not only causes detrimental structural changes to the disc in the long run but also at a young age, predisposing the disc to DDD during development by affecting ECM formation and composition. More significantly, our findings indicate that this process occurs independently of AGE accumulation as there was no difference in the AGE content between groups despite clear differences in their diabetic status (blood glucose, HbA1c, etc.). Rather, hyperglycemia appears to

predispose the disc to DDD during development by altering matrix composition, with diabetic animals demonstrating elevated proteoglycan content in the inner AF paired with greater fiber disorganization in these regions.

Selection of a diabetic model which would appropriately parallel our *in vitro* observations from Chapter 2 was of critical concern. Given the TE-IVD model utilized in our previous studies[18-24] involves the generation of immature disc constructs which rely on cell contractile forces to drive their alignment, as well as the important role that proteoglycans play in AF and fibrocartilage formation during embryonic development[1-8], the most appropriate comparison would involve an examination of spontaneous diabetes transferred from the mother and its effect on the developing disc over time. There are two distinct approaches to animal models of diabetes, whereby the disease is triggered by either a) diet or b) genetically modified changes to the organism[25-30]. Diet-induced models of diabetes tend to focus on obesity and on how manipulation of environmental factors rather than genetics produces obesity in order to mimic the human condition, and involve high fat feeding in order to lead the animals to gain weight[25]. Genetic models of spontaneous diabetes, then, are more in line with the goals of this study. Of the genetic models, db/db mice are the most widely used model for type 2 diaebetes (T2D), where diabetes is caused by a spontaneous mutation to the leptin receptor gene[26-30]. The mutation then results in an abnormal phenotype leading to the development of symptoms such as obesity, hyperphagia, insulin resistance, etc.[25,31-35]. Additionally, hyperglycemia in db/db mice is reported as early as 8 weeks of age while as the animal is still growing, enabling parallels to be drawn to the developing disc.

Specific Aim 3

In chapter 4, we sought to develop a resorbable support structure to deliver our composite TE-IVDs into a new large animal model with the goal of providing temporary

mechanical support until the mature implant achieved successful integration with the host tissue. When subjected to mechanical loading as a means of validating material strength, cage prototypes were deemed capable of withstanding uniform compression exerted by the cervical spine. Following implantation, two-piece designs failed almost immediately while the one-piece designs maintained disc height for the duration of the study. Upon collecting the cages for post-mortem analysis, however, all cage designs demonstrated comparable damage to the posterior region, indicating that the cages were likely subject to repeated and non-uniform loading concentrated to this area. Geometric constraints of the porcine cervical spine rather than material properties, then, likely accounted for the structural failure of the implants; this conclusion was supported following a reconstruction of the cervical vertebral endplate which indicated the presence of a prominent bony process rather than a smooth surface. In preparation for further *in vivo* studies, TE-IVD culture was also successfully adapted to enable discs to mature within the cage constructs, highlighting the tunability of our system. These findings encompass significant progress in developing a novel means of protecting immature disc constructs prior to integration, a necessity in advancing the technology towards clinical use due to the complex loading profiles of large animal spines.

Dogs are an established model of disc degeneration and an attractive choice for the study of TE-TDR strategies. Some canine breeds, including beagles and dachshunds, do not retain their immature notochord population with age[36,37] and are known to spontaneously develop DDD as well as receive surgical treatment. As a result, they may not only demonstrate similar degenerative processes to humans but have the potential to respond to treatment and undergo healing in a comparable manner as well. Additionally, the canine cervical spine demonstrates a similar loading profile to that seen in humans[37-42]. However, the cervical spine displays a primarily kyphotic curvature as compared to the lordotic curvature of the human cervical spine[43]. This higher degree

of curvature resulted in near 100% displacement of constructs implanted at certain levels[23,24], suggesting the need for an additional large animal model with a more upright cervical spine comparable to that of humans. Göttingen minipigs meanwhile demonstrate slower progression of disc degeneration despite retaining their notochord population throughout adulthood, which may serve as an appropriate parallel for natural degenerative processes in humans[44]. Porcine discs are also anatomically, structurally, and mechanically relevant models[44-49]. Geometrically, they are large-scaled discs with similar bone structure and vertebral proportions, and are of a comparable contour and shape. Although pigs are quadrupedal, the biomechanical properties resemble those seen in humans, in part due to a similar weight range. Discs also possess similar stiffness values, and in response to applied compressive or shear loads yield comparable injuries.

While to our knowledge the ability of a PLA construct to facilitate the delivery of a TE-IVD implant into the spine has not been investigated, the Mauck group has utilized poly(caprolactone) (PCL), which resembles PLA, in the AF portions of their engineered constructs and documented their use extensively both *in vitro* and *in vivo*[49-53]. Resorbable structures composed of various PLA copolymer formulations have also been used in spinal fusion applications[54-61]. These studies utilized rectangular or cylindrical constructs in conjunction with bone grafts in sheep, goat, and pig models for study durations ranging from 12 weeks to 48 months, recording the immune response as well as extent of cage absorption. Biocompatibility was generally favorable across all studies, though the copolymer formulations with increased degradation times yielded more extensive foreign body response[57,59] while the longer studies resulted in mild to moderate immune responses[55,56,58,60,61]. Though microcracks were observed in multiple studies, the majority retained their mechanical integrity for sufficient time to maintain segment stability and allow for proper fusion. We have also previously demonstrated the feasibility of an 85:15 poly(lactic-co-glycolic acid), or PLGA, structure to prevent

implant displacement in our *in vivo* canine model[23]. The addition of a commercially available resorbable plate/screw system (Rapidsorb®, Depuy Synthes Co. Johnson & Johnson, West Chester, PA), commonly used for human cranio-maxillofacial trauma, restored over 25% of compressive control motion segment stiffness and prevented extrusion of the engineered implant at both experimental levels[24], though the effect was more significant at C3/4 than C5/6.

Future Directions

The research presented in this dissertation lays a foundation upon which subsequent work can expand with regards to future hypotheses and investigative directions. Some of these potential directions are outlined herein, focusing on further optimization of *in vitro* engineered discs and validation of the glucose observations *in vivo*; more closely analyzing the diabetic discs and expanding the work into larger animal models; and addressing aspects of the cage design as well as minipig anatomy to generate a delivery vehicle for successful implantation of engineered constructs into the cervical spine.

Specific Aim 1

As we observed from the work in Chapter 2, coupled with previous studies from our lab in meniscal constructs[9,10], media glucose provides an effective means of manipulating fiber formation and organization in engineered fibrocartilage. However, the long-term effects of glucose on engineered constructs have yet to be explored *in vivo*. While low physiologic concentrations of glucose produced TE-IVDs with the highest degree of alignment as well as effective stiffness, biochemical and biomechanical values are still orders of magnitude lower than what is seen in native discs. Given that our previous work indicates successful tissue integration and

mechanical stimulation in the disc space yields functional discs with native-like properties, we hypothesize that glucose treatment ultimately produces a primed template for disc engineering by enhancing the immature matrix[20,23]. The translation of this work to an *in vivo* animal model would confirm whether reducing the amount of glucose to which the discs are exposed in culture successfully optimizes matrix organization *in vivo* as we saw *in vitro*.

Biochemical and biomechanical behavior of the TE-IVDs may also continue to be improved *in vitro* by supplementing low glucose culture with additional techniques. Growth factors are commonly used in tissue engineering as well as in IVD regenerative therapies in an attempt to regulate disc metabolism and matrix maintenance by the cellular population. Members of the transforming growth factor β (TGF- β) and bone morphogenic protein (BMP) families, platelet-derived growth factor (PDGF), and growth differentiation factor 5 (GDF-5) have all been explored, among others[62]. Dynamic mechanical stimulation has also been shown to improve properties of engineered cartilage and to be instrumental for matrix regulation in the native IVD[63-71]. Previous work from our group has demonstrated that dynamic loading increased both effective stiffness and biochemical content in TE-IVDs, with full effects seen at 5% strain[72]. Lastly, culture in hypoxic conditions is often utilized to prime cells for disc engineering[73,74]. Given the largely avascular nature of the IVD, AF and NP cells *in vivo* are normally subjected to 1-5% O_2[75]; oxygen levels in normoxic culture, meanwhile, average 18-20% O_2[76]. Hypoxic culture of both cells and engineered constructs has shown increased stiffness in TE-IVDs as well as enhanced biochemical content[22]. Combining any of the aforementioned culture strategies with reduced glucose culture, then, is a logical next step in effectively priming TE-IVDs *in vitro* prior to *in vivo* implantation.

Specific Aim 2

While the work in Chapter 3 demonstrated significant differences in the caudal IVDs between diabetic and wild type mice, compositional changes were largely assessed using bulk assays. More specific assays for the characterization of disc composition, particularly with respect to proteoglycan and collagen content, could allow for better quantification of the changes between diabetic and wild type discs. As DDD progresses, there is a shift in collagen content in both the NP and AF, with the ratio of type I to type II collagen increasing in the NP and outer AF[77]. To determine if these trends are also present in the developing disc, techniques such as enzyme-linked immunosorbent assay (ELISA), immunohistochemical staining, and Fourier Transform Infrared (FTIR) spectroscopy, among others, could prove useful. FTIR analysis would be useful in gaining insight into how collagen and proteoglycan distribution vary with region in diabetic discs[78] while the presence of specific molecules could be probed and identified through immunohistochemistry and ELISA analysis.

Though rodent models are the most commonly used for the study of T2D, they do not accurately model the manner in which the disease manifests in humans. To address these shortcomings, a variety of larger animals have been proposed for further study[79]: animals such as cats, non-human primates, and pigs, for example, are prone to spontaneous T2D development[80-92]. While dogs do not spontaneously develop diabetes as the others do, experimental induction of the disease has been successful[85,93,94]. The canine and porcine models are the most commonly used for translational studies[83], though the former is primarily utilized for diet-induced models of obesity[79,94] and the latter has been increasingly used as of late due to comparable metabolism to humans[82] and the existence of multiple strains of transgenic pigs[90,91]. As such, an investigation of the mechanics as well as matrix organization and composition of the diabetic disc in young pigs could be telling. In larger animals, studies assessing the impact of diabetic

medication on the progression of DDD would be potentially impactful, given that biguanides—which function to limit the production of sugar by the liver—are often prescribed to Type II diabetics upon diagnosis to control blood glucose levels. In this manner studies could determine to what extent controlling hyperglycemia in diabetic animals is able to delay the onset of DDD, and at what age this treatment is most effective.

The consequences of hyperglycemia on the developing disc should, however, ultimately be explored in the human context: children with juvenile diabetes (most often Type I) and individuals diagnosed with gestational diabetes during pregnancy, for example. Gestational diabetes, while treatable and often a concern only during pregnancy and childbirth, may increase the risk of developing diabetes later in life for both the parent and child[95]. Routine medical visits for all aforementioned at-risk individuals can be supplemented with MR imaging to grade their disc health and identify the onset of any degenerative changes. Doing so would enable more immediate and potentially more effective treatment, as well as contribute to determining at which timepoints hyperglycemia has a concrete identifiable effect on disc structure.

Specific Aim 3

The work in Chapter 3 demonstrated that while our cage designs were sufficiently mechanically robust to withstand intradiscal pressure in the cervical spine, geometric constraints imposed by the spine itself resulted in structural failure regardless of design or experimental level. Incorporation of the vertebral endplate anatomy for future designs, particularly the bony processes in the posterior region of the endplate, is a necessity to ensure successful tissue integration. Testing of our next-generation prototypes requires additional modeling analysis to iteratively assess prototype potential before delivery is possible. In order to replicate the high stress damage we observed in

samples collected post-operatively, mechanical testing of printed prototypes in cervical motion segments in conjunction with finite element analysis could assist in prototype validation.

A detailed degradation study should also be incorporated into this screening process with an attempt to parse out details on kinetics, to determine how rate of degradation impacts structural integrity. While we demonstrated that TE-IVD culture can be adapted to allow for construct maturation within the cages, PLA degrades via hydrolysis. Implants cultured in media at 37°C for upwards of 2 weeks likely will not fragment on such a short time scale but could still potentially soften or show other mild signs of loss of structural integrity. Cage dimensions could be used to develop a mold template to provide appropriate geometry to the constructs during culture, which could then be transferred to the proper cage directly prior to implantation and thus maintain the implant's full mechanical properties.

Concluding Remarks

Overall, the long-term goals of this dissertation were to advance biologic TDR options for use as a viable alternative to standard surgical procedures in the treatment of degenerative disc diseases. This work examined the relationship between fiber formation and matrix composition in the developing IVD both *in vitro* and *in vivo*, highlighting culture techniques necessary to generate a mechanically robust template for disc engineering. Additionally, supplementary surgical techniques were proposed to provide mechanical support and aid in scaling up to a new, clinically relevant large animal model. In doing so, this dissertation lays the groundwork and provides guidelines for future work in adapting TE-IVD strategies for use in the clinic.

REFERENCES

[1] Hayes AJ, Isaacs MD, Hughes C, Caterson B, Ralphs JR. Collagen fibrillogenesis in the development of the annulus fibrosus of the intervertebral disc. *Eur Cell Mater*. 2011;22:226-241.

[2] Lawson LY, Harfe BD. Developmental mechanisms of intervertebral disc and vertebral column formation. *Wiley Interdiscip Rev Dev Biol*. 2017;6(6):10.

[3] Colombier P, Clouet J, Hamel O, Lescaudron L, Guicheux J. The lumbar intervertebral disc: from embryonic development to degeneration. Joint Bone Spine. 2014;81(2):125-129.

[4] Kelleher CM, McLean SE, Mecham RP. Vascular extracellular matrix and aortic development. *Curr Top Dev Biol*. 2004;62:153-188.

[5] Iozzo RV, Schaefer L. Proteoglycan form and function: A comprehensive nomenclature of proteoglycans. *Matrix Biol*. 2015;42:11-55.

[6] Iozzo RV, Murdoch AD. Proteoglycans of the extracellular environment: clues from the gene and protein side offer novel perspectives in molecular diversity and function. *FASEB J*. 1996;10(5):598-614.

[7] Banos CC, Thomas AH, Kuo CK. Collagen fibrillogenesis in tendon development: current models and regulation of fibril assembly. *Birth Defects Res C Embryo Today*. 2008;84(3):228-244.

[8] Kalamajski S, Oldberg A. The role of small leucine-rich proteoglycans in collagen fibrillogenesis. *Matrix Biol*. 2010;29(4):248-253.

[9] McCorry MC, Kim J, Springer NL, Sandy J, Plaas A, Bonassar LJ. Regulation of proteoglycan production by varying glucose concentrations controls fiber formation in tissue engineered menisci. *Acta Biomater*. 2019;100:173-183.

[10] Kim J, Boys AJ, Estroff LA, Bonassar LJ. Combining TGF-β1 and Mechanical Anchoring to Enhance Collagen Fiber Formation and Alignment in Tissue-Engineered Menisci. *ACS Biomater Sci Eng*. 2021;7(4):1608-1620.

[11] Mobasheri A, Vannucci SJ, Bondy CA, Carter SD, Innes JF, Arteaga MF, Trujillo E, Ferraz I, Shakibaei M, Martín-Vasallo P. Glucose transport and metabolism in chondrocytes: a key to understanding chondrogenesis, skeletal development and cartilage degradation in osteoarthritis. *Histol Histopathol*. 2002;17(4):1239-1267.

[12] Prydz K, Dalen KT. Synthesis and sorting of proteoglycans. *J Cell Sci*. 2000;113 Pt 2:193-205.

[13] Zhang Y, Proenca R, Maffei M, Barone M, Leopold L, Friedman JM. Positional cloning of the mouse obese gene and its human homologue [published correction appears in Nature 1995 Mar 30;374(6521):479]. *Nature*. 1994;372(6505):425-432.

[14] Waldron AL, Schroder PA, Bourgon KL, Bolduc JK, Miller JL, Pellegrini AD, Dubois AL, Blaszkiewicz M, Townsend KL, Rieger S. Oxidative stress-dependent MMP-13 activity underlies glucose neurotoxicity. *J Diabetes Complications*. 2018;32(3):249-257.

[15] Chen YJ, Chan DC, Lan KC, Wang CC, Chen CM, Chao SC, Tsai KS, Yang RS, Liu SH. PPARγ is involved in the hyperglycemia-induced inflammatory responses and collagen degradation in human chondrocytes and diabetic mouse cartilages. *J Orthop Res*. 2015;33(3):373-381.

[16] Chen YJ, Chan DC, Chiang CK, Wang CC, Yang TH, Lan KC, Chao SC, Tsai KS, Yang RS, Liu SH. Advanced glycation end-products induced VEGF production and inflammatory responses in human synoviocytes via RAGE-NF-κB pathway activation. *J Orthop Res*. 2016;34(5):791-800.

[17] Wang J, Hu J, Chen X, Huang C, Lin J, Shao Z, Gu M, Wu Y, Tian N, Gao W, Zhou Y, Wang X, Zhang X. BRD4 inhibition regulates MAPK, NF-κB signals, and autophagy to suppress MMP-13 expression in diabetic intervertebral disc degeneration. *FASEB J*. 2019;33(10):11555-11566.

[18] Lintz ML, Bonassar LJ. Physiologic Levels of Glucose Drive Fiber Alignment in Tissue-Engineered Intervertebral Discs. In preparation 2021.

[19] Bowles RD, Williams RM, Zipfel WR, Bonassar LJ. Self-assembly of aligned tissue-engineered annulus fibrosus and intervertebral disc composite via collagen gel contraction. *Tissue Eng Part A*. 2010;16(4):1339-1348.

[20] Bowles RD, Gebhard HH, Härtl R, Bonassar LJ. Tissue-engineered intervertebral discs produce new matrix, maintain disc height, and restore biomechanical function to the rodent spine. *Proc Natl Acad Sci U S A*. 2011;108(32):13106-13111.

[21] Bowles RD, Gebhard HH, Dyke JP, Ballon DJ, Tomasino A, Cunningham ME, Härtl R, Bonassar, LJ. Image-based tissue engineering of a total intervertebral disc implant for restoration of function to the rat lumbar spine. *NMR Biomed*. 2012;25(3):443-451.

[22] Hudson KD, Bonassar LJ. Hypoxic Expansion of Human Mesenchymal Stem Cells Enhances Three-Dimensional Maturation of Tissue-Engineered Intervertebral Discs. *Tissue Eng Part A*. 2017;23(7-8):293-300.

[23] Moriguchi Y, Mojica-Santiago J, Grunert P, Pennicooke B, Berlin C, Khair T, Navarro-Ramirez R, Arbona RJR, Nguyen J, Härtl R, Bonassar LJ. Total disc replacement using tissue-engineered intervertebral discs in the canine cervical spine. *PLoS One*. 2017;12(10):e0185716.

[24] Mojica-Santiago JA, Lang GM, Navarro-Ramirez R, Hussain I, Härtl R, Bonassar LJ. Resorbable plating system stabilizes tissue-engineered intervertebral discs implanted ex vivo in canine cervical spines. *JOR Spine*. 2018;1(3):e1031.

[25] King AJ. The use of animal models in diabetes research. *Br J Pharmacol*. 2012;166(3):877-94.

[26] Szabadfi K, Pinter E, Reglodi D, Gabriel R. Neuropeptides, trophic factors, and other substances providing morphofunctional and metabolic protection in experimental models of diabetic retinopathy. *Int Rev Cell Mol Biol*. 2014;311:1-121.

[27] Mohammed-Ali Z, Carlisle RE, Nademi S, Dickhout JG. Animal models of kidney disease. In: *Animal Models for the Study of Human Disease (2nd ed.),* edited by Conn PM. London, UK: Academic Press. 2017; 379–417.

[28] Hummel KP, Dickie MM, Coleman DL. Diabetes, a new mutation in the mouse. *Science*. 1966;153(3740):1127-1128.

[29] Susztak K, Sharma K, Schiffer M, McCue P, Ciccone E, Böttinger EP. Genomic strategies for diabetic nephropathy. *J Am Soc Nephrol*. 2003;14(8 Suppl 3):S271-S278.

[30] Susztak K, Böttinger E, Novetsky A, Liang D, Zhu Y, Ciccone E, Wu D, Dunn S, McCue P, Sharma K. Molecular profiling of diabetic mouse kidney reveals novel genes linked to glomerular disease. *Diabetes*. 2004;53(3):784-794.

[31] Yoshida S, Tanaka H, Oshima H, Yamazaki T, Yonetoku Y, Ohishi T, Matsui T, Shibasaki M. AS1907417, a novel GPR119 agonist, as an insulinotropic and β-cell preservative agent for the treatment of type 2 diabetes. *Biochem Biophys Res Commun*. 2010;400(4):745-751.

[32] Park JS, Rhee SD, Kang NS, Jung WH, Kim HY, Kim JH, Kang SK, Cheon HG, Ahn JH, Kim KY. Anti-diabetic and anti-adipogenic effects of a novel selective 11β-hydroxysteroid dehydrogenase type 1 inhibitor, 2-(3-benzoyl)-4-hydroxy-1,1-dioxo-2H-1,2-benzothiazine-2-yl-1-phenylethanone (KR-66344). *Biochem Pharmacol*. 2011; 81(8):1028-1035.

[33] Gault VA, Kerr BD, Harriott P, Flatt PR. Administration of an acylated GLP-1 and GIP preparation provides added beneficial glucose-lowering and insulinotropic actions over single incretins in mice with Type 2 diabetes and obesity. *Clin Sci (Lond)*. 2011;121(3):107-117.

[34] Chen D, Wang MW. Development and application of rodent models for type 2 diabetes. *Diabetes Obes Metab*. 2005;7(4):307-317.

[35] King A, Bowe J. Animal models for diabetes: Understanding the pathogenesis and finding new treatments. *Biochem Pharmacol*. 2016;99:1-10.

[36] Bach FC, Willems N, Penning LC, Ito K, Meij BP, Tryfonidou MA. Potential regenerative treatment strategies for intervertebral disc degeneration in dogs. *BMC Vet Res*. 2014;10:3.

[37] Bergknut N, Rutges JP, Kranenburg HJ, Smolders LA, Hagman R, Smidt HJ, et al. The dog as an animal model for intervertebral disc degeneration? *Spine (Phila Pa 1976)*. 2012; 37(5):351–8.

[38] Lotz JC. Animal models of intervertebral disc degeneration: lessons learned. *Spine (Phila Pa 1976)*. 2004; 29 (23):2742–50.

[39] O'Connell GD, Vresilovic EJ, Elliott DM. Comparison of animals used in disc research to human lumbar disc geometry. *Spine (Phila Pa 1976)*. 2007; 32(3):328–33.

[40] Showalter BL, Beckstein JC, Martin JT, Beattie EE, Espinoza Orias AA, Schaer TP, et al. Comparison of animal discs used in disc research to human lumbar disc: torsion mechanics and collagen content. *Spine (Phila Pa 1976)*. 2012; 37(15): E900–7.

[41] Lim TH, Goel VK, Weinstein JN, Kong W. Stress analysis of a canine spinal motion segment using the finite element technique. *J Biomech*. 1994; 27(10):1259–69.

[42] Smit TH. The use of a quadruped as an in vivo model for the study of the spine–biomechanical considerations. *Eur Spine J*. 2002; 11(2):137–44.

[43] Sheng SR, Wang XY, Xu HZ, Zhu GQ, Zhou YF. Anatomy of large animal spines and its comparison to the human spine: a systematic review. *Eur Spine J*. 2010;19(1):46-56.

[44] Omlor GW, Nerlich AG, Wilke HJ, Pfeiffer M, Lorenz H, Schaaf-Keim M, Bertram H, Richter W, Carstens C, Guehring T. A new porcine in vivo animal model of disc degeneration: response of anulus fibrosus cells, chondrocyte-like nucleus pulposus cells, and notochordal nucleus pulposus cells to partial nucleotomy. *Spine (Phila Pa 1976)*. 2009;34(25):2730-2739.

[45] Daly C, Ghosh P, Jenkin G, Oehme D, Goldschlager T. A Review of Animal Models of Intervertebral Disc Degeneration: Pathophysiology, Regeneration, and Translation to the Clinic. *Biomed Res Int*. 2016;2016:5952165.

[46] Alini M, Eisenstein SM, Ito K, Little C, Kettler AA, Masuda K, Melrose J, Ralphs J, Stokes I, Wilke HJ. Are animal models useful for studying human disc disorders/degeneration?. *Eur Spine J*. 2008;17(1):2-19.

[47] Kääpä E, Zhang LQ, Muona P, Holm S, Vanharanta H, Peltonen J. Expression of type I, III, and VI collagen mRNAs in experimentally injured porcine intervertebral disc. *Connect Tissue Res*. 1994;30(3):203-214.

[48] Wang JL, Tsai YC, Wang YH. The leakage pathway and effect of needle gauge on degree of disc injury post anular puncture: a comparative study using aged human and adolescent porcine discs. *Spine (Phila Pa 1976)*. 2007;32(17):1809-1815.

[49] Ribitsch I, Baptista PM, Lange-Consiglio A, Melotti L, Patruno M, Jenner F, Schnabl-Feichter E, Dutton LC, Connolly DJ, van Steenbeek FG, Dudhia J, Penning LC. Large Animal Models in Regenerative Medicine and Tissue Engineering: To Do or Not to Do. *Front Bioeng Biotechnol*. 2020;8:972.

[50] Ashinsky BG, Gullbrand SE, Bonnevie ED, Wang C, Kim DH, Han L, Mauck RL, Smith HE. Sacrificial Fibers Improve Matrix Distribution and Micromechanical Properties in a Tissue-Engineered Intervertebral Disc. *Acta Biomater*. 2020;111:232-241.

[51] Kim DH, Martin JT, Gullbrand SE, Elliott DM, Smith LJ, Smith HE, Mauck RL. Fabrication, maturation, and implantation of composite tissue-engineered total discs formed from native and mesenchymal stem cell combinations. *Acta Biomater*. 2020;114:53-62.

[52] Martin JT, Gullbrand SE, Kim DH, et al. In Vitro Maturation and In Vivo Integration and Function of an Engineered Cell-Seeded Disc-like Angle Ply Structure (DAPS) for Total Disc Arthroplasty. *Sci Rep*. 2017;7(1):15765.

[53] Martin JT, Kim DH, Milby AH, Pfeifer CG, Smith LJ, Elliott DM, Smith HE, Mauck RL. In vivo performance of an acellular disc-like angle ply structure (DAPS) for total disc replacement in a small animal model. *J Orthop Res*. 2017;35(1):23-31.

[54] van Dijk M, Smit TH, Sugihara S, Burger EH, Wuisman PI. The effect of cage stiffness on the rate of lumbar interbody fusion: an in vivo model using poly(l-lactic Acid) and titanium cages. *Spine (Phila Pa 1976)*. 2002;27(7):682-688.

[55] Wuisman PI, van Dijk M, Smit TH. Resorbable cages for spinal fusion: an experimental goat model. *J Neurosurg*. 2002;97(4 Suppl):433-439.

[56] Toth JM, Wang M, Scifert JL, et al. Evaluation of 70/30 D,L-PLa for use as a resorbable interbody fusion cage. *Orthopedics*. 2002;25(10 Suppl):s1131-s1140.

[57] Cahill DW, Martin GJ Jr, Hajjar MV, Sonstein W, Graham LB, Engelman RW. Suitability of bioresorbable cages for anterior cervical fusion. *J Neurosurg*. 2003;98(2 Suppl):195-201.

[58] Krijnen MR, Smit TH, Strijkers GJ, Nicolay K, Pouwels PJ, Wuisman PI. The use of high-resolution magnetic resonance imaging for monitoring interbody fusion and bioabsorbable cages: an ex vivo pilot study. *Neurosurg Focus*. 2004;16(3):E3.

[59] Pflugmacher R, Schleicher P, Gumnior S, Turan O, Scholz M, Eindorf T, Haas NP, Kandziora F. Biomechanical comparison of bioabsorbable cervical spine interbody fusion cages. *Spine (Phila Pa 1976)*. 2004;29(16):1717-1722.

[60] Smit TH, Krijnen MR, van Dijk M, Wuisman PI. Application of polylactides in spinal cages: studies in a goat model. *J Mater Sci Mater Med*. 2006;17(12):1237-1244.

[61] Abbah SA, Lam CX, Ramruttun AK, Goh JC, Wong HK. Fusion performance of low-dose recombinant human bone morphogenetic protein 2 and bone marrow-derived multipotent stromal cells in biodegradable scaffolds: a comparative study in a large animal model of anterior lumbar interbody fusion. *Spine (Phila Pa 1976)*. 2011;36(21):1752-1759.

[62] Kennon JC, Awad ME, Chutkan N, DeVine J, Fulzele S. Current insights on use of growth factors as therapy for Intervertebral Disc Degeneration. *Biomol Concepts*. 2018;9(1):43-52.

[63] Chan SC, Ferguson SJ, Gantenbein-Ritter B. The effects of dynamic loading on the intervertebral disc [published correction appears in Eur Spine J. 2011 Nov;20(11):1813]. *Eur Spine J*. 2011;20(11):1796-1812.

[64] Wuertz K, Godburn K, MacLean JJ, Barbir A, Donnelly JS, Roughley PJ, Alini M, Iatridis JC. In vivo remodeling of intervertebral discs in response to short- and long-term dynamic compression. *J Orthop Res*. 2009;27(9):1235-1242.

[65] Mauck RL, Soltz MA, Wang CC, Wong DD, Chao PH, Valhmu WB, Hung CT, Ateshian GA. Functional tissue engineering of articular cartilage through dynamic loading of chondrocyte-seeded agarose gels. *J Biomech Eng*. 2000;122(3):252-260.

[66] Hunter CJ, Imler SM, Malaviya P, Nerem RM, Levenston ME. Mechanical compression alters gene expression and extracellular matrix synthesis by chondrocytes cultured in collagen I gels. *Biomaterials*. 2002;23(4):1249-1259.

[67] Bonassar LJ, Grodzinsky AJ, Frank EH, Davila SG, Bhaktav NR, Trippel SB. The effect of dynamic compression on the response of articular cartilage to insulin-like growth factor-I. *J Orthop Res*. 2001;19(1):11-17.

[68] Buschmann MD, Gluzband YA, Grodzinsky AJ, Hunziker EB. Mechanical compression modulates matrix biosynthesis in chondrocyte/agarose culture. *J Cell Sci*. 1995;108 (Pt 4):1497-1508.

[69] Waldman SD, Couto DC, Grynpas MD, Pilliar RM, Kandel RA. A single application of cyclic loading can accelerate matrix deposition and enhance the properties of tissue-engineered cartilage. *Osteoarthritis Cartilage*. 2006;14(4):323-330.

[70] Davisson T, Kunig S, Chen A, Sah R, Ratcliffe A. Static and dynamic compression modulate matrix metabolism in tissue engineered cartilage. *J Orthop Res*. 2002;20(4):842-848.

[71] Salvatierra JC, Yuan TY, Fernando H, Castillo A, Gu WY, Cheung HS, Huant CY. Difference in Energy Metabolism of Annulus Fibrosus and Nucleus Pulposus Cells of the Intervertebral Disc. *Cell Mol Bioeng*. 2011;4(2):302-310.

[72] Hudson KD, Mozia RI, Bonassar LJ. Dose-dependent response of tissue-engineered intervertebral discs to dynamic unconfined compressive loading. *Tissue Eng Part A*. 2015;21(3-4):564-572.

[73] Risbud MV, Albert TJ, Guttapalli A, Vresilovic EJ, Hillibrand AS, Vaccaro AR, Shapiro IM. Differentiation of mesenchymal stem cells towards a nucleus pulposus-like phenotype in vitro: implications for cell-based transplantation therapy. *Spine (Phila Pa 1976)*. 2004;29(23):2627-2632.

[74] Risbud MV, Guttapalli A, Stokes DG, Hawkins D, Danielson KG, Schaer TP, Albert TJ, Shapiro IM. Nucleus pulposus cells express HIF-1 alpha under normoxic culture conditions: a metabolic adaptation to the intervertebral disc microenvironment. *J Cell Biochem*. 2006;98(1):152-159.

[75] Grunhagen T, Wilde G, Soukane DM, Shirazi-Adl SA, Urban JP. Nutrient supply and intervertebral disc metabolism. *J Bone Joint Surg Am*. 2006;88 Suppl 2:30-35.

[76] Wenger RH, Kurtcuoglu V, Scholz CC, Marti HH, Hoogewijs D. Frequently asked questions in hypoxia research. *Hypoxia (Auckl)*. 2015;3:35-43.

[77] Dowdell J, Erwin M, Choma T, Vaccaro A, Iatridis J, Cho SK. Intervertebral Disk Degeneration and Repair. *Neurosurgery*. 2017;80(3S):S46-S54.

[78] Khanarian NT, Boushell MK, Spalazzi JP, Pleshko N, Boskey AL, Lu HH. FTIR-I compositional mapping of the cartilage-to-bone interface as a function of tissue region and age. *J Bone Miner Res*. 2014;29(12):2643-2652.

[79] King A, Bowe J. Animal models for diabetes: Understanding the pathogenesis and finding new treatments. *Biochem Pharmacol*. 2016;99:1-10.

[80] Bellinger DA, Merricks EP, Nichols TC. Swine models of type 2 diabetes mellitus: insulin resistance, glucose tolerance, and cardiovascular complications. *ILAR J*. 2006;47(3):243-258.

[81] Koopmans SJ, Mroz Z, Dekker R, Corbijn H, Ackermans M, Sauerwein H. Association of insulin resistance with hyperglycemia in streptozotocin-diabetic pigs: effects of metformin at isoenergetic feeding in a type 2-like diabetic pig model. *Metabolism*. 2006;55(7):960-971.

[82] Koopmans SJ, Schuurman T. Considerations on pig models for appetite, metabolic syndrome and obese type 2 diabetes: From food intake to metabolic disease. *Eur J Pharmacol*. 2015;759:231-239.

[83] Fang JY, Lin CH, Huang TH, Chuang SY. In Vivo Rodent Models of Type 2 Diabetes and Their Usefulness for Evaluating Flavonoid Bioactivity. *Nutrients*. 2019;11(3):530.

[84] Wagner JE, Kavanagh K, Ward GM, Auerbach BJ, Harwood HJ Jr, Kaplan JR. Old world nonhuman primate models of type 2 diabetes mellitus. *ILAR J*. 2006;47(3):259-271.

[85] Rand JS, Fleeman LM, Farrow HA, Appleton DJ, Lederer R. Canine and feline diabetes mellitus: nature or nurture?. *J Nutr*. 2004;134(8 Suppl):2072S-2080S.

[86] Rand JS. Pathogenesis of feline diabetes. *Vet Clin North Am Small Anim Pract*. 2013;43(2):221-231.

[87] Henson MS, O'Brien TD. Feline models of type 2 diabetes mellitus. *ILAR J*. 2006;47(3):234-242.

[88] Hoenig M. The cat as a model for human obesity and diabetes. *J Diabetes Sci Technol*. 2012;6(3):525-533.

[89] Grüssner R, Nakhleh R, Grüssner A, Tomadze G, Diem P, Sutherland D. Streptozotocin-induced diabetes mellitus in pigs. *Horm Metab Res*. 1993;25(4):199-203.

[90] Renner S, Fehlings C, Herbach N, Hofmann A, von Waldthausen DC, Kessler B, Ulrichs K, Chodnevskaja I, Moskalenko V, Amselgruber W, Göke B, Pfeifer A, Wanke R, Wolf E. Glucose intolerance and reduced proliferation of pancreatic beta-cells in transgenic pigs with impaired glucose-dependent insulinotropic polypeptide function. *Diabetes*. 2010;59(5):1228-1238.

[91] Umeyama K, Watanabe M, Saito H, Kurome M, Tohi S, Matsunari H, Miki K, Nagashima H. Dominant-negative mutant hepatocyte nuclear factor 1alpha induces diabetes in transgenic-cloned pigs. *Transgenic Res*. 2009;18(5):697-706.

[92] Lutz TA, Rand JS. Pathogenesis of feline diabetes mellitus. *Vet Clin North Am Small Anim Pract*. 1995;25(3):527-552.

[93] Pagliassotti MJ, Moore MC, Neal DW, Cherrington AD. Insulin is required for the liver to respond to intraportal glucose delivery in the conscious dog. *Diabetes*. 1992;41(10):1247-1256.

[94] Ionut V, Liu H, Mooradian V, Castro AV, Kabir M, Stefanovski D, Zheng D, Kirkman EL, Bergman RN. Novel canine models of obese prediabetes and mild type 2 diabetes. *Am J Physiol Endocrinol Metab*. 2010;298(1):E38-E48.

[95] U.S. Department of Health and Human Services. *Gestational diabetes*. National Institute of Diabetes and Digestive and Kidney Diseases.